2012-03-14

Damage Tolerance of Unidirectional Carbon and Fiberglass Composites with Aramid Sleeves

Charles Andrew Sika
Brigham Young University - Provo

Damage Tolerance of Unidirectional Carbon and Fiberglass Composites with Aramid Sleeves

Charles Andrew Sika

A thesis submitted to the faculty of
Brigham Young University
in partial fulfillment of the requirements for the degree of

Master of Science

David W. Jensen, Chair
Richard J. Balling
Fernando S. Fonseca

Department of Civil and Environmental Engineering

Brigham Young University

April 2012

ABSTRACT

Damage Tolerance of Unidirectional Fiberglass and Carbon Composites with Aramid Sleeves

Charles Andrew Sika
Department of Civil and Environmental Engineering, BYU
Master of Science

Unidirectional carbon fiber and fiberglass epoxy composite elements consolidated with aramid sleeves were radially impacted at 5 J (3.7 ft-lbs) and 10 J (7.4 ft-lbs), tested under compression, and compared to undamaged control specimens. These structural elements represent local members of open three-dimensional composite lattice structures (e.g., based on isogrid or IsoTruss® technologies). Advanced three-dimensional braiding techniques were used to continuously fabricate these specimens. The unidirectional core specimens, 8 mm (5/16 in) in diameter, were manufactured with various sleeve patterns. Bi-directional braided sleeves and unidirectional spiral sleeves ranged from a nominal full to half coverage. These specimens were tested for compression strength after impact. This research used an unsupported length of 50.8 mm (2.0 in) specimens to ensure a strength-controlled compression failure. Compression strength of undamaged unidirectional carbon fiber and fiberglass epoxy composites is virtually unaffected by sleeve type and sleeve coverage. Fiberglass/epoxy configurations exhibited approximately 1/2 and 2/3 reduction in compression strength relative to undamaged configurations after impact with 5 J (3.7 ft-lbs) and 10 J (7.4 ft-lbs), respectively. Increasing aramid sleeve coverage and/or increasing the interweaving of an aramid sleeve (i.e., braid vs. spiral) increases the damage tolerance of fiberglass/epoxy composite elements. Damaged carbon/epoxy composites exhibited an approximate decrease in strength of 70% and 75% after 5 J and 10 J of impact, respectively, relative to undamaged configurations. The results verify that an aramid sleeve, regardless of type (braid or spiral), facilitates consolidation of the carbon fiber and fiberglass epoxy core. Not surprisingly, full coverage configurations exhibit greater compression strength after impact than half coverage configurations.

Keywords: carbon, fiberglass, fiber/epoxy composite, damage tolerance, IsoTruss®, compression strength after impact (CSAI), unidirectional, kevlar/aramid sleeves

ACKNOWLEDGEMENTS

First, I thank my graduate advisor Dr. David W. Jensen for presenting to me this research opportunity. His expertise has given me invaluable guidance and direction to complete my portion of this research. He has also provided opportunity to submit and present parts of this thesis as a conference paper to the AIAA/ASME/ASCE/AHS/ASC Structures, Structural Dynamics and Materials Conference, held in Honolulu, HI, in April 2012.

I acknowledge the support of Novatek, Inc., the sponsor of this research, under the leadership of Mr. David Hall, and all of the Novatek Inc. employees. Mark Jensen also provided additional technical support from Altus Poles, LLC.

I would also like to thank my graduate committee at Brigham Young University for their time and input to fine-tune the quality of this thesis. I thank my colleagues at the Center for Advanced Structural Composites whom I have worked alongside and who have contributed tremendously to the completion this research.

Finally, I gratefully thank my family and friends for their tireless support, particularly my wife Haley, for her patience and encouragement throughout the duration of this process.

TABLE OF CONTENTS

LIST OF TABLES

LIST OF FIGURES

1 INTRODUCTION

The damage tolerance of unidirectional carbon fiber and fiberglass epoxy composite elements with aramid sleeves subjected to impact damage has been examined. These cylindrical elements represent the local members of open 3-dimensional lattice structures based on IsoTruss® or isogrid technologies [1], where unidirectional fibers in an epoxy matrix are consolidated and co-cured using various aramid sleeve patterns. Specimen configurations varied in their sleeve type (bi-directional braid or unidirectional spiral) and the nominal amount of coverage provided by the sleeve (half or full). Various specimens were radially impacted at either 5 J (3.7 ft-lbs.) or 10 J (7.4 ft-lbs.) prior to measuring the residual Compression Strength After Impact (CSAI). These results were compared to the compression strength of non-impacted control specimens and to the results from related tests previously performed by Allen on basalt/epoxy [2] [3].

This research extends the work conducted by Allen [2-3] from basalt/epoxy to carbon fiber and fiberglass epoxy composite elements. The primary purpose of sleeves in this research was to properly consolidate the core fibers. Presence of sleeves has been shown to confine the core fibers, thus eliminating micro-buckling [4] when compressed, and effectively consolidating the core fibers, which increases the tensile capacity of the resin [5]. Because of the brittle nature of composite materials, even low impact energies can degrade structural performance, particularly in compression. Sleeves were therefore, used as a secondary purpose to improve damage

tolerance. Wisnom [6] has shown that an aramid sleeve protects the core and increases the compression strength by nearly half. A related study on basalt/epoxy composites, performed by Allen [2] [7] showed that aramid sleeves improve the damage tolerance by diffusing impact energy: i.e., sleeves absorb a portion of the total impact energy and spread out the impact energy over a larger area of the core. The influence of both type and coverage of such sleeves was quantified in the current research document.

Manufacturing IsoTruss structures with braided rather than spiral sleeves increases the manufacturing complexity since it requires a larger machine capability [8], but even the most complex IsoTruss structure geometries can be manufactured with automated processes, as shown by Kesler [9] [10]. The interlocking inherent in braided sleeves provides a mechanical advantage over spiral wrapped sleeves, which could potentially unravel if damaged. On the other hand, a full spiral sleeve yields a smoother surface on the core composite because of the uniform pressure applied by the consistent pattern, whereas full braided sleeves produce a dimpled pattern on the surface. With regards to impact, full coverage sleeves obviously provide better protection to the core than half coverage sleeves. Conversely, half coverage saves material and manufacturing time, which, in turn, reduces cost.

1.1 Description of IsoTruss® Grid Structure

IsoTruss® structures offer a lightweight [11] and efficient alternative to typical steel, wood, aluminum, and even other traditional composite structures. The unique geometry of the IsoTruss not only poses an advantage when it comes to inspection, but also enables tremendous support to axial, torsional, and flexural loads. The IsoTruss is composed of longitudinal and helical members. Typical orientations with joints for the longitudinal and helical members are illustrated in Figure 1.1. The longitudinal and helical members are composed of transversely

isotropic composite tows consolidated with sleeves (the influence of sleeves on damage tolerance was quantified in this research). In IsoTruss structures, axial loads are carried primarily by the longitudinal members, while torsional loads are carried by the helical members. Helical members also increase the overall stiffness of the structure by reducing the un-braced length of the longitudinal members which can be susceptible to buckling [1] [12].

1.2 Automated Manufacturing of IsoTruss Structures

The unidirectional carbon and fiberglass composite members were manufactured using an IsoTruss machine built specifically for the purpose of creating automated and continuous production [8] [13]. These members were continuously fabricated with dry aramid fiber sleeves, tension wound around the core composite members [10]. The details and specifics of how these cylindrical unidirectional members were fabricated are documented by Allen [2].

Figure 1.1: Example of a Typical Geometry of IsoTruss® Structures

1.3 Related Research

The geometric specifics including equations and nomenclature used in IsoTruss descriptions and analysis were documented by Kesler [9], Winkel [14], Scoresby [15] and McCune [16]. Kesler [9] revealed a significant reduction in scatter in both stiffness and strength with an increased number of braiders.

Stoutis [4] tested pultruded carbon/epoxy rods under compression, similar to the tests done for this thesis except Stoutis only used undamaged specimens. In the research described in this current document, sleeves were used to confine the core fibers and minimize the effects of micro buckling, which was the failure mode observed by Stoutis.

Hansen [5] tested encapsulated and interwoven joints of IsoTruss structures. Different sleeve types were used to consolidate the core fibers resulting in a significant improvement in stiffness and strength. His specimens were undamaged, leading to the conclusion that braided sleeves exhibited a more consistent strength and stiffness than other sleeve types.

Wisnom [6] post-wrapped carbon fiber rods with aramid sleeves and tested for residual Compression Strength After Impact (CSAI). Research in the current thesis used aramid sleeves to consolidate the core fibers, and aramid sleeves were co-cured with members during manufacture. The aramid sleeves improve performance by confining the cores, preventing splitting of the core fibers, and acting as an impact energy diffuser.

The current research on the CSAI of carbon/epoxy and fiberglass/epoxy composites compliments the previous CSAI research on basalt/epoxy composites by Allen [2], and buckling strength research of longer members on basalt, carbon, and fiberglass fiber/epoxy composites conducted by Embley [17] [18].

General conclusions from related research by Allen [2] [3] are as follows:

1. Braided and spiral sleeves properly consolidate continuously-manufactured unidirectional basalt/epoxy composites.
2. The ultimate compression strength and compression stiffness of undamaged basalt/epoxy composites are not significantly affected (for better or worse) by sleeve type or sleeve coverage.
3. The ultimate strength of basalt/epoxy composites decreases with increasing impact energy levels (approximately one-third and two-thirds with 5 and 10 J (3.7 and 7.4 ft-lbs), respectively).
4. Basalt/epoxy composites with an 8 mm (5/16 in) diameter (same diameter as in this research) are not significantly affected by sleeve type. Full coverage specimens, however, exhibit 45% higher CSAI than partial coverage.

Conclusions from related research by Embley [17] [18] are as follows:

1. The influence of sleeve type and sleeve coverage is not consistent among carbon, fiberglass, and basalt fiber/epoxy composite rods.
2. Braided sleeves can be up to 34% stronger than spiral sleeves.
3. Full coverage can be up to 38% stronger than half coverage.
4. Buckling strength of carbon/epoxy composites decreases with increasing impact energy. Fiberglass and basalt composites, however, are more flexible and some configurations do not exhibit degradation in compression strength after impact at lower impact energy levels.

1.4 Scope of Investigation

The specific geometry of open composite lattice structures determines the dominant type of failure mode. In particular, the length-to-diameter ratio of the individual members controls the failure mode. For example, composite lattice structures with short bay lengths are more likely to exhibit local compression failure of members (depending on the member diameter, of course); whereas composite lattice structures with longer bay lengths are generally more likely to experience local buckling failure (see IsoTruss structure examples in Figure 1.2) [19].

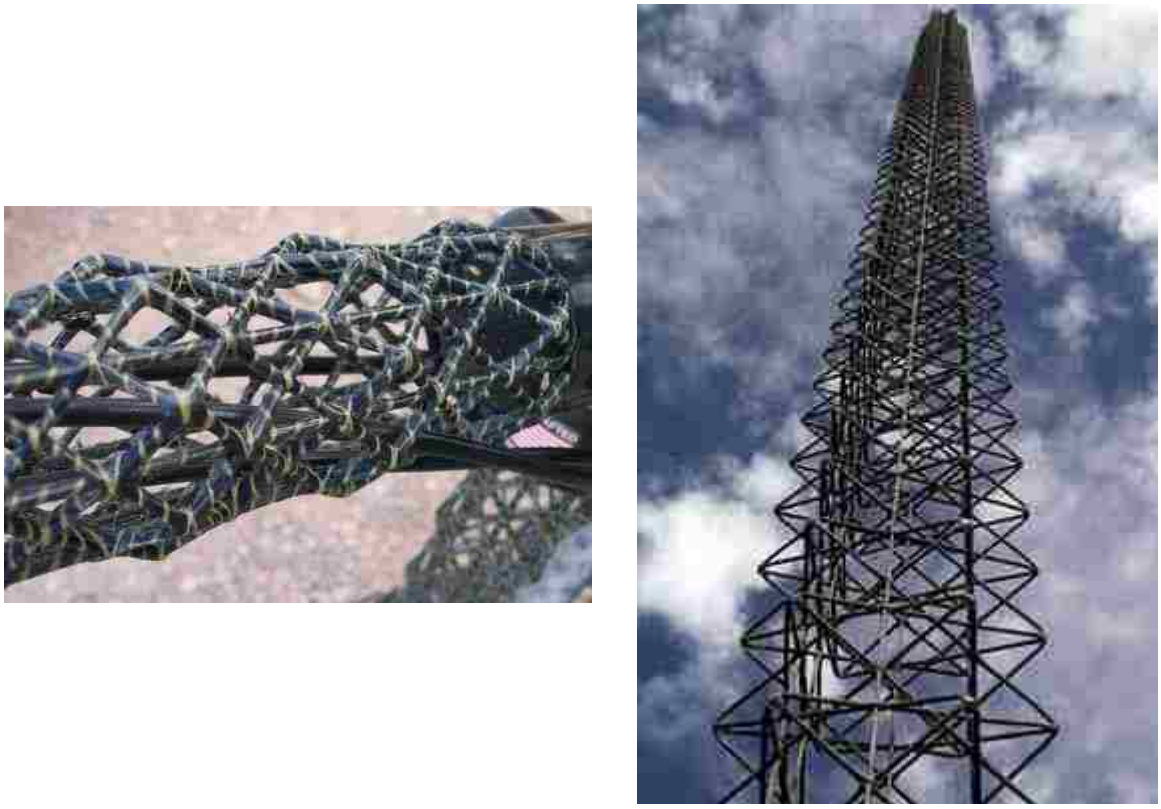

Figure 1.2: IsoTruss® Structure: A) Bicycle Frame (Left); and, B) Tower (Right)

The focus of this research was to quantify the influence of sleeves on damaged unidirectional carbon fiber and fiberglass epoxy composite rods under compression failure.

Specifically, this research answers the following design questions about fiber/epoxy composite rods under compression after radial impact:

1. Is the compression strength of undamaged carbon/epoxy composite rods manufactured using the automated continuous machine, independent of sleeve type or sleeve coverage, as demonstrated by Hansen [5]?
2. Are the conclusions from related research by Allen [2] on basalt/epoxy composites equally applicable to carbon/epoxy and/or fiberglass/epoxy composites?
    - Do co-cured braided sleeves on carbon/epoxy and fiberglass/epoxy composites yield sufficiently higher mechanical properties than spiral sleeves to justify the increased manufacturing complexity?
    - Do full coverage sleeves on carbon/epoxy and fiberglass/epoxy composites yield sufficiently higher mechanical properties than half coverage sleeves to justify the increased manufacturing complexity?
    - Do carbon/epoxy and fiberglass/epoxy composites exhibit similar damage tolerance characteristics to basalt/epoxy composites with respect to sleeve type and coverage?
    - Do carbon/epoxy and fiberglass/epoxy composites exhibit similar damage tolerance characteristics to basalt/epoxy composites as a function of impact energy?

To answer these fundamental questions, unidirectional carbon fiber and fiberglass epoxy composite rods with different aramid sleeve patterns were fabricated and tested in longitudinal compression with and without radial impact damage. Sleeve configurations were either bi-

directional braids or unidirectional spiral wraps and sleeve coverage was either full or half, nominally. Specimens were nominally 8 mm (5/16 in) in diameter and short enough to ensure local compression failure. Various specimens were radially impacted about mid-length with impact energy levels of 5 and 10 J (3.7 and 7.4 ft-lbs) prior to performing compression tests. The CSAI was measured and compared to the results of undamaged specimens and to the results of previous tests by Allen [2] and Hansen [5].

1.5 Thesis Overview

The experimental approach and data reduction procedure are described in Chapter Two. Chapter Three contains the test results for each test configuration. Chapters Four and Five summarize the averages for carbon fiber and fiberglass epoxy configuration results, respectively. Chapter Six describes normalized average compression stress and strain for all fiber/epoxy composites. Chapter Seven compares the test results for all tested fiber/epoxy materials, and Chapter Eight summarizes the final conclusions and provides recommendations.

2 EXPERIMENTAL APPROACH

This chapter details the test variables, manufacturing process, specimen preparation, and testing procedure used in this research.

2.1 Experimental Variables

Variables examined in this research include fiber material in the core, sleeve type, sleeve coverage, and impact energy.

2.1.1 Material

Fiber/epoxy composites using carbon fiber and fiberglass epoxy were investigated as specimen cores. These unidirectional rods were consolidated and co-cured with aramid sleeves. A list of each of the materials, manufacturers, and type is shown in Table 2.1. The nominal mechanical properties for each of the materials are shown in Table 2.2 [20-24].

Table 2.1: List of Specimen Materials, Manufacturer, and Type

Material and Use	Manufacturer	Type
Carbon Fiber Core	Toho	UTS50 E13 12K 800 Tex
Fiberglass Core	Owens Corning	X-Strand HPXSS EPX10 600 Tex
Epoxy Matrix	TCR Composites	UF3330-100
Aramid Sleeve	Dupont	49- 7100 Denier

Table 2.2: Properties of Specimen Materials

Material	Tensile Modulus [GPa (10^6 psi)]		Tensile Strength [MPa (ksi)]		Density [g/cm^3 (lb/ft^3)]		Filament Diameter [μm]	Filaments per Tow
Carbon	243	(35.2)	4860	(705)	1.79	(112)	7	12,000
Fiberglass	91.7	(13.3)	3300-4060	(479-589)	2.45	(153)	17	10,000
Epoxy	112	(16.3)	3000	(435)	1.44	(89.9)	12	4,700
Aramid	2830	(410)	68.9	(10.0)	1.21	(75.5)	--	--

2.1.2 Sleeve Type and Coverage

Sleeve type was either bi-directional (asymmetric) braid wrap or unidirectional spiral wrap and sleeve coverage ranged from full to half nominally. Figure 2.1 shows all four sleeve configurations (full braid, half braid, full spiral, and half spiral). In this research, specimens without sleeves were not considered, since the sleeves were needed to consolidate the specimens.

Figure 2.1: Sleeve Configurations from Left to Right: Full Braid, Half Braid, Full Spiral, and Half Spiral

2.1.3 Impact Energy

For consistency and future comparison purposes, the same impact energy levels that Allen [2] used were repeated in this research. This research used 50.8 mm (2 in) long specimens with 8 mm (5/16 in) diameter carbon and fiberglass cores, impacted at 5 and 10 J (3.7 and 7.4 ft-lbs) of impact energy, and later compared to non-impacted specimens.

2.1.4 Test Matrix

The different test variables resulted in a total of twenty-four possible configurations. Each of the twenty-four possible configurations is shown in Table 2.3. Nominally, five specimens of each configuration were tested.

Table 2.3: Test Matrix

Material	Diameter [mm (in)]	Sleeve Type	Sleeve Coverage	Impact Energy [J (ft-lbs)]
Carbon	8 (5/16)	Braid	Full	0 (0.0)
				5 (3.7)
				10 (7.4)
			Half	0 (0.0)
				5 (3.7)
				10 (7.4)
		Spiral	Full	0 (0.0)
				5 (3.7)
				10 (7.4)
			Half	0 (0.0)
				5 (3.7)
				10 (7.4)
Fiberglass	8 (5/16)	Braid	Full	0 (0.0)
				5 (3.7)
				10 (7.4)
			Half	0 (0.0)
				5 (3.7)
				10 (7.4)
		Spiral	Full	0 (0.0)
				5 (3.7)
				10 (7.4)
			Half	0 (0.0)
				5 (3.7)
				10 (7.4)

2.2 Specimen Manufacturing

The specimens were fabricated on an advanced three-dimensional, prototype braiding machine developed specifically for the manufacture of IsoTruss® and isogrid type composite lattice structures, see Figure 2.2. For a complete and detailed report outlining the manufacturing method, creation of sleeve patterns, and consolidation, refer to Allen [2]. The member was kept in constant tension while cured in an in-line oven.

Figure 2.2: Test Specimen Being Fabricated on Prototype IsoTruss Machine

2.3 Specimen Preparation

This section contains a summary of the specimen preparation procedure. The preparation steps in this research were followed in a manner similar to parallel research previously conducted by Allen [2] and Embley [17].

2.3.1 Unsupported Length

Preliminary tests by Allen [3] determined the critical length of 50.8 mm (2 in) long specimens to be used in the current research. This unsupported length of carbon fiber and fiberglass epoxy composite rods ensured compression failure. Similar but longer elements created a separate research performed by Embley [17-18]. To allow room for bonding in end caps, an additional 38 mm (1.5 in) was added to the specimens' unsupported length. The total specimen length was therefore, 88.9 mm (3.5 in).

Leco CM-10 cutting jig with a diamond tip blade was used to cut the specimens to length, as shown in Figure 2.3. To create a flat end surface, a polishing machine, Leco Spectrum System 2000, was used together with a special sanding fixture attachment, as shown in Figure 2.3. The attachment ensured a proper vertical alignment of specimens to polishing surface.

Figure 2.3: Specimen Preparation Equipment: A) Cutting Jig with Diamond Tip Blade (Left); and, B) Polisher with Vertical Aligning Attachment (Right)

2.3.2 Label Notation

Using a random number generator the specimens were assigned impact energy levels and testing order. Each specimen was labeled in the **5CA43FLC-2** notation. This example denotes an 8 mm (**5**/16 in) diameter specimen using **C**arbon fiber for the core and **A**ramid fiber for the sleeve. The three-dimensional braiding machine wall pattern used to make the braided sleeve was the **43** pattern [2]. This specimen sleeve coverage was **F**ull, impacted with **L**ow energy, and tested for **C**ompression failure. This was Specimen #**2** of 5 for this configuration. The details of this notation (number and letter designation) for each of the test variables are listed in Table 2.4.

Table 2.4: Specimen Label Notation Convention

Diameter	8 mm (5/16 in)	**5**
Core Material	Carbon	**C**
	Fiberglass	**G**
Sleeve Material	Aramid	**A**
Sleeve Type	Braid	**43**
	Spiral	**10**
Sleeve Coverage	Full	**F**
	Half	**H**
Impact Energy	Undamaged	**N**
	5 J (3.7 ft-lbs)	**L**
	10 J (7.4 ft-lbs)	**S**
Test	Compression	**C**
Specimen	Number	**1-6**

2.3.3 Bonding in End Caps

Loctite 5-minute epoxy was used to bond steel caps to each end of the specimens. End caps prevented splaying of the ends of each specimen when compressed; and allowed proper alignment in the test fixture by creating an even surface for uniform load distribution. A setting fixture specifically designed for this research, shown in Figure 2.4, was used to vertically align

the specimens when bonding on end caps. Excess epoxy was cleaned off the end caps using the Leco Spectrum System 2000 polishing machine (see Figure 2.3).

Figure 2.4: Vertical Aligning Fixture used to Bond Specimens in End Caps

2.4 Microscope Measurements

Precise measurements of specimen cross-sectional area, specimen offset from center, and the percent of sleeve coverage were recorded using Leco Olympus SZX12 microscope and Pax-it software. The software enabled 7X magnified pictures of the ends and sleeves of each specimen to be recorded.

2.4.1 Cross-Sectional Area

The magnified pictures of each end of the specimens were used to take cross-sectional area measurements. Using the Pax-it software, the core of the specimen was changed to a bright green color and the area of the green was measured as shown in Figure 2.5. The average of both ends' cross-sectional area was used as the final area for the individual specimen. The cross-sectional areas for each specimen are listed in Table A.1 – Table A.4.

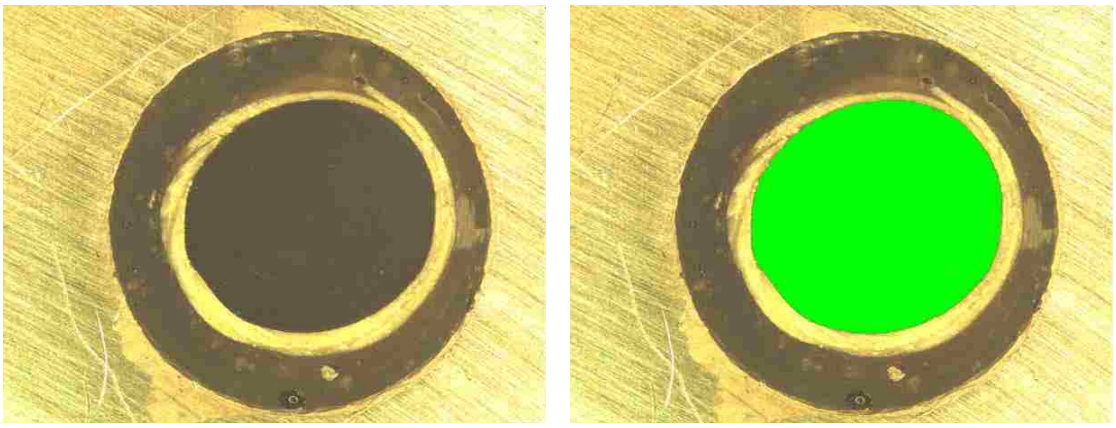

Figure 2.5: Cross-Sectional Area Measurements with Microscope and Pax-it Software

2.4.2 Offset Measurements

Specimens were not always perfectly bonded in the center of end caps. To later determine if this misalignment had any effect on specimen stiffness or strength, the offsets from center were measured were recorded. Crosshairs printed on a transparent sheet were placed on the end of the specimen and aligned with crosshairs on the Pax-it software. The offset was measured as the distance from the center of the crosshairs to the center of the specimen as shown in Figure 2.6. Offset measurements for each individual configuration is listed in Table A.5 – Table A.8.

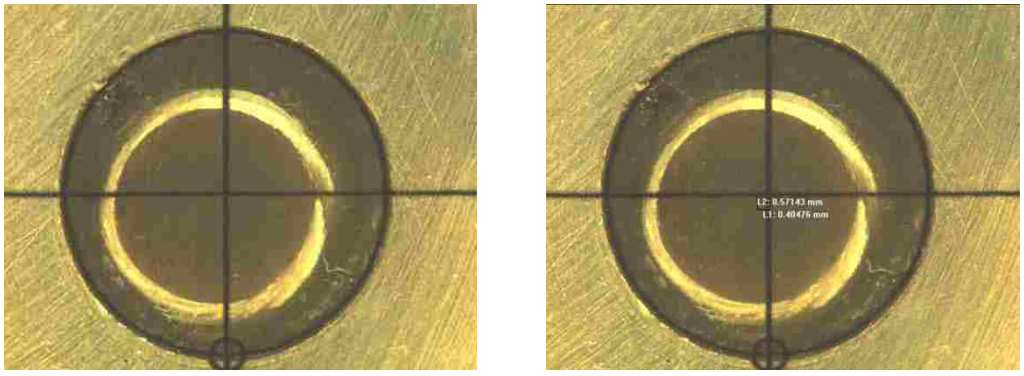

Figure 2.6: Offset from Center Measurements with Microscope and Pax-it Software

2.4.3 Sleeve Coverage

Measurements were taken to determine the actual percent coverage for the nominally half covered specimens only. Similar to the cross-sectional area measurements, the visible portion of the core was colored green with the Pax-it software and the area of the green was measured as shown in Figure 2.7. Each half coverage specimen was rotated approximately every 90 degrees to take four pictures for sleeve coverage measurement. The average of the four recorded measurements was reported as the actual percent coverage. Coverage measurements for each individual specimen are listed in Table A.9 – Table A.10.

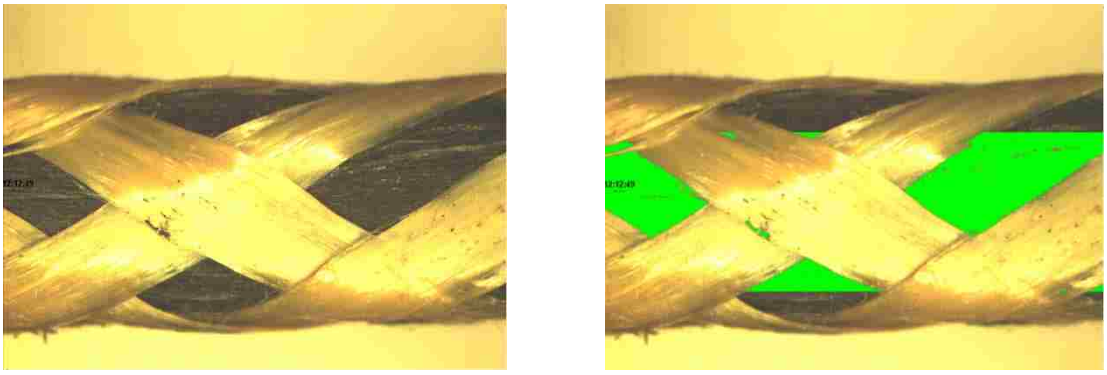

Figure 2.7: Sleeve Coverage Measurements with Microscope and Pax-it Software

2.5 Test Procedure

This section is a summary of the impact and compression test procedure, similarly conducted in related research by Allen [2] and Embley [17].

2.5.1 Impact Test Procedure

Impact tests were performed using the Dynatup® 8200 drop weight impact test machine shown on the right in Figure 2.8. The different levels of impact energy (5 and 10 J (3.7 and 7.4

ft-lbs)) were achieved by adjusting the drop weight height. Although the direct measure of damage inflicted on specimens was not measured, the total impact energy still provides a basis for comparison [25]. In this research, the internal damage was not investigated, only the impact energy was quantified.

Specimens were clamped in v-blocks fixed to a steel plate and radially impacted at mid-length with a cylindrical tup as shown in Figure 2.8. It is important to note that the specimens were bonded in end caps prior to impact, resulting in fixed-end conditions. This is a conservative approach compared to practical applications. Typically, three dimensional lattice structures will be flexible and absorb impact energy, resulting in less damage to local members.

Figure 2.8: Dynatup® 8200 Drop Weight Impact Test Machine

2.5.2 Compression Test Procedure

Compression tests were performed using 89 kN (20 kip) Instron model 1321, as shown in Figure 2.9. Also shown in Figure 2.10, is the alignment of the test specimen in the test fixture.

The test specimen receptacles were designed specifically to hold the end caps, making it quick and easy to align each specimen. The receptacles were clamped in the machine and a tungsten-carbide puck was used between the receptacle and the specimen to eliminate repeated use damage and to ensure uniform load introduction. The specimens were loaded at a stroke-controlled rate of 1.27 mm/min (0.05 in/min). Refer to Figure B.1–Figure B.8 for a picture of each specimen after failure.

Preliminary tests showed that the extensometer provided unreliable results [2-3]. An extensometer was therefore not used to measure deformation in this research. A correction factor was derived to remove deformations in the system from the measured machine displacement. The details of this correction factor derivation are found in Appendix E in Allen's thesis [2].

Figure 2.9: Instron Test Machine

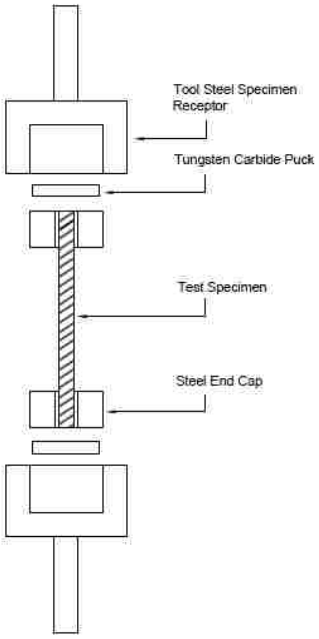

Figure 2.10: Schematics of Testing Fixture

2.6 Data Reduction and Statistical Analysis

A statistical conservative criterion, Chauvenet's criterion, used in parallel research by Embley [17], was repeated to determine if any tested specimens qualify as outliers and should therefore be excluded from the averages. This criterion provides an envelope based on a 1/2n probability and is calculated using a specified ratio (1.65 and 1.73 for 5 and 6 samples, respectively), the average, and the standard deviation.

A range of probable values representing 90% reliability with 95% confidence are shown for the average stress-strain curves and the average ultimate strengths of each test configuration. Details of this statistical analysis and equations for computation of the lower and upper limit envelope were documented in previous related research by Embley [17].

2.7 Offset Adjustment

Curve plots of the offset angle vs. compression strength after impact were prepared for each specimen (see Appendix D). For the most part, offset angle had insignificant or no effect on the specimens' compression modulus nor ultimate compression strength. Therefore, test results were not adjusted due to offsets in this research.

3 TEST RESULTS

Detail of results for each of the twenty-four test configurations along with the statistical analysis procedures used in this research are illustrated in this chapter. Tables that summarize average values (compression Young's modulus, compression strain at ultimate strength, and ultimate compression strength) for each test configuration are followed by their respective stress-strain curve plots.

3.1 Test Results

This section contains summary tables and stress-strain plots for each configuration. For a cleaner stress-strain plot presentation for each configuration, the stress-strain curves were truncated the first time stress dropped below 60% of the maximum stress. In the plots, 90% reliability and 95% confidence envelope are shown to illustrate ranges where data points are within averages and specimens that were ultimately discarded due to outlier characteristics.

3.1.1 Full Braid Carbon Specimens

Test results for undamaged full braid carbon/epoxy specimens (5CA43FNC) are summarized in Table 3.1 and the stress-strain curves are shown in Figure 3.1.

Test results for full braid carbon/epoxy specimens impacted at 5 J (3.7 ft-lbs) (5CA43FLC) are summarized in Table 3.2 and the stress-strain curves are shown in Figure 3.2.

Table 3.1: Properties of Full Braid, Undamaged, Carbon Specimens (5CA43FNC)

Full Braided Sleeve at No Impact	Compression Young's Modulus		Ultimate Compression Strength		Compression Strain at Ultimate Strength
	[GPa	(10^6 psi)]	[MPa	(ksi)]	[10^3 με]
1	123.3	17.88	964	139.8	8.42
2	144.6	20.97	1025	148.7	7.82
3	139.8	20.27	976	141.5	7.36
4	124.9	18.12	889	129.0	7.58
5	144.4	20.94	796	115.4	5.87
Average	135.4	19.64	930	134.9	7.41
Standard Deviation	10.5	1.52	90	13.0	0.95
[%]	7.8		10		13

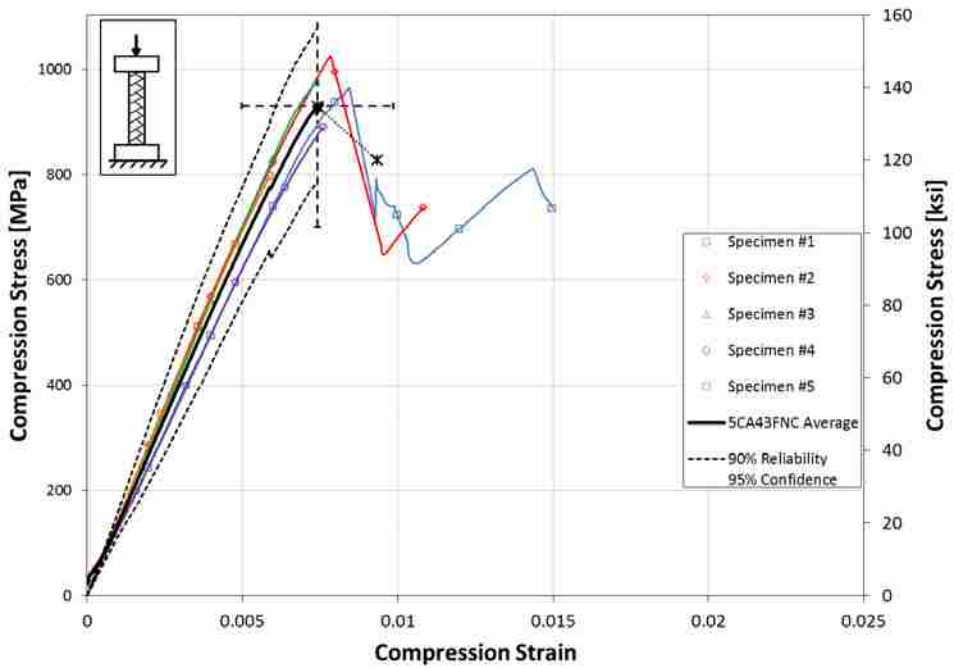

Figure 3.1: Stress-Strain Curves for Full Braid, Undamaged, Carbon Specimens (5CA43FNC)

Table 3.2: Properties of Full Braid, 5 J (3.7 ft-lbs) Impact, Carbon Specimens (5CA43FLC)

Full Braided Sleeve at 5 J (3.7 ft-lbs) Impact	Compression Young's Modulus		Ultimate Compression Strength		Compression Strain at Ultimate Strength
	[GPa	(10^6 psi)]	[MPa	(ksi)]	[10^3 με]
1	92.9	13.47	293	42.5	3.76
2	92.1	13.35	334	48.4	10.70
3	124.5	18.05	265	38.4	2.48
4	105.2	15.26	247	35.9	3.22
5	111.1	16.11	325	47.2	11.85
Average	105.1	15.25	293	42.5	6.40
Standard Deviation	13.5	1.96	37	5.4	4.49
[%]	13		13		70

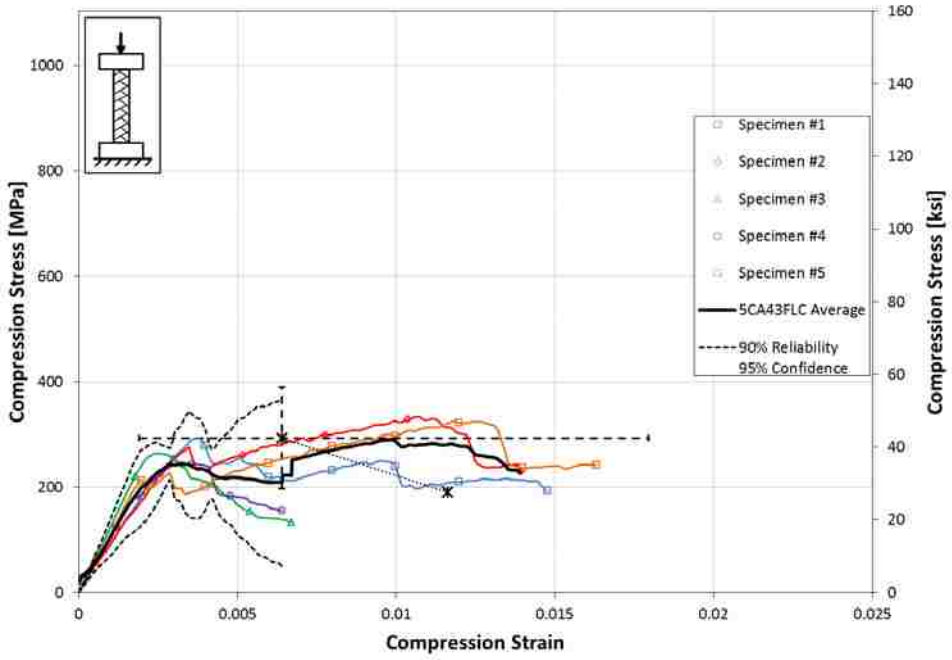

Figure 3.2: Stress-Strain Curves for Full Braid, 5 J (3.7 ft-lbs) Impact, Carbon Specimens (5CA43FLC)

Test results for full braid carbon/epoxy specimens impacted at 10 J (7.4 ft-lbs) (5CA43FSC) are summarized in Table 3.3 and the stress-strain curves are shown in Figure 3.3. After the initial test for full braid carbon/epoxy specimens impacted at 10 J (7.4 ft-lbs) (5CA43FSC), the compression modulus of Specimen 1 was lower than the Chauvenet minimum. A sixth specimen was tested and after reapplying Chauvenet's criterion to all six specimens, the stress-strain curve of Specimen 1 fell 28.4% outside Chauvenet's envelope (see Figure C.1) verifying that Specimen 1 was an outlier and was therefore excluded from the final data set.

Table 3.3: Properties of Full Braid, 10 J (7.4 ft-lbs) Impact, Carbon Specimens (5CA43FSC)

Full Braid Sleeve at 10 J (7.4 ft-lbs) Impact	Compression Young's Modulus		Ultimate Compression Strength		Compression Strain at Ultimate Strength
	[GPa	(10^6 psi)]	[MPa	(ksi)]	[10^3 με]
1*	*57.5*	*8.33*[+]	*334*	*48.4*	*11.43*
2	78.8	11.43	303	43.9	6.12
3	92.2	13.38	263	38.1	7.79
4	91.0	13.20	274	39.7	17.23
5	99.1	14.38	290	42.1	16.71
6	118.4	17.17	288	41.8	7.44
Average [1-5]	83.7	12.14	293	42.5	11.85
Standard Deviation [1-5]	16.4	2.38	28	4.0	5.05
[%]	20		9.5		43
Average [2-6]	95.9	13.91	284	41.1	11.06
Standard Deviation [2-6]	14.6	2.11	16	2.3	5.4
[%]	15		5.5		49

*Specimen eliminated using Chauvenet's criterion; italicized values not included in average or standard deviation.
[+]Properties used to eliminate specimen.

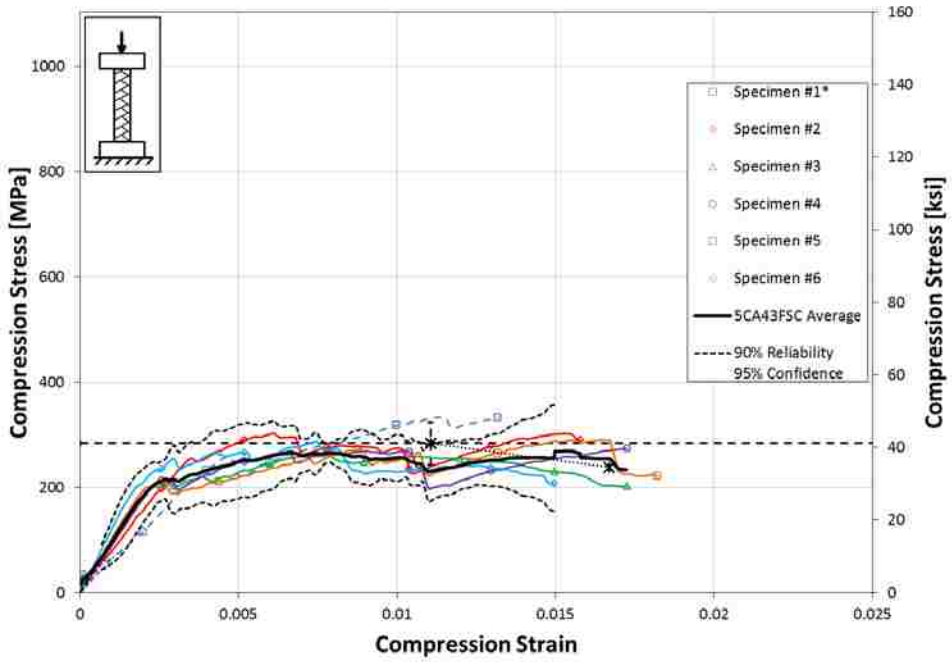

Figure 3.3: Stress-Strain Curves for Full Braid, 10 J (7.4 ft-lbs) Impact, Carbon Specimens (5CA43FSC)

3.1.2 Half Braid Carbon Specimens

Test results for undamaged half braid carbon/epoxy specimens (5CA43HNC) are summarized in Table 3.4 and the stress-strain curves are shown in Figure 3.4. After the initial test for undamaged half braid carbon/epoxy specimens (5CA43HNC), the compression stiffness and ultimate strength of Specimen 5 were lower than Chauvenet's minimum. One more specimen was tested and after reapplying Chauvenet's criterion to all six specimens, the compression modulus and ultimate strength of Specimen 5 were still lower than the Chauvenet minima and its stress-strain curve fell 87.3% outside Chauvenet's envelope (see Figure C.3). Specimen 5 was an outlier and was therefore excluded from the final data set.

Table 3.4: Properties of Half Braid, Undamaged, Carbon Specimens (5CA43HNC)

Half Braided Sleeve at No Impact	Compression Young's Modulus		Ultimate Compression Strength		Compression Strain at Ultimate Strength
	[GPa	(10^6 psi)]	[MPa	(ksi)]	[10^3 με]
1	140.4	20.36	954	138.4	7.42
2	133.8	19.41	1016	147.4	8.41
3	143.9	20.87	940	136.3	7.23
4	151.7	22.00	1078	156.3	8.22
5*	*117.7*	*17.06+*	*480*	*69.7+*	*4.55+*
6	142.1	20.62	947	137.4	7.33
Average [1-6]	138.3	20.05	903	130.9	7.19
Standard Deviation [1-6]	11.6	1.69	214	31.0	1.39
[%]	8.4		24		19
Average [1-4,6]	142.4	20.65	987	143.2	7.72
Standard Deviation [1-4,6]	6.4	0.93	59	8.5	0.6
[%]	4.5		6.0		7.1

*Specimen eliminated using Chauvenet's criterion; italicized values not included in average or standard deviation.
+Properties used to eliminate specimen.

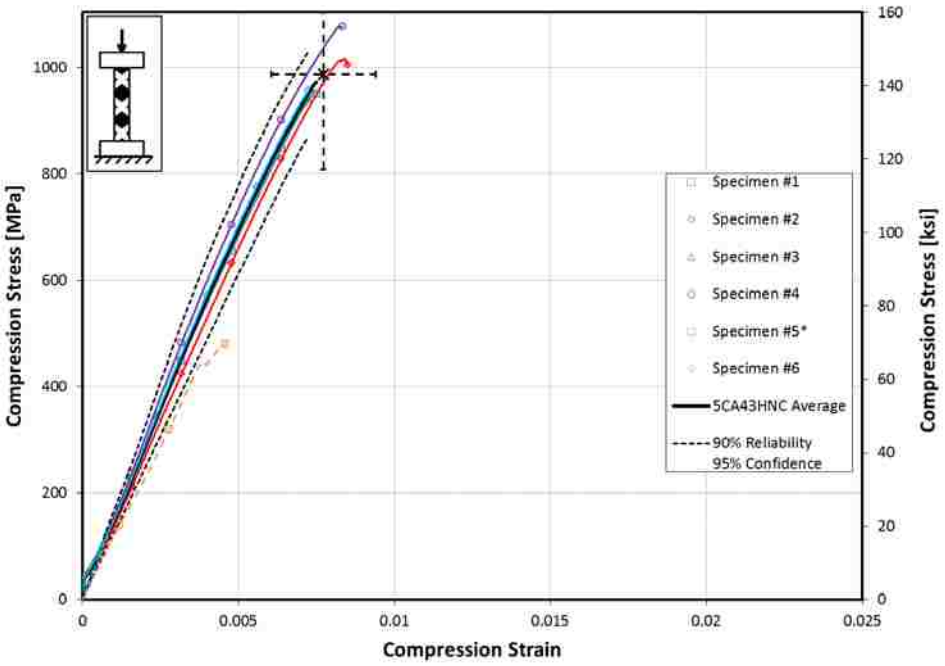

Figure 3.4: Stress-Strain Curves for Half Braid, Undamaged, Carbon Specimens (5CA43HNC)

Test results for half braid carbon/epoxy specimens impacted with 5 J (3.7 ft-lbs) (5CA43HLC) are summarized in Table 3.5 and the stress-strain curves are shown in Figure 3.5. After the initial test, the compression modulus of Specimen 1 was higher than the Chauvenet maximum. One more specimen was tested, and after reapplying Chauvenet's criterion to all six specimens, the stress-strain curve of Specimen 1 fell 57.9% outside Chauvenet's envelope (see Figure C.4). Specimen 1 was an outlier and was therefore excluded from the final data set.

Test results for half braid carbon/epoxy specimens impacted with 10 J (7.4 ft-lbs) (5CA43HSC) are summarized in Table 3.6 and the stress-strain curves are shown in Figure 3.6.

Table 3.5: Properties of Half Braid, 5 J (3.7 ft-lbs) Impact, Carbon Specimens (5CA43HLC)

Half Braided Sleeve Impacted at 5 J (3.7 ft-lbs)	Compression Young's Modulus		Ultimate Compression Strength		Compression Strain at Ultimate Strength
	[GPa	(10^6 psi)]	[MPa	(ksi)]	[10^3 με]
1*	*149.3*	*21.66+*	*309*	*44.8*	*2.25*
2	106.8	15.49	295	42.8	3.03
3	106.5	15.44	216	31.3	2.58
4	104.8	15.20	260	37.6	2.82
5	123.7	17.94	332	48.2	2.79
6	107.3	15.56	207	30.0	2.21
Average [1-5]	118.2	17.15	282	40.9	2.69
Standard Deviation [1-5]	19.0	2.76	45	6.6	0.30
[%]	16		16		11
Average [2-6]	109.8	15.93	262	38.0	2.69
Standard Deviation [2-6]	7.8	1.13	53	7.7	0.3
[%]	7.1		20		11

*Specimen eliminated using Chauvenet's criterion; italicized values not included in average or standard deviation.
+Properties used to eliminate specimen.

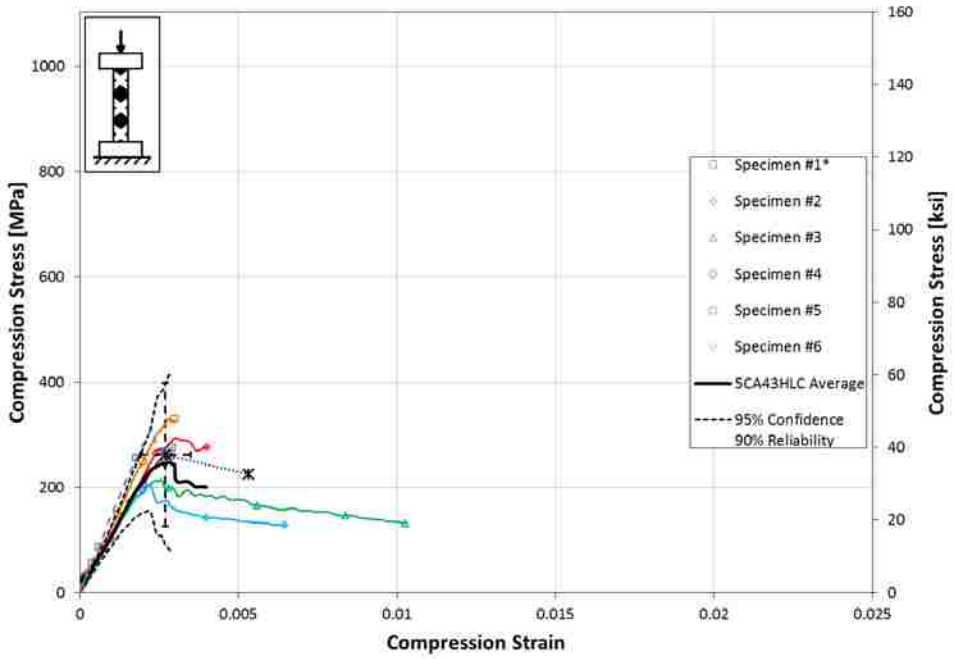

Figure 3.5: Stress-Strain Curves for Half Braid, 5 J (3.7 ft-lbs) Impact, Carbon Specimens (5CA43HLC)

Table 3.6: Properties of Half Braid, 10 J (7.4 ft-lbs) Impact, Carbon Specimens (5CA43HSC)

Half Braided Sleeve Impacted at 10 J (7.4 ft-lbs)	Compression Young's Modulus		Ultimate Compression Strength		Compression Strain at Ultimate Strength
	[GPa	(10^6 psi)]	[MPa	(ksi)]	[10^3 με]
1	116.4	16.88	199	28.8	2.35
2	113.3	16.43	193	28.1	2.43
3	66.4	9.63	123	17.8	2.99
4	55.5	8.04	121	17.6	2.91
5	83.2	12.07	165	23.9	2.56
Average	87.0	12.61	160	23.2	2.65
Standard Deviation	27.3	3.96	37	5.4	0.29
[%]	31		23		11

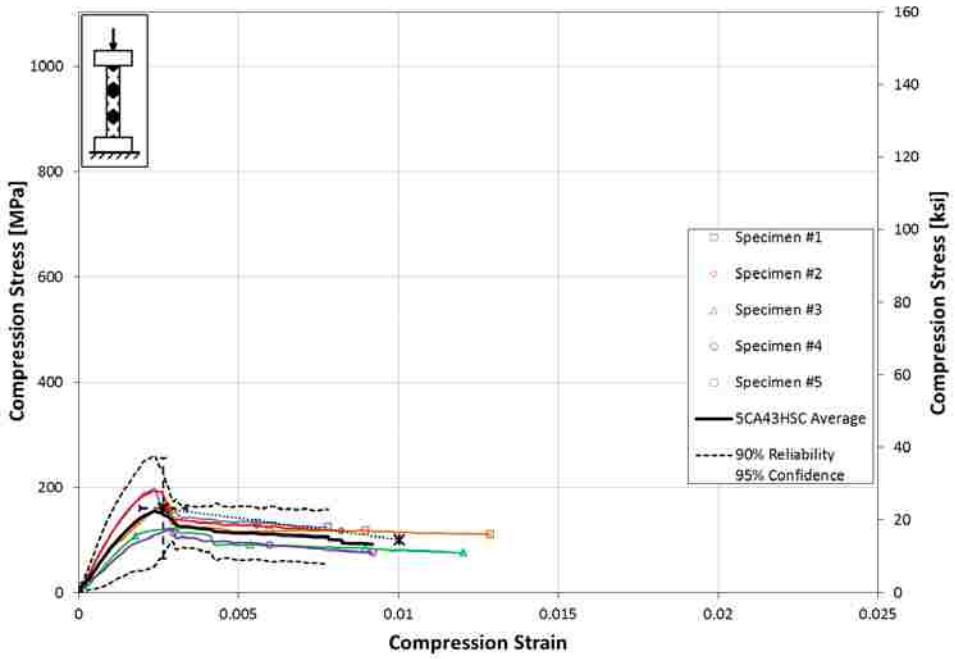

Figure 3.6: Stress-Strain Curves for Half Braid, 10 J (7.4 ft-lbs) Impact, Carbon Specimens (5CA43HSC)

3.1.3 Full Spiral Carbon Specimens

Test results for undamaged full spiral carbon/epoxy specimens (5CA10FNC) are summarized in Table 3.7 and the stress-strain curves are shown in Figure 3.7. After the initial test of undamaged full spiral carbon/epoxy specimens (5CA10FNC), the compression stiffness of Specimen 1 was lower than the Chauvenet minimum. One more specimen was tested and after reapplying Chauvenet's criterion to all six specimens, the modulus of Specimen 1 was still lower than the Chauvenet minimum and the stress-strain curve fell 89.4% outside Chauvenet's envelope (see Figure C.5). Specimen 1 was therefore eliminated and its properties are not included in the final average test results.

Table 3.7: Properties of Full Spiral, Undamaged, Carbon Specimens (5CA10FNC)

Full Spiral Sleeve at No Impact	Compression Young's Modulus		Ultimate Compression Strength		Compression Strain at Ultimate Strength
	[GPa	(10^6 psi)]	[MPa	(ksi)]	[10^3 με]
1*	*126.6*	*18.36*[+]	*902*	*130.8*	*7.45*
2	136.8	19.84	903	130.9	6.97
3	140.2	20.33	896	129.9	6.96
4	138.1	20.03	915	132.7	7.16
5	133.4	19.34	899	130.4	7.20
6	137.4	19.93	883	128.0	6.93
Average [1-6]	135.4	19.64	899	130.4	7.11
Standard Deviation [1-6]	4.8	0.70	10	1.5	0.20
[%]	3.6		1.2		2.8
Average [2-6]	137.2	19.89	899	130.4	7.04
Standard Deviation [2-6]	2.5	0.36	12	1.7	0.1
[%]	1.8		1.3		1.8

*Specimen eliminated using Chauvenet's criterion; italicized values not included in average or standard deviation.
[+]Properties used to eliminate specimen.

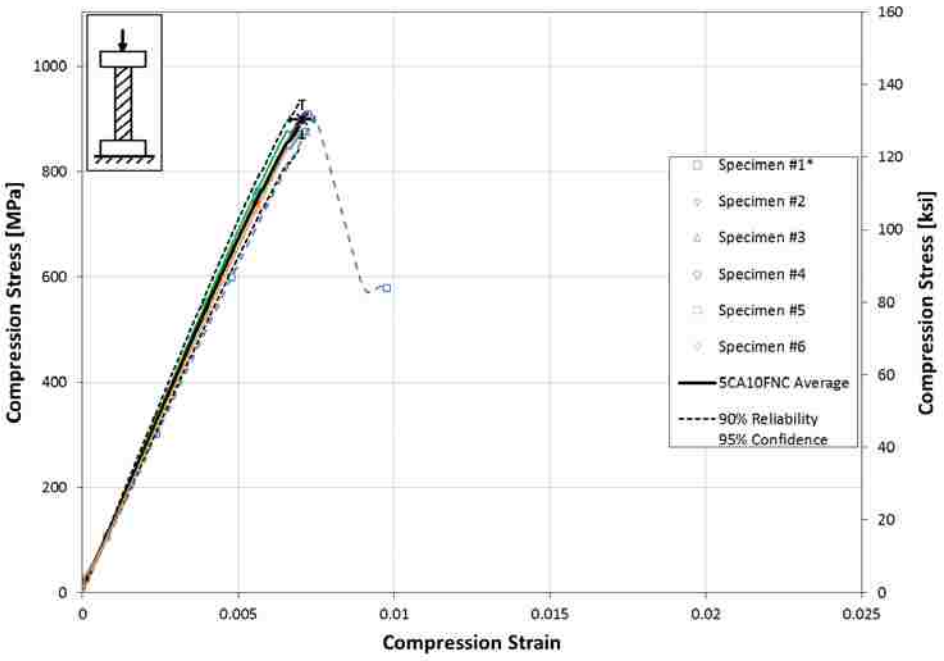

Figure 3.7: Stress-Strain Curves for Full Spiral, Undamaged, Carbon Specimens (5CA10FNC)

Test results for full spiral carbon/epoxy specimens impacted with 5 J (3.7 ft-lbs) (5CA10FLC) are summarized in Table 3.8 and the stress-strain curves are shown in Figure 3.8. After the initial test of full spiral carbon/epoxy specimens impacted with 5 J (3.7 ft-lbs) (5CA10FLC), the ultimate strength and strain of Specimen 4 were higher than the Chauvenet maximum and its stress-strain curve fell 9.1% outside Chauvenet's envelope (see Figure C.6). One more specimen was tested, and after reapplying Chauvenet's criterion to all six specimens, Specimen 4 was excluded from the final data set.

Test results for full spiral carbon/epoxy specimens impacted with 10 J (7.4 ft-lbs) (5CA10FSC) are summarized in Table 3.9 and the stress-strain curves are shown in Figure 3.9.

Table 3.8: Properties of Full Spiral, 5 J (3.7 ft-lbs) Impact, Carbon Specimens (5CA10FLC)

Full Spiral Sleeve Impacted at 5 J (3.7 ft-lbs)	Compression Young's Modulus		Ultimate Compression Strength		Compression Strain at Ultimate Strength
	[GPa	(10^6 psi)]	[MPa	(ksi)]	[10^3 με]
1	126.0	18.27	348	50.5	3.21
2	124.2	18.02	324	47.0	3.08
3	89.9	13.04	261	37.8	3.07
4*	*84.2*	*12.21*	*399*	*57.9*[+]	*3.70*
5	101.9	14.78	272	39.5	2.77
6	113.9	16.51	276	40.0	2.99
Average [1-5]	105.2	15.26	321	46.5	3.17
Standard Deviation [1-5]	19.2	2.79	57	8.2	0.34
[%]	18		18		11
Average [1-3,5-6]	111.2	16.13	296	43.0	3.02
Standard Deviation [1-3,5-6]	15.3	2.22	38	5.5	0.2
[%]	14		13		5.4

*Specimen eliminated using Chauvenet's criterion; italicized values not included in average or standard deviation.
[+]Properties used to eliminate specimen.

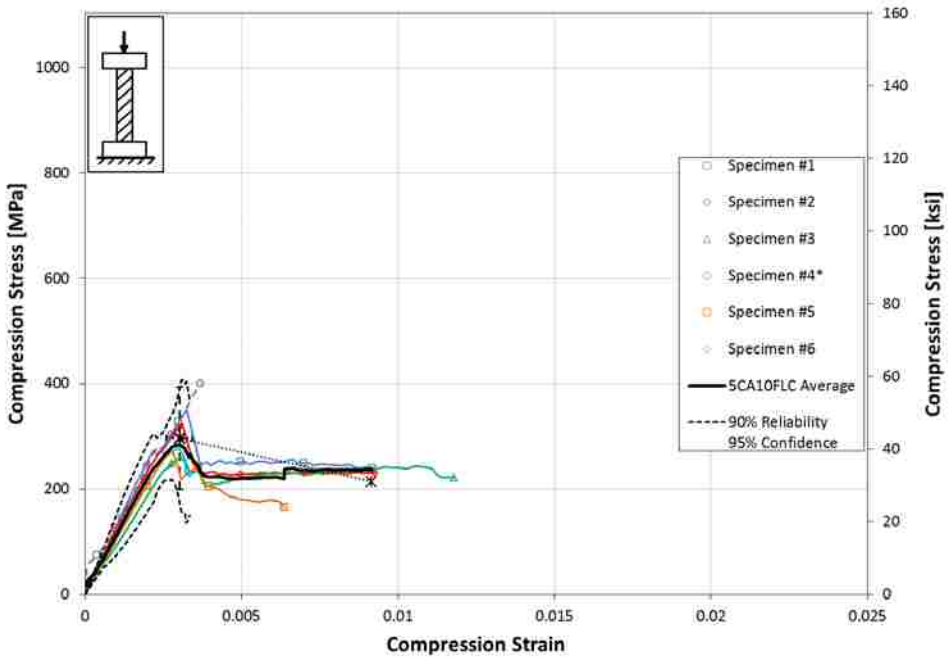

Figure 3.8: Stress-Strain Curves for Full Spiral, 5 J (3.7 ft-lbs) Impact, Carbon Specimens (5CA10FLC)

Table 3.9: Properties of Full Spiral, 10 J (7.4 ft-lbs) Impact, Carbon Specimens (5CA10FSC)

Full Spiral Sleeve Impacted at 10 J (7.4 ft-lbs)	Compression Young's Modulus		Ultimate Compression Strength		Compression Strain at Ultimate Strength
	[GPa	(10^6 psi)]	[MPa	(ksi)]	[10^3 με]
1	108.4	15.72	250	36.3	3.53
2	110.3	16.00	279	40.5	3.80
3	97.2	14.10	263	38.1	3.61
4	82.1	11.91	206	29.9	4.92
5	65.4	9.48	223	32.4	4.11
Average [1-5]	92.7	13.44	244	35.4	3.99
Standard Deviation [1-5]	18.9	2.75	30	4.3	0.57
[%]	20		12		14

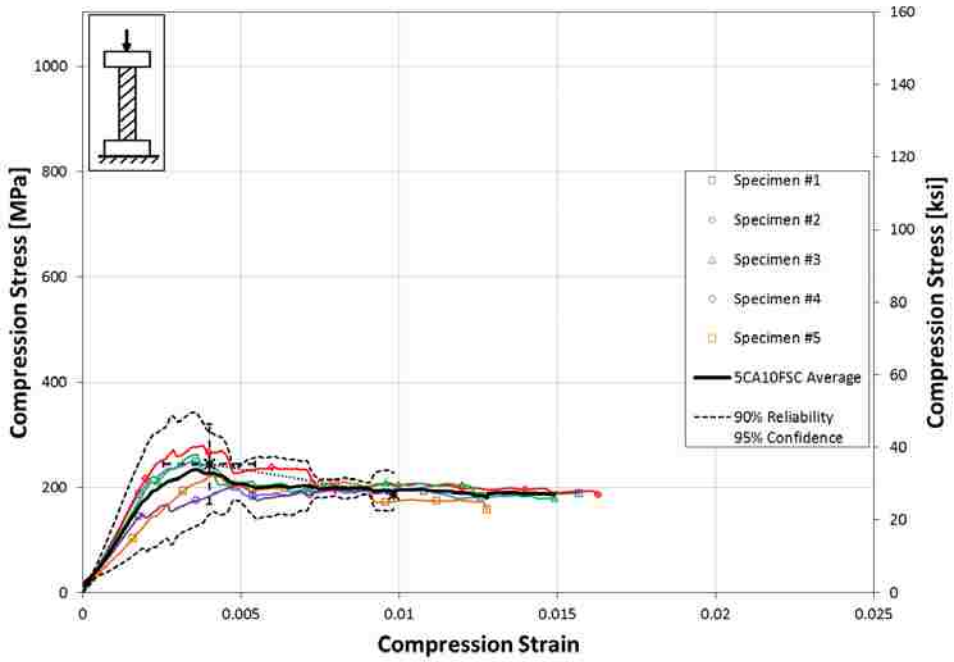

Figure 3.9: Stress-Strain Curves for Full Spiral, 10 J (7.4 ft-lbs) Impact, Carbon Specimens (5CA10FSC)

3.1.4 Half Spiral Carbon Specimens

Test results for undamaged half spiral carbon/epoxy specimens (5CA10HNC) are summarized in Table 3.10 and the stress-strain curves are shown in Figure 3.10. After the initial test of undamaged half spiral carbon/epoxy specimens (5CA10HNC), the ultimate compression strength of Specimen 3 was lower than the Chauvenet minimum. One more specimen was tested and after reapplying Chauvenet's criterion to all six specimens, the stress-strain curve for Specimen 3 fell 17.1% outside Chauvenet's envelope and was therefore excluded from the final data set (see Figure C.8).

Table 3.10: Properties of Half Spiral, Undamaged, Carbon Specimens (5CA10HNC)

Half Spiral Sleeve at No Impact	Compression Young's Modulus		Ultimate Compression Strength		Compression Strain at Ultimate Strength
	[GPa	(10^6 psi)]	[MPa	(ksi)]	[10^3 με]
1	145.7	21.13	934	135.5	7.11
2	162.0	23.50	1060	153.7	7.71
3*	*135.3*	*19.62*	*729*	*105.8*[+]	*5.62*
4	134.5	19.50	895	129.9	6.98
5	132.2	19.17	913	132.4	7.21
6	159.4	23.12	989	143.5	6.91
Average [1-5]	141.9	20.59	906	131.5	6.93
Standard Deviation [1-5]	12.4	1.79	118	17.1	0.78
[%]	8.7		13		11.3
Average [1-2,4-6]	146.8	21.28	958	139.0	7.18
Standard Deviation	13.8	1.99	67	9.7	0.3
[%]	9.4		7.0		4.4

*Specimen eliminated using Chauvenet's criterion; italicized values not included in average or standard deviation.
[+]Properties used to eliminate specimen.

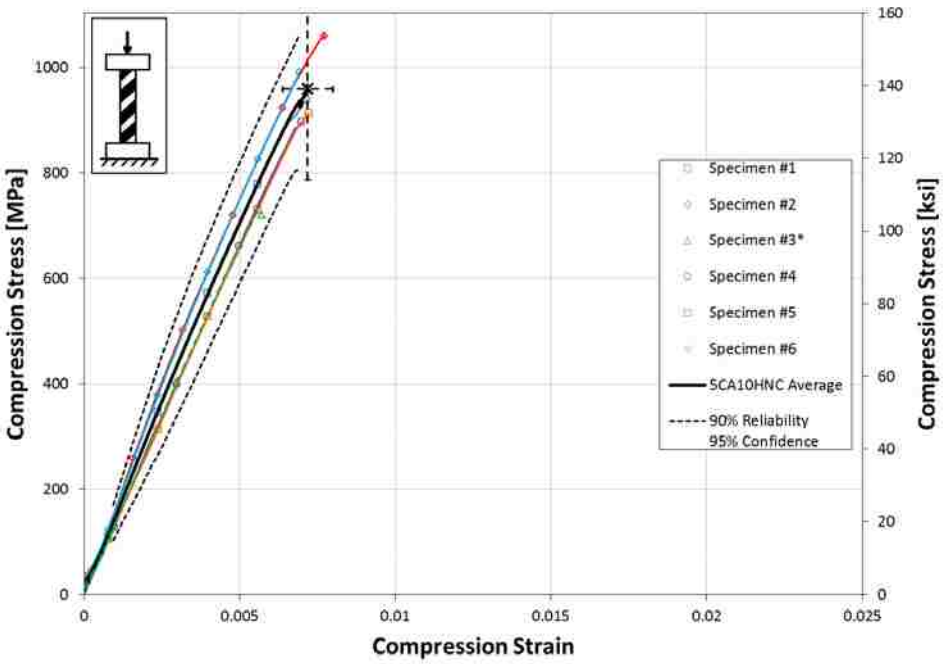

Figure 3.10: Stress-Strain Curves for Half Spiral, Undamaged, Carbon Specimens (5CA10HNC)

Test results for half spiral carbon/epoxy specimens (5CA10HLC) impacted with 5 J (3.7 ft-lbs) are summarized in Table 3.11 and the stress-strain curves are shown in Figure 3.11.

Test results for half spiral carbon/epoxy specimens impacted with 10 J (7.4 ft-lbs) (5CA10HSC) are summarized in Table 3.12 and the stress-strain curves are shown in Figure 3.12. After the initial test of half spiral carbon/epoxy specimens impacted with 10 J (7.4 ft-lbs) (5CA10HSC), the ultimate compression strength of Specimen 2 was lower than the Chauvenet minimum. One more specimen was tested and after reapplying Chauvenet's criterion to all six specimens, the ultimate strength of Specimen 2 was still lower than the Chauvenet minimum and the stress-strain curve fell 45.2% outside Chauvenet's envelope (see Figure C.10). Specimen 2 was therefore excluded from the final data set.

Table 3.11: Properties of Half Spiral, 5 J (3.7 ft-lbs) Impact, Carbon Specimens (5CA10HLC)

Full Spiral Sleeve Impacted at 5 J (3.7 ft-lbs)	Compression Young's Modulus		Ultimate Compression Strength		Compression Strain at Ultimate Strength
	[GPa	(10^6 psi)]	[MPa	(ksi)]	[10^3 με]
1	109.6	15.89	180	26.1	2.41
2	106.8	15.49	372	54.0	3.64
3	138.7	20.11	313	45.4	3.54
4	118.7	17.22	262	38.0	2.69
5	87.9	12.75	283	41.0	2.98
Average	112.3	16.29	282	40.9	3.05
Standard Deviation	18.5	2.68	71	10.3	0.53
[%]	16		25		17

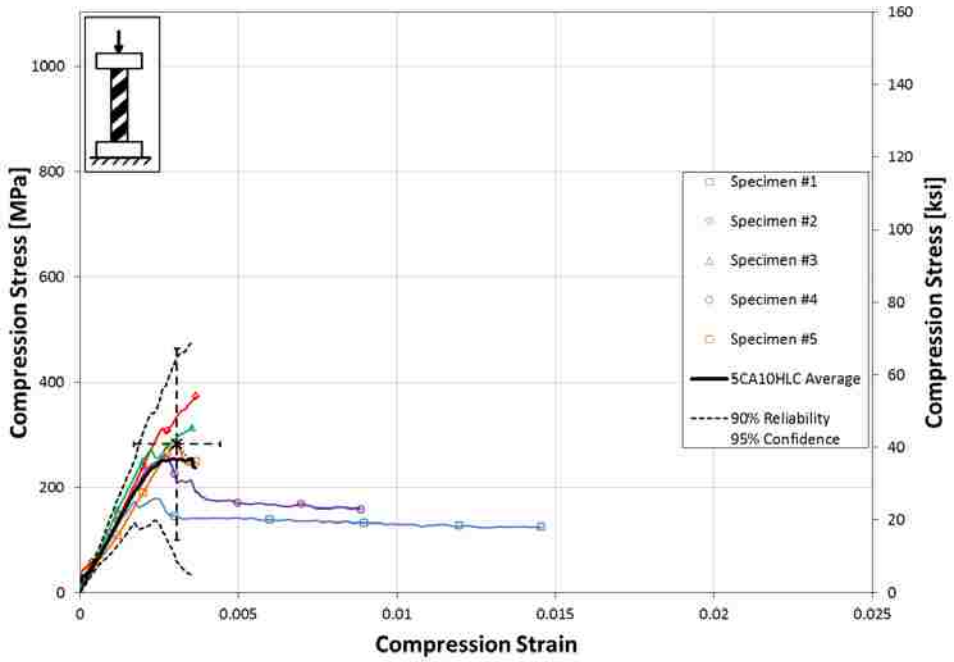

Figure 3.11: Stress-Strain Curves for Half Spiral, 5 J (3.7 ft-lbs) Impact, Carbon Specimens (5CA10HLC)

Table 3.12: Properties of Half Spiral, 10 J (7.4 ft-lbs) Impact, Carbon Specimens (5CA10HSC)

Half Spiral Sleeve Impacted at 10 J (7.4 ft-lbs)	Compression Young's Modulus		Ultimate Compression Strength		Compression Strain at Ultimate Strength
	[GPa	(10^6 psi)]	[MPa	(ksi)]	[10^3 με]
1	79.2	11.49	182	26.4	2.33
2*	*68.0*	*9.86*	*117*	*17.0+*	*3.41*
3	79.8	11.57	187	27.1	2.39
4	69.3	10.05	185	26.8	2.70
5	79.1	11.47	183	26.5	2.65
6	79.4	11.52	173	25.1	2.97
Average [1-6]	75.8	10.99	171	24.8	2.74
Standard Deviation [1-6]	5.6	0.81	27	3.9	0.40
[%]	7.3		16		15
Average [1,3-6]	77.4	11.22	182	26.4	2.61
Standard Deviation [1,3-6]	4.5	0.65	5	0.8	0.3
[%]	5.8		3.0		9.9

*Specimen eliminated using Chauvenet's criterion; italicized values not included in average or standard deviation.
+Properties used to eliminate specimen.

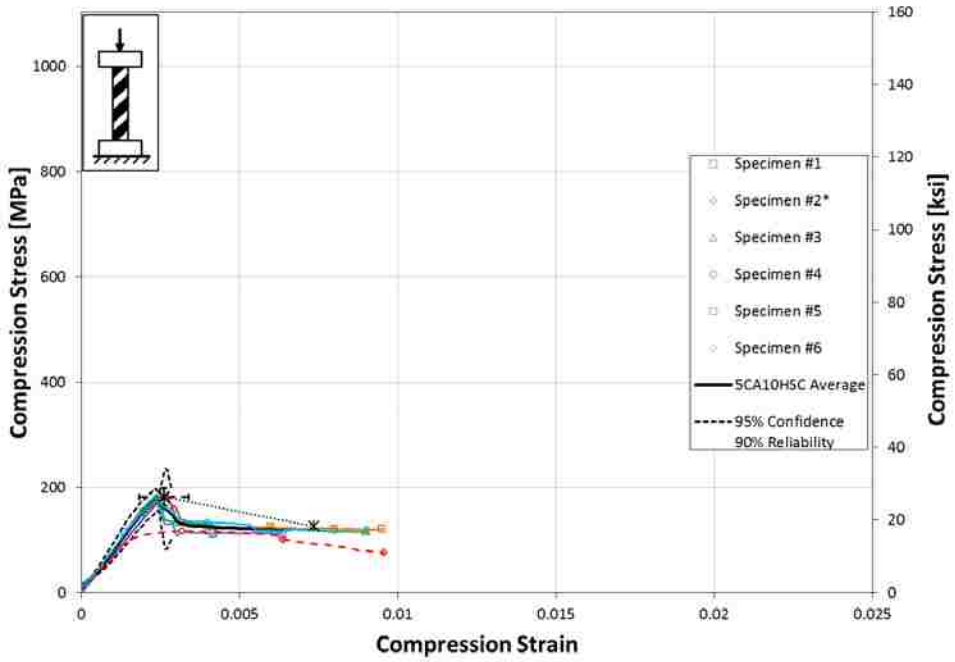

Figure 3.12: Stress-Strain Curves for Half Spiral, 10 J (7.4 ft-lbs) Impact, Carbon Specimens (5CA10HSC)

3.1.5 Full Braid Fiberglass Specimens

Test results for undamaged full braid fiberglass specimens (5GA43FNC) are summarized in Table 3.13 and the stress-strain curves are shown in Figure 3.13.

Test results for full braid fiberglass specimens (5GA43FLC) impacted with 5 J (3.7 ft-lbs) are summarized in Table 3.14 and the stress-strain curves are shown in Figure 3.14. After the initial test of full braid fiberglass specimens impacted with 5 J (3.7 ft-lbs) (5GA43FLC), the ultimate compression strength of Specimen 4 was lower than the Chauvenet minimum. One more specimen was tested and after reapplying Chauvenet's criterion to all six specimens, the ultimate strength of Specimen 4 was still lower than the Chauvenet minimum and the stress-strain curve fell 28.4% outside Chauvenet's envelope (see Figure C.12). Specimen 4 was therefore eliminated and its properties are not included in the final test results.

Table 3.13: Properties of Full Braid, Undamaged, Fiberglass Specimens (5GA43FNC)

Full Braided Sleeve at No Impact	Compression Young's Modulus		Ultimate Compression Strength		Compression Strain at Ultimate Strength
	[GPa	(10^6 psi)]	[MPa	(ksi)]	[10^3 με]
1	57.6	8.35	985	142.9	16.78
2	59.2	8.58	825	119.7	14.88
3	61.2	8.87	851	123.4	15.65
4	60.3	8.75	972	141.0	17.25
5	61.9	8.97	955	138.6	16.77
Average [1-5]	60.0	8.70	918	133.1	16.27
Standard Deviation [1-5]	1.7	0.25	74	10.8	0.97
[%]	2.8		8.1		6.0

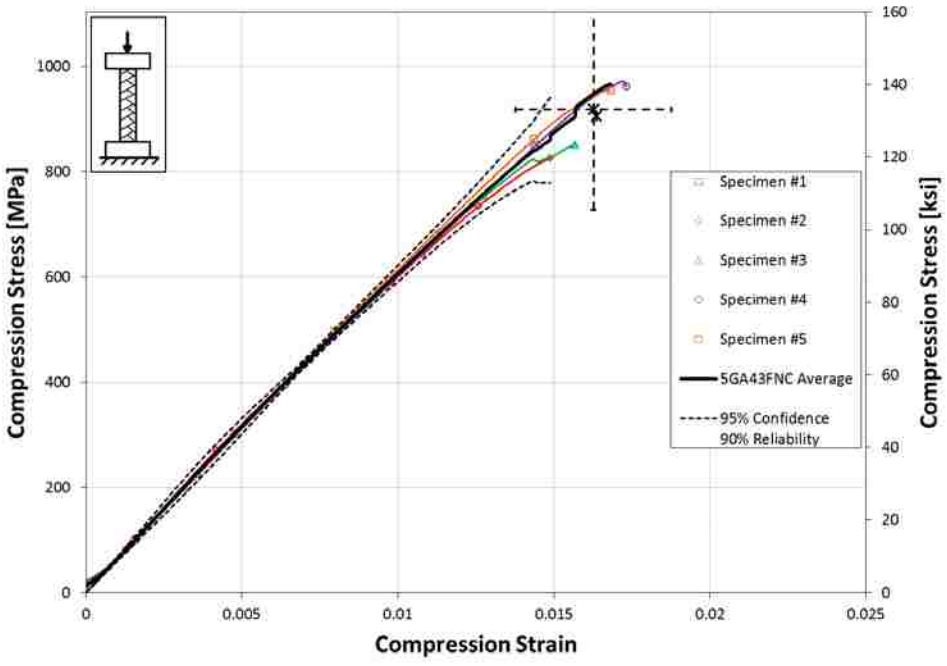

Figure 3.13: Stress-Strain Curves for Full Braid, Undamaged, Fiberglass Specimens (5GA43FNC)

Table 3.14: Properties of Full Braid, 5 J (3.7 ft-lbs) Impact, Fiberglass Specimens (5GA43FLC)

Full Braided Sleeve Impacted at 5 J (3.7 ft-lbs)	Compression Young's Modulus		Ultimate Compression Strength		Compression Strain at Ultimate Strength
	[GPa	(10^6 psi)]	[MPa	(ksi)]	[10^3 με]
1	64.9	9.42	559	81.1	10.29
2	68.7	9.96	597	86.6	10.00
3	61.8	8.96	506	73.4	9.01
4*	*63.9*	*9.27*	*342*	*49.6*[+]	*5.60*[+]
5	63.3	9.19	498	72.2	9.15
6	68.0	9.87	481	69.8	8.08
Average [1-5]	64.5	9.36	501	72.6	8.81
Standard Deviation [1-5]	2.6	0.38	97	14.1	1.88
[%]	4.0		19		21
Average [1-3,5-6]	65.4	9.48	528	76.6	9.31
Standard Deviation [1-3,5-6]	3.0	0.43	48	7.0	0.9
[%]	4.6		9.1		9.4

*Specimen eliminated using Chauvenet's criterion; italicized values not included in average or standard deviation.
[+]Properties used to eliminate specimen.

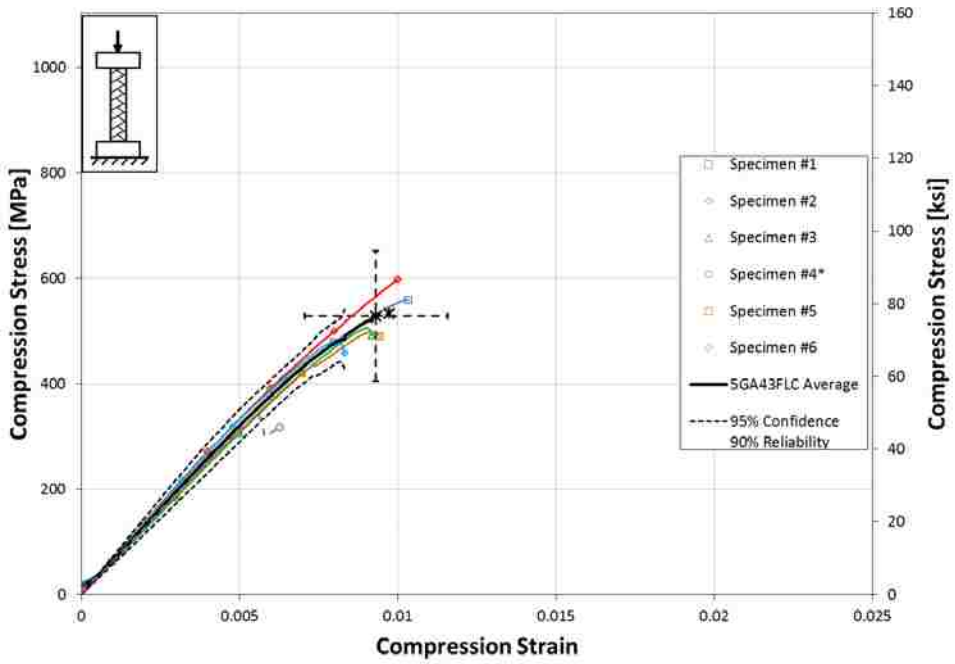

Figure 3.14: Stress-Strain Curves for Full Braid, 5 J (3.7 ft-lbs) Impact, Fiberglass Specimens (5GA43FLC)

Test results for full braid fiberglass specimens impacted with 10 J (7.4 ft-lbs) (5GA43FSC) are summarized in Table 3.15 and the stress-strain curves are shown in Figure 3.15. After the initial test of full braid fiberglass specimens impacted with 10 J (7.4 ft-lbs) (5GA43FSC), the ultimate compression strength and compression modulus of Specimen 3 were higher than the Chauvenet maximum. One more specimen was tested and after reapplying Chauvenet's criterion to all six specimens, the ultimate strength and modulus of Specimen 3 were still higher than the Chauvenet maximum and the stress-strain curve fell 84.9% outside Chauvenet's envelope (see Figure C.13). Specimen 3 was therefore eliminated and its properties are not included in the final test results.

Table 3.15: Properties of Full Braid, 10 J (7.4 ft-lbs) Impact, Fiberglass Specimens (5GA43FSC)

Full Braided Sleeve Impacted at 10 J (7.4 ft-lbs)	Compression Young's Modulus		Ultimate Compression Strength		Compression Strain at Ultimate Strength
	[GPa	(10^6 psi)]	[MPa	(ksi)]	[10^3 με]
1	60.7	8.80	301	43.7	5.85
2	62.9	9.13	335	48.6	6.31
3*	*70.5*	*10.23*	*599*	*86.9*[+]	*9.98*
4	61.2	8.88	380	55.1	6.70
5	59.9	8.69	395	57.3	7.24
6	57.0	8.26	283	41.1	6.32
Average [1-5]	63.1	9.15	402	58.3	7.21
Standard Deviation [1-5]	4.3	0.63	116	16.9	1.63
[%]	6.9		29		23
Average [1-2,4-6]	60.3	8.75	339	49.2	6.48
Standard Deviation [1-2,4-6]	2.2	0.32	48	7.0	0.5
[%]	3.6		14		8.0

*Specimen eliminated using Chauvenet's criterion; italicized values not included in average or standard deviation.
[+]Property used to eliminate specimen.

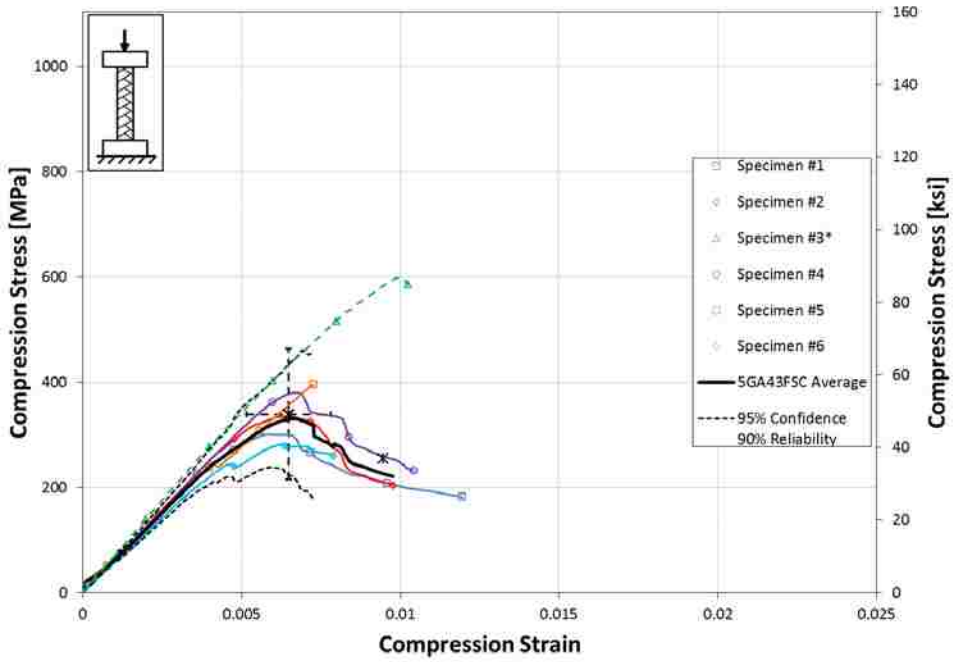

Figure 3.15: Stress-Strain Curves for Full Braid, 10 J (7.4 ft-lbs) Impact, Fiberglass Specimens (5GA43FSC)

3.1.6 Half Braid Fiberglass Specimens

Test results for undamaged half braid fiberglass specimens (5GA43HNC) are summarized in Table 3.16 and the stress-strain curves are shown in Figure 3.16.

Test results for half braid fiberglass specimens impacted with 5 J (3.7 ft-lbs) (5GA43HLC) are summarized in Table 3.17 and the stress-strain curves are shown in Figure 3.17. After the initial test of half braid fiberglass specimens impacted with 5 J (3.7 ft-lbs) (5GA43HLC), the compression modulus of Specimen 4 was lower than the Chauvenet minimum. One more specimen was tested and after reapplying Chauvenet's criterion to all six specimens, the modulus was still lower than the Chauvenet minimum and the stress-strain curve fell 57.1% outside Chauvenet's envelope (see Figure C.15). Specimen 4 was therefore eliminated and its properties are not included in the final test results.

Test results for half braid fiberglass specimens impacted with 10 J impact (5GA43HSC) are summarized in Table 3.18 and the stress-strain curves are shown in Figure 3.18.

Table 3.16: Properties of Half Braid, Undamaged, Fiberglass Specimens (5GA43HNC)

Half Braided Sleeve at No Impact	Compression Young's Modulus		Ultimate Compression Strength		Compression Strain at Ultimate Strength
	[GPa	(10^6 psi)]	[MPa	(ksi)]	[10^3 με]
1	63.3	9.18	827	119.9	14.46
2	55.5	8.05	968	140.4	16.79
3	56.1	8.13	953	138.2	17.16
4	56.3	8.17	993	144.0	17.02
5	61.1	8.86	831	120.5	14.35
Average [1-5]	58.5	8.48	914	132.6	15.96
Standard Deviation [1-5]	3.5	0.51	79	11.5	1.3
[%]	6.0		8.7		8.0

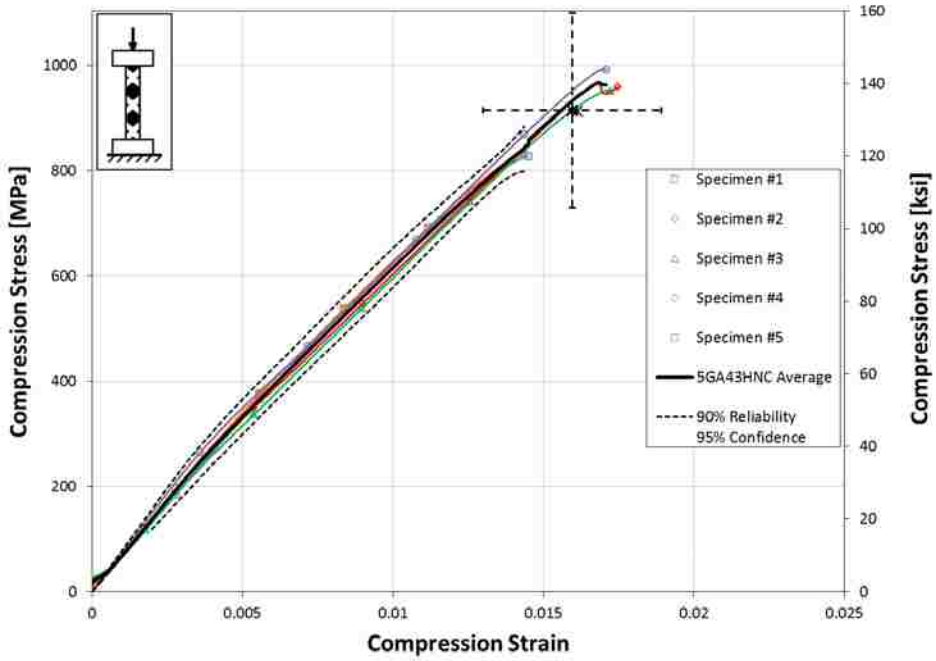

Figure 3.16: Stress-Strain Curves for Half Braid, Undamaged, Fiberglass Specimens (5GA43HNC)

Table 3.17: Properties of Half Braid, 5 J (3.7 ft-lbs) Impact, Fiberglass Specimens (5GA43HLC)

Half Braided Sleeve Impacted at 5 J (3.7 ft-lbs)	Compression Young's Modulus		Ultimate Compression Strength		Compression Strain at Ultimate Strength
	[GPa	(10^6 psi)]	[MPa	(ksi)]	[10^3 με]
1	75.5	10.95	693	100.5	11.38
2	72.8	10.56	589	85.5	10.74
3	70.5	10.22	457	66.2	9.07
4*	*63.7*	*9.24+*	*458*	*66.5*	*9.15*
5	74.2	10.76	488	70.8	9.50
6	77.0	11.17	565	81.9	9.91
Average [1-5]	71.3	10.35	537	77.9	9.97
Standard Deviation [1-5]	4.6	0.67	102	14.9	1.03
[%]	6.5		19		10
Average [1-3,5,6]	74.0	10.73	558	81.0	10.12
Standard Deviation [1-3,5,6]	2.5	0.36	93	13.4	0.9
[%]	3.4		17		9.2

*Specimen eliminated using Chauvenet's criterion; italicized values not included in average or standard deviation.
+Property used to eliminate specimen.

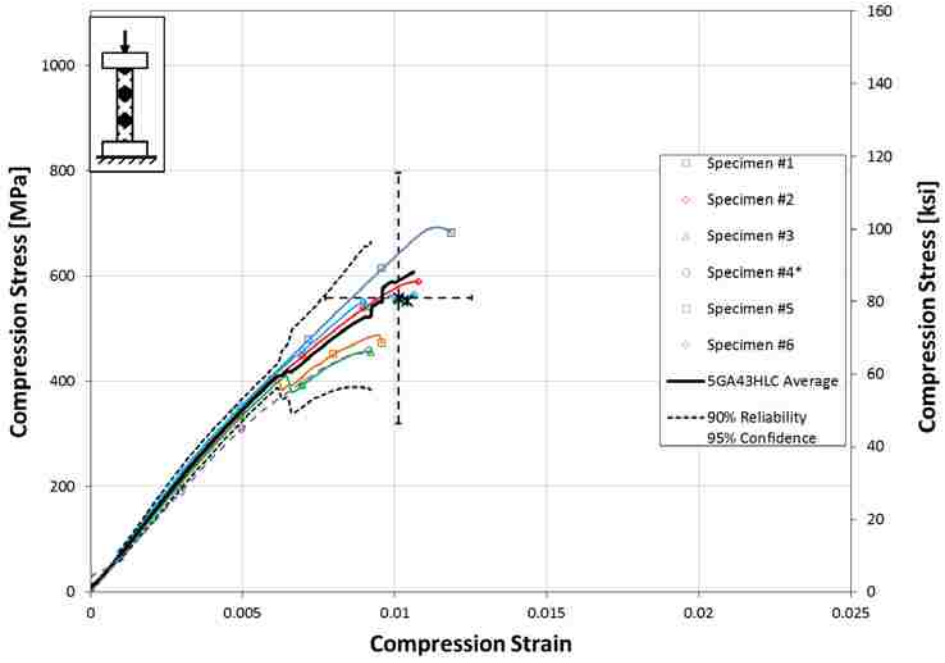

Figure 3.17: Stress-Strain Curves for Half Braid, 5 J (3.7 ft-lbs) Impact, Fiberglass Specimens (5GA43HLC)

Table 3.18: Properties of Half Braid, 10 J (7.4 ft-lbs) Impact, Fiberglass Specimens (5GA43HSC)

Half Braided Sleeve Impacted at 10 J (7.4 ft-lbs)	Compression Young's Modulus		Ultimate Compression Strength		Compression Strain at Ultimate Strength
	[GPa	(10^6 psi)]	[MPa	(ksi)]	[10^3 με]
1	62.6	9.08	289	41.9	5.80
2	64.5	9.36	321	46.5	6.26
3	68.6	9.95	342	49.6	6.17
4	69.5	10.08	286	41.4	5.66
5	67.5	9.80	369	53.5	8.60$^+$
Average [1-5]	66.6	9.65	321	46.6	6.50
Standard Deviation [1-5]	2.9	0.42	35	5.1	1.20
[%]	4.3		11		18

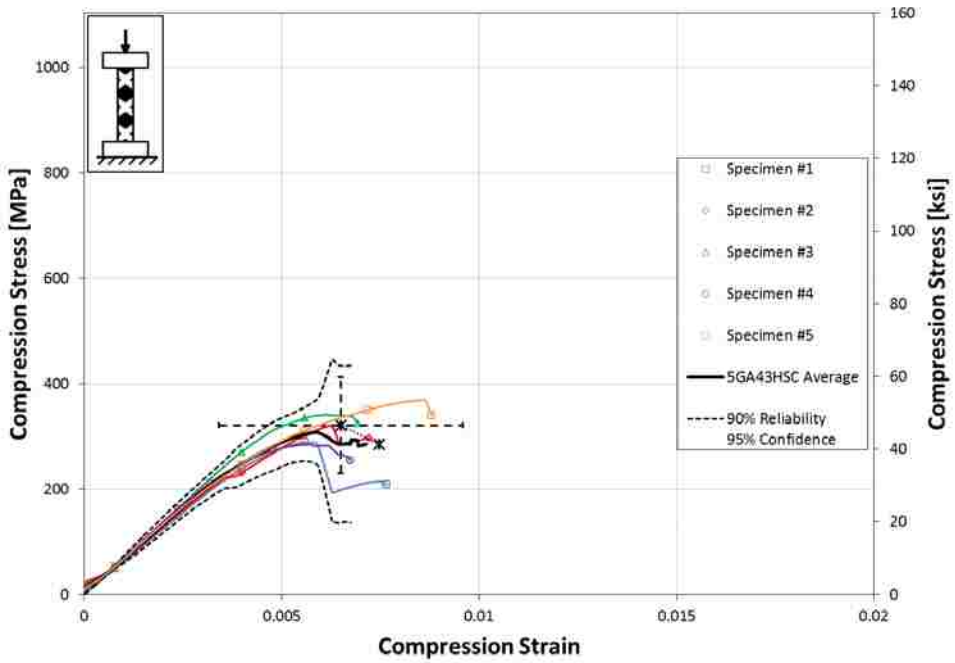

Figure 3.18: Stress-Strain Curves for Half Braid, 10 J (7.4 ft-lbs) Impact, Fiberglass Specimens (5GA43HSC)

3.1.7 Full Spiral Fiberglass Specimens

Test results for undamaged full spiral fiberglass specimens (5GA10FNC) are summarized in Table 3.19 and the stress-strain curves are shown in Figure 3.19.

Test results for full spiral fiberglass specimens at 5 J (3.7 ft-lbs) (5GA10FLC) of impact, are summarized in Table 3.20 and the stress-strain curves are shown in Figure 3.20.

Test results for full spiral fiberglass specimens impacted with 10 J (7.4 ft-lbs) (5GA10FSC) are summarized in Table 3.21 and the stress-strain curves are shown in Figure 3.21. After the initial test of full spiral fiberglass specimens impacted with 10 J (7.4 ft-lbs) (5GA10FSC), the compression stiffness of Specimen 2 was lower than the Chauvenet minimum. One more specimen was tested and after reapplying Chauvenet's criterion to all six specimens, the modulus was still lower than the Chauvenet minimum and the stress-strain curve fell 59.6% outside Chauvenet's envelope (see Figure C.19). Specimen 2 was therefore eliminated and its properties are not included in the final test results.

Table 3.19: Properties of Full Spiral, Undamaged, Fiberglass Specimens (5GA10FNC)

Full Spiral Sleeve Impacted at 5 J (3.7 ft-lbs)	Compression Young's Modulus		Ultimate Compression Strength		Compression Strain at Ultimate Strength
	[GPa	(10^6 psi)]	[MPa	(ksi)]	[10^3 με]
1	56.8	8.24	903	131.0	16.60
2	57.0	8.27	975	141.4	17.57
3	57.5	8.34	977	141.7	17.43
4	56.7	8.23	964	139.8	17.71
5	56.8	8.23	943	136.8	16.95
Average	57.0	8.26	952	138.1	17.25
Standard Deviation	0.3	0.05	31	4.4	0.46
[%]		0.6		3.2	2.7

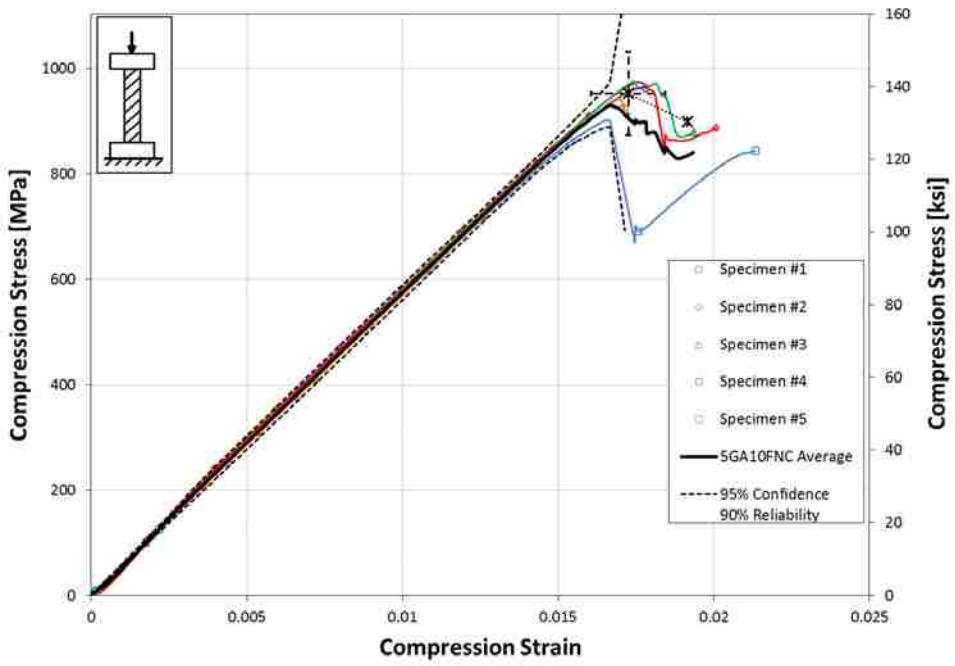

Figure 3.19: Stress-Strain Curves for Full Spiral, Undamaged, Fiberglass Specimens (5GA10FNC)

Table 3.20: Properties of Full Spiral, 5 J (3.7 ft-lbs) Impact, Fiberglass Specimens (5GA10FLC)

Full Spiral Sleeve Impacted at 5 J (3.7 ft-lbs)	Compression Young's Modulus		Ultimate Compression Strength		Compression Strain at Ultimate Strength
	[GPa	(10^6 psi)]	[MPa	(ksi)]	[10^3 με]
1	58.5	8.48	671	97.3	12.44
2	60.5	8.77	310	45.0	5.21
3	63.9	9.27	686	99.5	12.33
4	64.7	9.39	584	84.6	9.58
5	62.2	9.02	471	68.3	8.17
Average	62.0	8.99	544	79.0	9.55
Standard Deviation	2.5	0.37	156	22.7	3.04
[%]	4.1		28.7		31.8

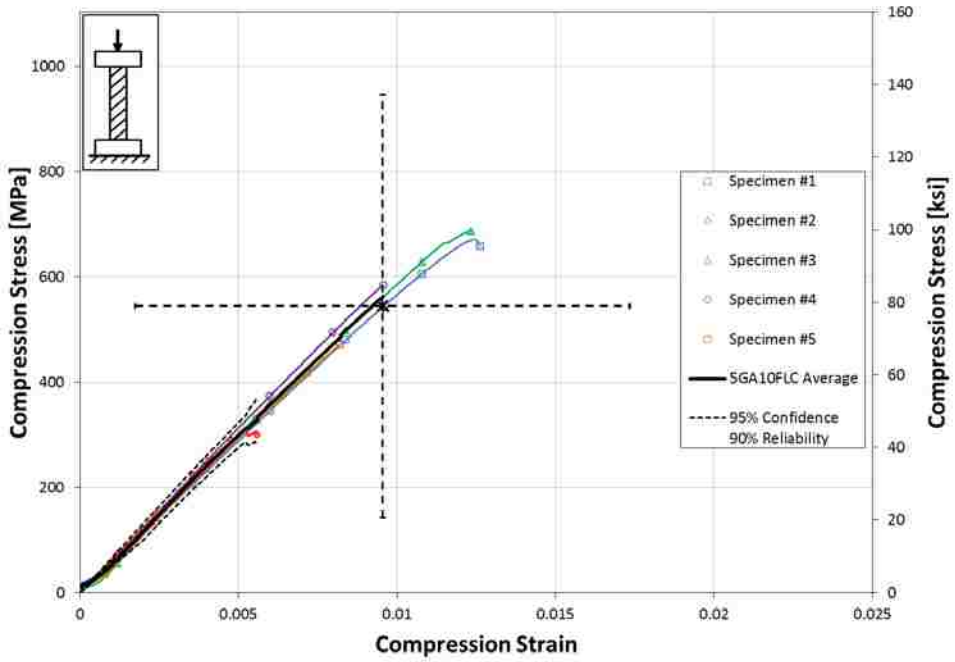

Figure 3.20: Stress-Strain Curves for Full Spiral, 5 J (3.7 ft-lbs) Impact, Fiberglass Specimens (5GA10FLC)

Table 3.21: Properties of Full Spiral, 10 J (7.4 ft-lbs) Impact, Fiberglass Specimens (5GA10FSC)

Full Spiral Sleeve Impacted at 10 J (7.4 ft-lbs)	Compression Young's Modulus		Ultimate Compression Strength		Compression Strain at Ultimate Strength
	[GPa	(10^6 psi)]	[MPa	(ksi)]	[10^3 με]
1	64.2	9.31	354	51.3	6.04
2*	*39.0*	*5.66+*	*156*	*22.6+*	*13.51+*
3	59.5	8.63	198	28.7	4.41
4	67.9	9.85	433	62.7	7.05
5	53.5	7.77	213	30.9	5.06
6	61.6	8.93	273	39.6	5.38
Average [1-5]	56.8	8.24	271	39.3	7.21
Standard Deviation [1-5]	11.3	1.64	117	17.0	3.66
[%]	20		43		51
Average [1,3-6]	61.3	8.90	294	42.7	5.59
Standard Deviation [1,3-6]	5.4	0.78	99	14.3	1.0
[%]	8.8		34		18

*Specimen eliminated using Chauvenet's criterion; italicized values not included in average or standard deviation.
+Property used to eliminate specimen.

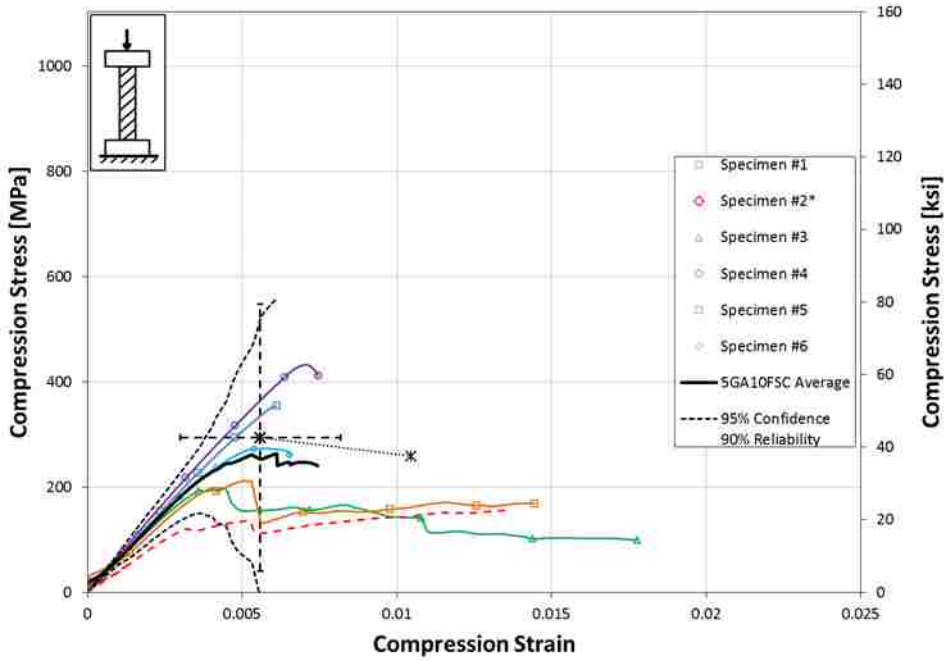

Figure 3.21: Stress-Strain Curves for Full Spiral, 10 J (7.4 ft-lbs) Impact, Fiberglass Specimens (5GA10FSC)

3.1.8 Half Spiral Fiberglass Specimens

Test results for undamaged half spiral fiberglass specimens (5GA10HNC) are summarized in Table 3.22 and the stress-strain curves are shown in Figure 3.22.

Test results for half spiral fiberglass specimens impacted with 5 J (3.7 ft-lbs) (5GA10HLC) are summarized in Table 3.23 and the stress-strain curves are shown in Figure 3.23. After the initial test of half spiral fiberglass specimens impacted with 5 J (3.7 ft-lbs) (5GA10HLC), the ultimate compression strength of Specimen 2 was higher than the Chauvenet's maximum. A sixth specimen was tested and after reapplying the Chauvenet's criterion to all six specimens, the ultimate compression strength of Specimen 2 was still higher than Chauvenet's maximum (see Figure C.21). Specimen 2 was therefore excluded from the final data results.

Test results for half spiral fiberglass specimens at 10 J (7.4 ft-lbs) (5GA10HSC) of impact, are summarized in Table 3.24 and the stress-strain curves are shown in Figure 3.24.

Table 3.22: Properties of Half Spiral, Undamaged, Fiberglass Specimens (5GA10HNC)

Full Spiral Sleeve Impacted at 0 J (3.7 ft-lbs)	Compression Young's Modulus		Ultimate Compression Strength		Compression Strain at Ultimate Strength
	[GPa	(10^6 psi)]	[MPa	(ksi)]	[10^3 με]
1	55.2	8.01	913	132.4	16.25
2	59.2	8.59	902	130.9	15.70
3	56.9	8.25	942	136.6	17.39
4	57.7	8.37	958	138.9	17.29
5	54.2	7.86	928	134.6	17.01
Average	56.7	8.22	929	134.7	16.73
Standard Deviation	2.0	0.29	22	3.2	0.73
[%]	3.5		2.4		4.3

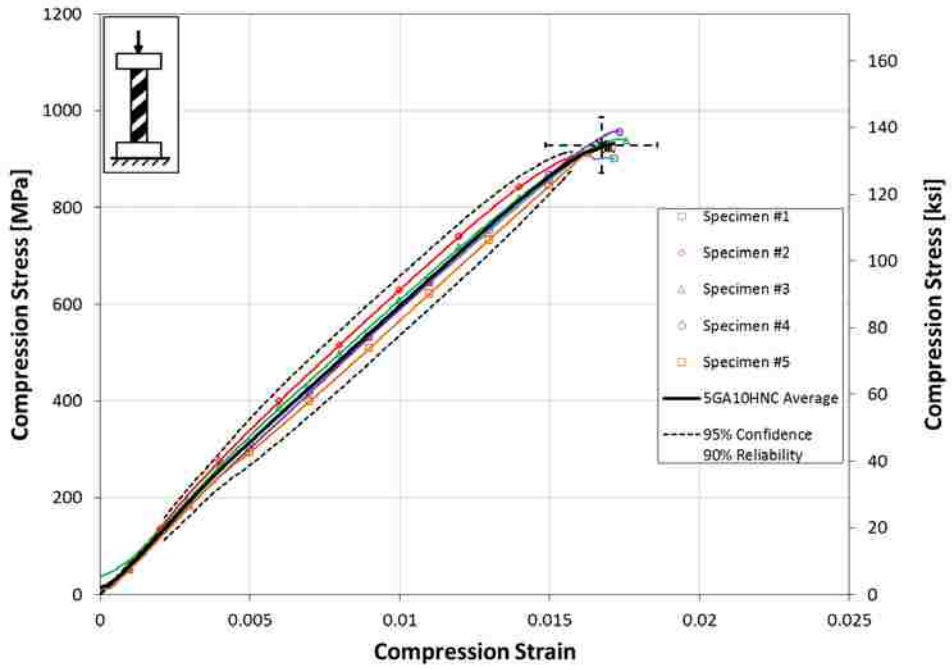

Figure 3.22: Stress-Strain Curves for Half Spiral, Undamaged, Fiberglass Specimens (5GA10HNC)

Table 3.23: Properties of Half Spiral, 5 J (3.7 ft-lbs) Impact, Fiberglass Specimens (5GA10HLC)

Half Spiral Sleeve Impacted at 5 J (3.7 ft-lbs)	Compression Young's Modulus		Ultimate Compression Strength		Compression Strain at Ultimate Strength
	[GPa	(10^6 psi)]	[MPa	(ksi)]	[10^3 με]
1	69.9	10.13	364	52.8	5.47
2*	*62.8*	*9.11*	*667*	*96.7+*	*11.82*
3	64.9	9.42	465	67.5	9.19
4	61.6	8.93	230	33.3	4.19
5	68.8	9.97	377	54.7	7.92
6	60.7	8.81	308	44.7	5.58
Average [1-5]	65.6	9.51	421	61.0	7.72
Standard Deviation [1-5]	3.6	0.53	161	23.4	3.02
[%]	5.5		38		39
Average [1,3-6]	65.2	9.45	349	50.6	6.47
Standard Deviation [1,3-6]	4.1	0.60	87	12.6	2.0
[%]	6.3		25		31

*Specimen eliminated using Chauvenet's criterion; italicized values not included in average or standard deviation.
+Property used to eliminate specimen.

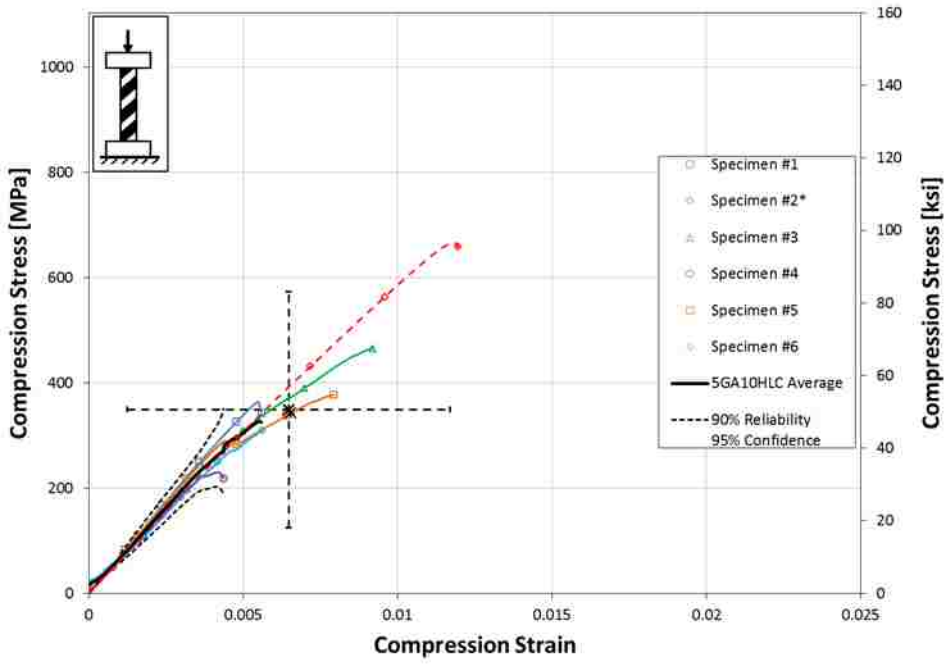

Figure 3.23: Stress-Strain Curves for Half Spiral, 5 J (3.7 ft-lbs) Impact, Fiberglass Specimens (5GA10HLC)

Table 3.24: Properties of Half Spiral, 10 J (7.4 ft-lbs) Impact, Fiberglass Specimens (5GA10HSC)

Half Spiral Sleeve Impacted at 10 J (7.4 ft-lbs)	Compression Young's Modulus		Ultimate Compression Strength		Compression Strain at Ultimate Strength
	[GPa	(10^6 psi)]	[MPa	(ksi)]	[10^3 με]
1	67.1	9.73	253	36.6	4.51
2	62.5	9.06	295	42.7	7.48
3	55.2	8.01	212	30.7	6.52
4	69.0	10.00	333	48.4	6.43
5	53.8	7.81	174	25.2	3.90
Average [1-5]	61.5	8.92	253	36.7	5.77
Standard Deviation [1-5]	6.8	0.99	64	9.2	1.50
[%]	11		25		26

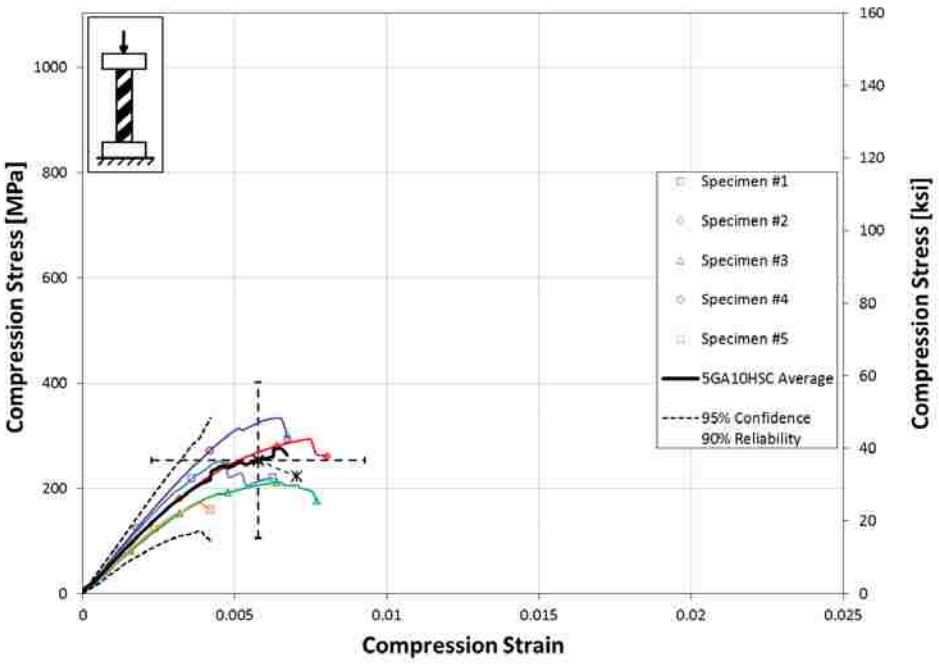

Figure 3.24: Stress-Strain Curves for Half Spiral, 10 J (7.4 ft-lbs) Impact, Fiberglass Specimens (5GA10HSC)

4 CONFIGURATION AVERAGES FOR CARBON/EPOXY COMPOSITES

This chapter presents the average stress-strain curves, the compression Young's modulus, compression strain at ultimate strength, and ultimate compression strength for carbon/epoxy configuration test results. Carbon/epoxy averages are summarized by configuration, impact energy level, sleeve type, and sleeve coverage. Figure 4.1 shows the average stress-strain curves for the twelve carbon/epoxy configurations (four sleeve types at each impact energy levels). Carbon/epoxy configurations exhibited a significant degradation in stiffness and strength due to impact damage. These observations are more closely examined in subsequent sections.

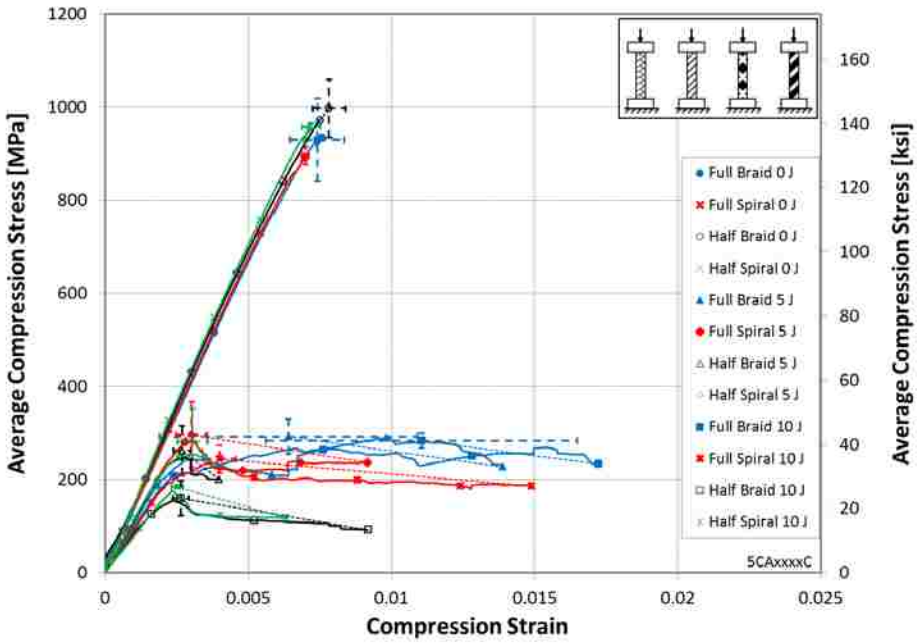

Figure 4.1: Average Stress-Strain Curves of All Twelve Carbon Configurations

4.1 Compression Young's Modulus

A summary of the average compression Young's modulus results for carbon/epoxy configurations is presented in Table 4.1. At no impact energy, there are insignificant variations in the stiffness among all four undamaged configurations, as illustrated 6% average variation in standard deviation. At 5 and 10 J (3.7 and 7.4 ft-lbs) of impact, however, compression modulus yielded slightly more variations, as shown by an average of 13% and 20% in standard deviation, respectively. Not surprisingly, the compression Young's modulus decreases with increasing impact energy; 22% and 38% reduction in stiffness relative to undamaged for the 5 and 10 J (3.7 and 7.4 ft-lbs) of impact energy.

Table 4.1: Compression Young's Modulus of Carbon Configurations

Configuration & Impact Energy		Compression Young's Modulus			Modulus Relative to Undamaged [%]
		Average	Standard Deviation		
		[GPa (10^6 psi)]	[GPa (10^6 psi)]	[%]	
Full Braid	Undamaged	135 (19.6)	10.5 (1.52)	8	--
	5 J (3.7 ft-lbs)	105 (15.3)	13.5 (1.96)	13	-22
	10 J (7.4 ft-lbs)	89.5 (13.0)	20.4 (2.96)	23	-34
Half Braid	Undamaged	142 (20.7)	7.44 (1.08)	5	--
	5 J (3.7 ft-lbs)	110 (15.9)	7.80 (1.13)	7	-23
	10 J (7.4 ft-lbs)	87.0 (12.6)	27.3 (3.96)	31	-39
Full Spiral	Undamaged	138 (20.0)	1.45 (0.21)	1	--
	5 J (3.7 ft-lbs)	111 (16.1)	15.3 (2.22)	14	-20
	10 J (7.4 ft-lbs)	92.7 (13.4)	18.9 (2.75)	20	-33
Half Spiral	Undamaged	147 (21.3)	13.8 (1.99)	9	--
	5 J (3.7 ft-lbs)	112 (16.3)	18.5 (2.68)	16	-24
	10 J (7.4 ft-lbs)	76.8 (11.1)	5.04 (0.73)	7	-48
All Configurations	Undamaged	140.5 (20.4)	8.30 (1.20)	6	--
	5 J (3.7 ft-lbs)	109.5 (15.9)	13.8 (2.01)	13	-22
	10 J (7.4 ft-lbs)	86.5 (12.5)	17.9 (2.60)	20	-38

4.2 Compression Strain at Ultimate Strength

A summary of the average compression strain at ultimate strength results for carbon/epoxy configurations is shown in Table 4.2. At no impact, there is virtually no difference in strain at ultimate strength among the four different undamaged sleeve configurations, as shown by less than 6% average in standard deviation. At both 5 and 10 J (3.7 and 7.4 ft-lbs) of impact energy, however, strain at ultimate strength yielded 25% and 19% average variations in standard deviation among all sleeve configurations, respectively.

Table 4.2: Compression Strain at Ultimate Strength of Carbon Configurations

Specimen Configuration & Impact Energy		Compression Strain at Max Stress		
		Average Max [10^3 με]	Standard Deviation	
			[10^3 με]	[%]
Full Braid	**0 J**	7.4	0.95	13
	5 J	6.4	4.49	70
	10 J	11	4.86	44
Half Braid	**0 J**	7.8	0.58	7
	5 J	2.7	0.31	11
	10 J	2.6	0.29	11
Full Spiral	**0 J**	7.0	0.10	1
	5 J	3.0	0.16	5
	10 J	4.0	0.57	14
Half Spiral	**0 J**	7.2	0.32	4
	5 J	3.1	0.53	17
	10 J	2.5	0.19	7

4.3 Ultimate Compression Strength

Average ultimate compression strength results for carbon/epoxy configurations are summarized in Table 4.3. Again, at no impact, there is virtually no variation in ultimate compression strength among all four sleeve configurations, as shown by 6% average in standard

deviation. At 5 and 10 J (3.7 and 7.4 ft-lbs) of impact, however, ultimate compression strength yielded slightly more variations, as shown by an average of 18% and 11% in standard deviation, respectively. The average ultimate compression strength of all undamaged carbon/epoxy configurations is 945 MPa (137.1 ksi) with a standard deviation of 59.7 MPa (8.7 ksi). The results for 5 and 10 J (3.7 and 7.4 ft-lbs) of impact energy exhibited significant effect on the ultimate compression strength among all sleeve configurations. Carbon configurations yielded 71% and 77% average reduction in ultimate strength relative to undamaged specimens for specimens with 5 and 10 J (3.7 and 7.4 ft-lbs) of impact energy, respectively.

Table 4.3: Ultimate Compression Strength of Carbon Configurations

Configuration & Impact Energy		Ultimate Compression Strength			Ultimate Strength Relative to Undamaged
		Average	Standard Deviation		
		[MPa (ksi)]	[MPa (ksi)]	[%]	[%]
Full Braid	Undamaged	930 (135)	89.6 (13)	10	--
	5 J (3.7 ft-lbs)	293 (42.5)	37.4 (5.4)	13	-68
	10 J (7.4 ft-lbs)	292 (42.3)	24.9 (3.6)	9	-67
Half Braid	Undamaged	997 (145)	63.0 (9.1)	6	--
	5 J (3.7 ft-lbs)	262 (38.0)	52.9 (7.7)	20	-74
	10 J (7.4 ft-lbs)	160 (23.2)	37.1 (5.4)	23	-84
Full Spiral	Undamaged	896 (130)	19.5 (2.8)	2	--
	5 J (3.7 ft-lbs)	296 (43.0)	37.7 (5.5)	13	-67
	10 J (7.4 ft-lbs)	244 (35.4)	29.7 (4.3)	12	-73
Half Spiral	Undamaged	958 (139)	66.8 (10)	7	--
	5 J (3.7 ft-lbs)	282 (40.9)	70.7 (10)	25	-71
	10 J (7.4 ft-lbs)	184 (26.7)	2.3 (0.3)	1	-81
All Configurations	Undamaged	945 (137.2)	59.7 (8.66)	6	--
	5 J (3.7 ft-lbs)	283 (41.1)	49.7 (7.21)	18	-71
	10 J (7.4 ft-lbs)	220 (31.9)	23.5 (3.41)	11	-77

4.4 Configuration Stress-Strain Curves

Stress-strain curves for carbon/epoxy full braid, half braid, full spiral, and half spiral configurations are shown in Figure 4.2, Figure 4.3, Figure 4.4, and Figure 4.5, respectively. Not surprisingly, compression modulus and ultimate compression strength decrease with increasing impact energy for each configuration. At each of the four sleeve configuration, there was an approximate 70% decrease in strength when impacted with 5 J (3.7 ft-lbs) of energy. Full braid carbon/epoxy configuration showed relatively no difference in strength at either impact levels (5 J and 10 J).

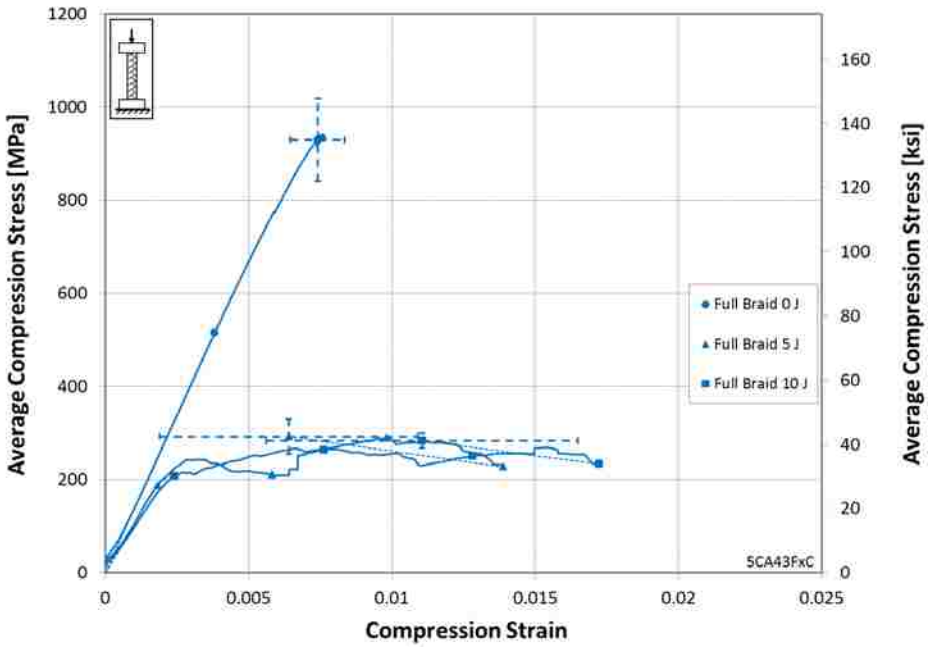

Figure 4.2: Average Stress-Strain Curves of Full Braid Carbon Configurations

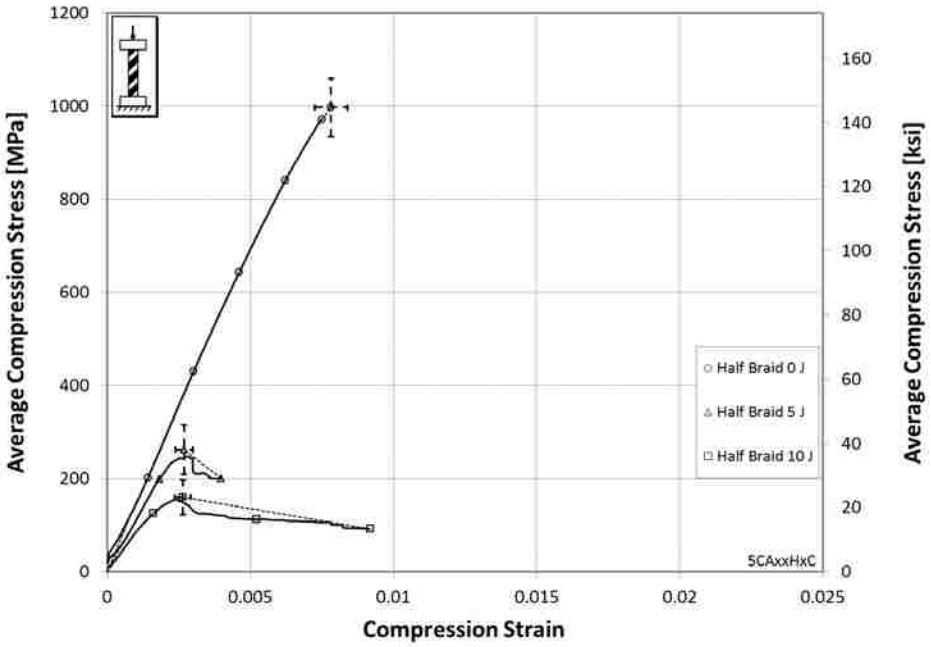

Figure 4.3: Average Stress-Strain Curves of Half Braid Carbon Configurations

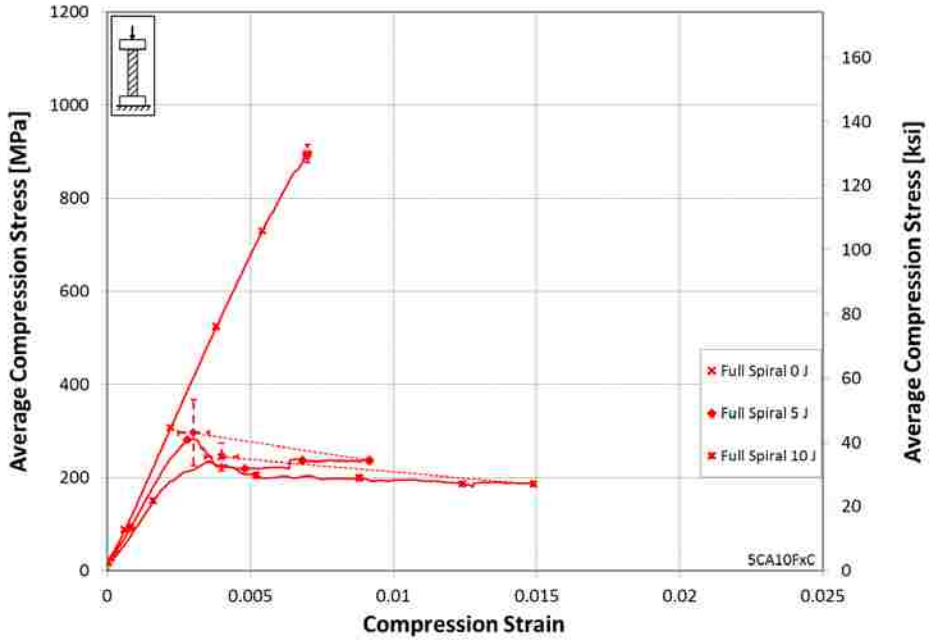

Figure 4.4: Average Stress-Strain Curves of Full Spiral Carbon Configurations

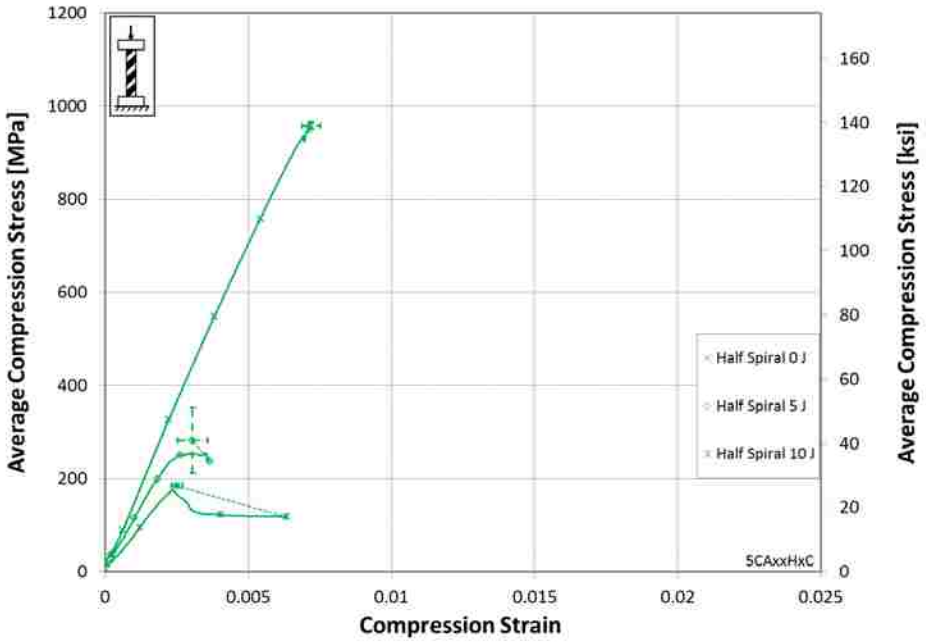

Figure 4.5: Average Stress-Strain Curves of Half Spiral Carbon Configurations

4.5 Influence of Impact Energy

A plot of the compression strength as a function of impact energy was prepared to illustrate the effect of impact energy on compression strength, as a function of sleeve type and coverage. Figure 4.6 compares trends of all sleeve configurations (full braid, full spiral, half braid, and half spiral) at each impact level (0 J, 5 J, 10 J). The dashed trend lines simply connect the averages of each sleeve configuration and should not be used for extrapolation. This plot shows that 5 J (3.7 ft-lbs) of impact energy significantly affects the ultimate strength of carbon/epoxy configurations and subsequently show an insignificant difference in strength when compared to specimens with 10 J (7.4 ft-lbs) of impact energy. More configurations would need to be tested with 1-4 J (0.7–3.0 ft-lbs) of impact energy to see if the carbon/epoxy configurations retain any compression strength after impact. Configurations impacted with 10 J (7.4 ft-lbs) of

energy show that the amount of coverage does matter; i.e., both full braided and full spiral sleeves have a higher strength than either of the half coverage sleeves.

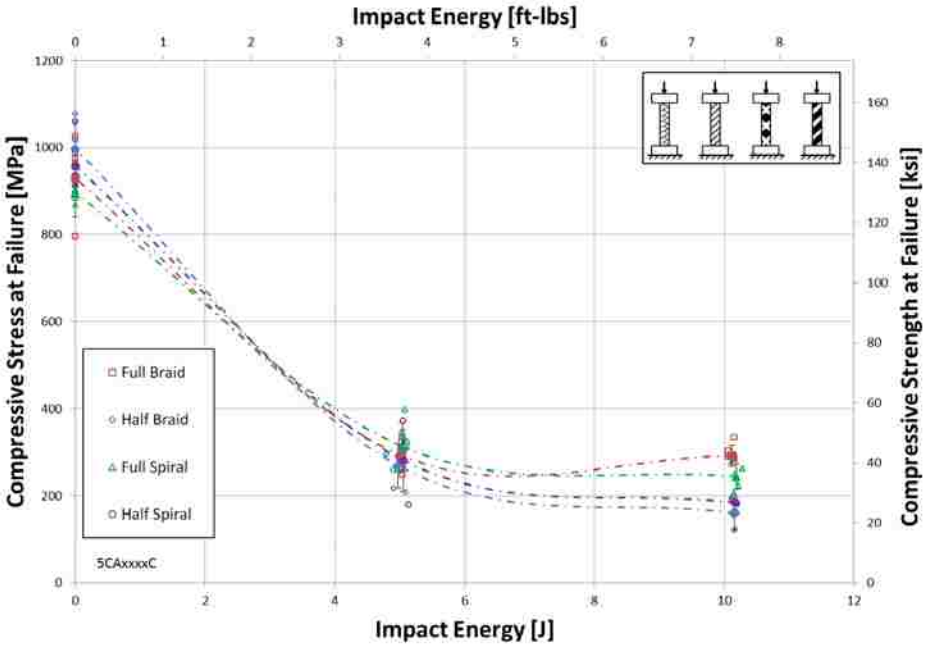

Figure 4.6: Compression Strength After Impact vs. Impact Energy for Carbon Configurations

4.6 Influence of Sleeve Type

To illustrate the effect of sleeve type (full braid vs. full spiral and half braid vs. half spiral) at each impact energy level, Figure 4.7 and Figure 4.8 were created to allow comparison of results for full coverage braided and spiral samples, and half coverage braided and spiral sleeves. For all undamaged configurations, there exhibits virtually no difference for modulus, strain at ultimate strength, or ultimate strength between sleeve types. For full coverage (braid vs. spiral), there isn't a clear distinction between the 5 and 10 J (3.7 and 7.4 ft-lbs) of impact energy. For half coverage (braid vs. spiral), however, there is more of a distinction between the impact

energy levels (5 and 10 J); interestingly, half braid and half spiral sleeves exhibited very similar behavior, and in fact almost identical as shown by Figure 4.8. The average stress-strain curves comparing full coverage braid vs. spiral and half coverage braid vs. spiral carbon/epoxy configurations are shown in Figure 4.7 and Figure 4.8, respectively.

4.7 Influence of Sleeve Coverage

Average stress-strain curves comparing full vs. half coverage braided sleeves for carbon/epoxy configurations are shown in Figure 4.9. Undamaged configurations exhibit virtually no difference between full and half coverage. With both 5 and 10 J (3.7 and 7.4 ft-lbs) of impact, however, full coverage specimens perform slightly better than half coverage.

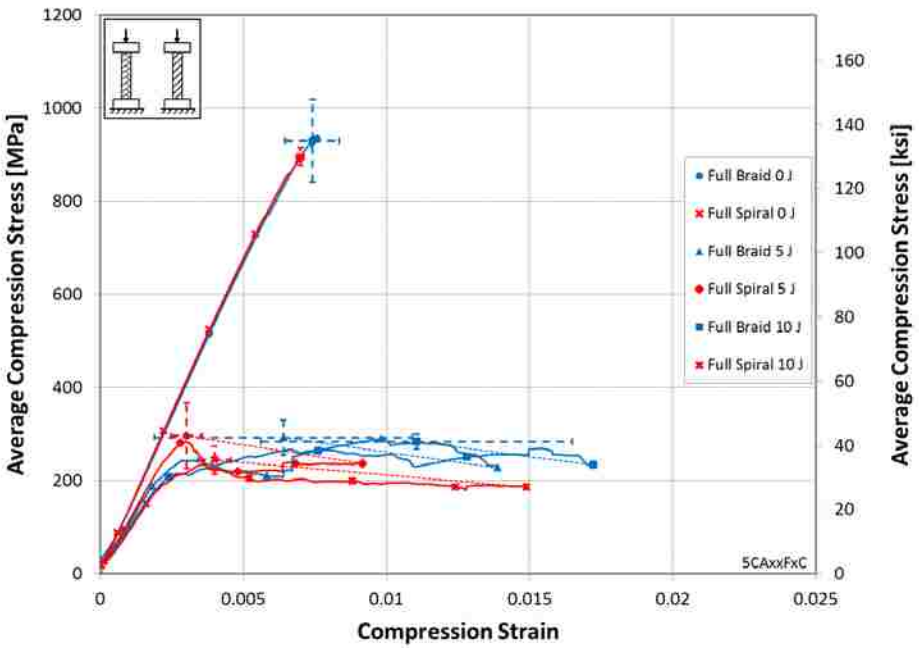

Figure 4.7: Average Stress-Strain Curves Comparing Full Coverage Braid vs. Spiral Carbon Configurations

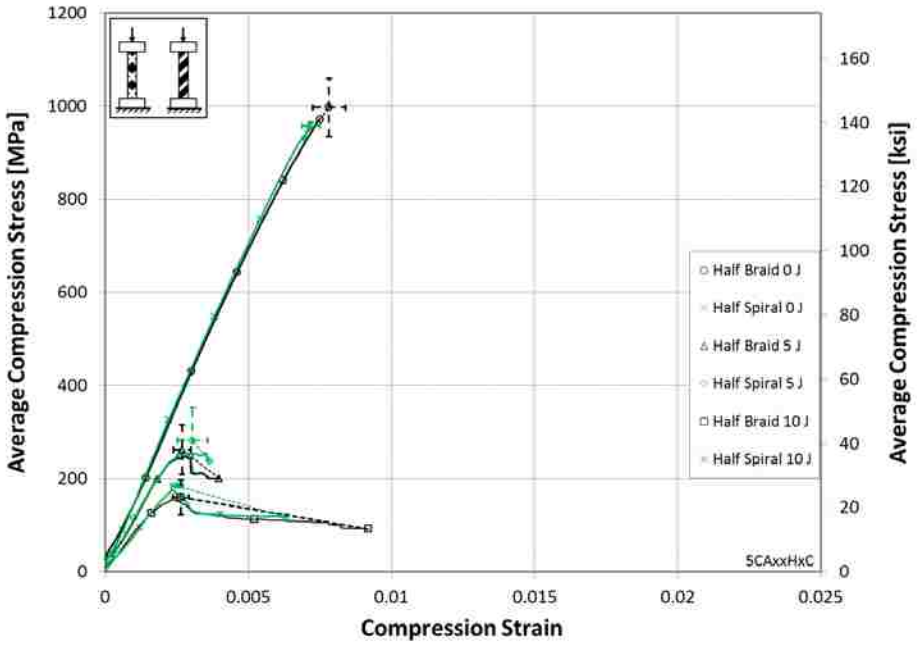

Figure 4.8: Average Stress-Strain Curves Comparing Half Coverage Braid vs. Spiral Carbon Configurations

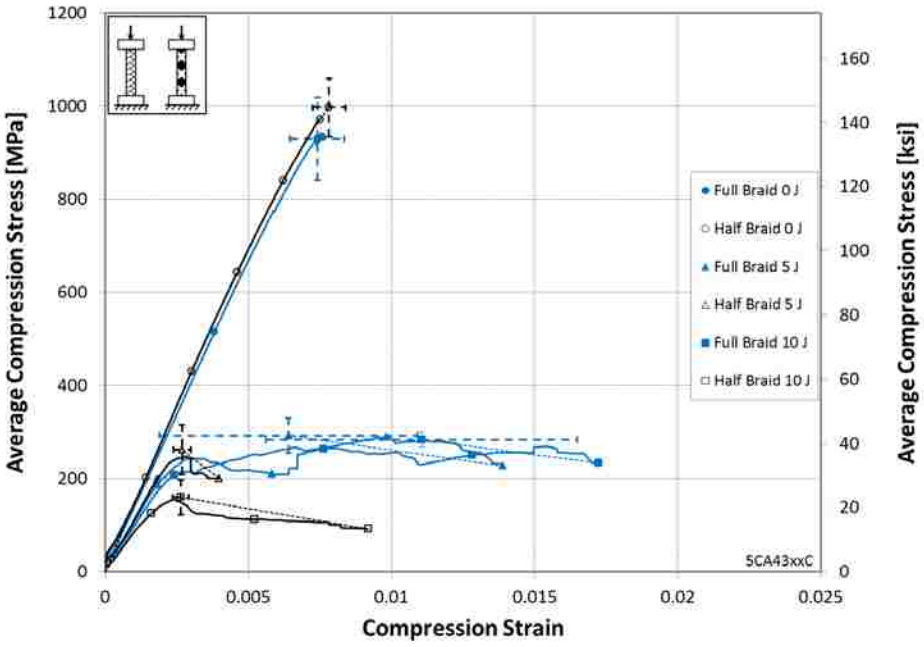

Figure 4.9: Average Stress-Strain Curves Comparing Full and Half Braid for Carbon Configurations

Average stress-strain curves comparing full vs. half coverage spiral sleeves for carbon/epoxy configurations are shown in Figure 4.10. Again, there is virtually no difference in modulus, strain at ultimate strength, or ultimate strength between full and half coverage for undamaged configurations. Similarly, at both 5 and 10 J (3.7 and 7.4 ft-lbs) of impact, full coverage performs better than half coverage sleeves.

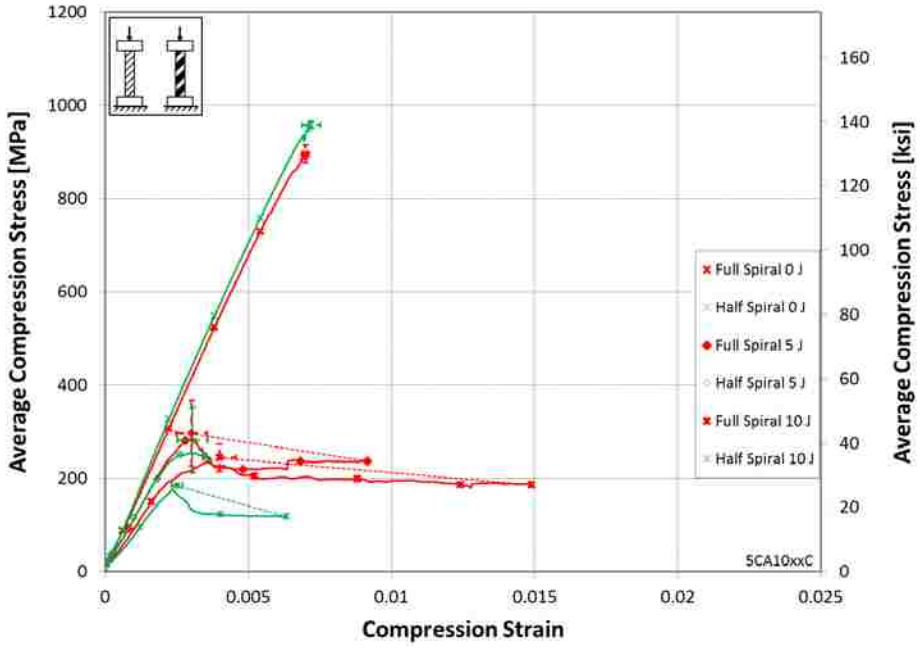

Figure 4.10: Average Stress-Strain Curves Comparing Full vs. Half Spiral for Carbon Configurations

5 CONFIGURATION AVERAGES FOR FIBERGLASS/EPOXY COMPOSITES

This chapter presents the average stress-strain curves, the compression Young's modulus, compression strain at ultimate strength, and ultimate compression strength for fiberglass/epoxy configuration test results. Fiberglass/epoxy averages are summarized by configuration, impact energy level, sleeve type, and sleeve coverage. Figure 5.1 shows the average stress-strain curves for the twelve fiberglass/epoxy configurations (four sleeve types at each of the three impact energy levels). Unlike carbon/epoxy configurations, fiberglass/epoxy specimens exhibited a distinctive reduction in compression strength for all three levels of impact energy.

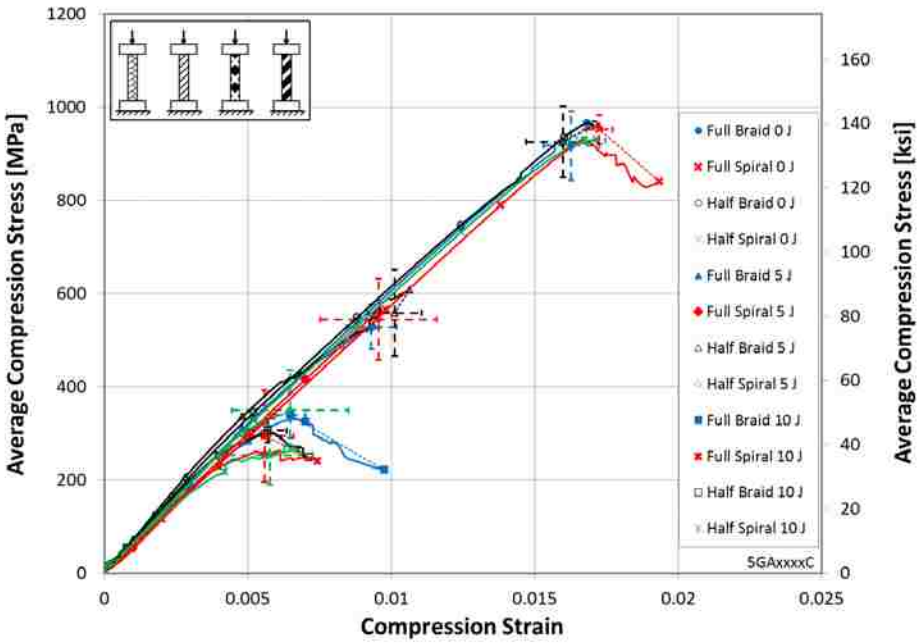

Figure 5.1: Average Stress-Strain Curves of All Twelve Fiberglass Configurations

5.1 Compression Young's Modulus

Average compression Young's modulus results for fiberglass configurations are summarized in Table 5.1. Variations of compression modulus for all configurations rest within the typical range, which is less than 10% variations for composites, except for the half spiral specimens with 10 J (7.4 ft-lbs) of impact, as shown by 19% variations. At 5 J (3.7 ft-lbs) of impact, the compression stiffness yielded 14% difference relative to undamaged specimens.

Table 5.1: Compression Young's Modulus of Fiberglass Configurations

Configuration & Impact Energy		Compression Young's Modulus					Modulus Relative to Undamaged
		Average		Standard Deviation			
		[GPa (10^6 psi)]		[GPa (10^6 psi)]		[%]	[%]
Full Braid	Undamaged	60.0	(8.70)	1.70	(0.25)	3	--
	5 J (3.7 ft-lbs)	65.4	(9.48)	2.98	(0.43)	5	9
	10 J (7.4 ft-lbs)	60.3	(8.75)	2.19	(0.32)	4	0
Half Braid	Undamaged	59.3	(8.59)	3.69	(0.54)	6	--
	5 J (3.7 ft-lbs)	74.0	(10.7)	2.51	(0.36)	3	25
	10 J (7.4 ft-lbs)	67.5	(9.79)	3.93	(0.57)	6	14
Full Spiral	Undamaged	57.0	(8.26)	0.31	(0.05)	1	--
	5 J (3.7 ft-lbs)	62.0	(8.99)	2.53	(0.37)	4	8
	10 J (7.4 ft-lbs)	61.3	(8.90)	5.38	(0.78)	9	7
Half Spiral	Undamaged	56.7	(8.22)	1.77	(0.26)	3	--
	5 J (3.7 ft-lbs)	65.2	(9.45)	4.12	(0.60)	6	15
	10 J (7.4 ft-lbs)	57.8	(8.38)	11.0	(1.60)	19	2
All Configurations	Undamaged	58.3	(8.44)	1.87	(0.28)	3	--
	5 J (3.7 ft-lbs)	66.7	(9.66)	3.04	(0.44)	5	14
	10 J (7.4 ft-lbs)	61.7	(8.96)	5.63	(0.82)	10	5

5.2 Compression Strain at Ultimate Strength

Average compression strain at ultimate strength results for fiberglass configurations are summarized in Table 5.2. As expected, the compression strain at maximum strength decreases with increasing impact energy for all configurations. At no impact, there is virtually no difference in strain at ultimate strength among the four different undamaged sleeve configurations. For spiral configurations, in particular, both 5 and 10 J (3.7 and 7.4 ft-lbs) of impact energy, exhibited more variation on strain at ultimate strength, demonstrated with 32% and 18%, and 31% and 18% variations, respectively.

Table 5.2: Compression Strain at Ultimate Strength of Fiberglass Configurations

Specimen Configuration & Impact Energy		Compression Strain at Max Stress		
		Average Max [10^3 με]	Standard Deviation	
			[10^3 με]	[%]
Full Braid	**0 J**	16.3	0.97	6
	5 J	9.31	0.88	9
	10 J	6.48	0.52	8
Half Braid	**0 J**	16.0	1.27	8
	5 J	10.1	0.93	9
	10 J	5.69	0.67	12
Full Spiral	**0 J**	17.3	0.46	3
	5 J	9.55	3.04	32
	10 J	5.59	1.01	18
Half Spiral	**0 J**	16.7	0.72	4
	5 J	6.47	2.03	31
	10 J	5.89	1.37	23

5.3 Ultimate Compression Strength

Average ultimate compression strength results for fiberglass configurations are summarized in Table 5.3. Again, at no impact energy, there is virtually no variation in ultimate

compression strength among all four sleeve configurations. The average ultimate compression strength of all undamaged carbon/epoxy configurations is 934 MPa (135.5 ksi) with a standard deviation of 53.8 MPa (7.8 ksi). The results for 5 and 10 J (3.7 and 7.4 ft-lbs) of impact energy exhibited significant effect on the ultimate strength among all sleeve configurations, as illustrated by 47% and 69% reduction in strength relative to undamaged configurations, respectively. All other configurations except for half spiral with 5 J (3.7 ft-lbs) of impact, achieved just a little over half the ultimate compression strength of their respective undamaged configurations, and logically much less for the specimens with 10 J of impact.

Table 5.3: Ultimate Compression Strength of Fiberglass Configurations

Configuration & Impact Energy		Ultimate Compression Strength			Ultimate Strength Relative to Undamaged
		Average	Standard Deviation		
		[MPa (ksi)]	[MPa (ksi)]	[%]	[%]
Full Braid	Undamaged	918 (133)	74.2 (10.8)	8	--
	5 J (3.7 ft-lbs)	528 (76.6)	48.3 (7.01)	9	-42
	10 J (7.4 ft-lbs)	339 (49.2)	48.4 (7.03)	14	-63
Half Braid	Undamaged	926 (134)	76.4 (11.1)	8	--
	5 J (3.7 ft-lbs)	558 (81.0)	92.6 (13.4)	17	-40
	10 J (7.4 ft-lbs)	306 (44.3)	24.7 (3.58)	8	-67
Full Spiral	Undamaged	952 (138)	30.7 (4.45)	3	--
	5 J (3.7 ft-lbs)	544 (79.0)	156 (22.7)	29	-43
	10 J (7.4 ft-lbs)	294 (42.7)	98.7 (14.3)	34	-69
Half Spiral	Undamaged	940 (136)	34.0 (4.93)	4	--
	5 J (3.7 ft-lbs)	349 (50.6)	87.1 (12.6)	25	-63
	10 J (7.4 ft-lbs)	238 (34.5)	68.4 (9.92)	29	-75
All Configurations	Undamaged	934 (136)	53.8 (7.81)	6	--
	5 J (3.7 ft-lbs)	495 (77.9)	96.0 (13.9)	20	-47
	10 J (7.4 ft-lbs)	294 (42.6)	60.1 (8.72)	21	-69

5.4 Configuration Stress-Strain Curves

Stress-strain curves for fiberglass full braid, half braid, full spiral, and half spiral configurations are shown in Figure 5.2, Figure 5.3, Figure 5.4, and Figure 5.5, respectively. Not surprisingly, compression modulus and ultimate compression strength decrease with increasing impact energy for each configuration. Half spiral coverage specimens yielded about 70% reduction in strength when impacted with 5 J (3.7 ft-lbs) of energy. At 10 J (7.4 ft-lbs) of impact energy, all configurations achieved an approximate of 30% in strength relative to undamaged specimens.

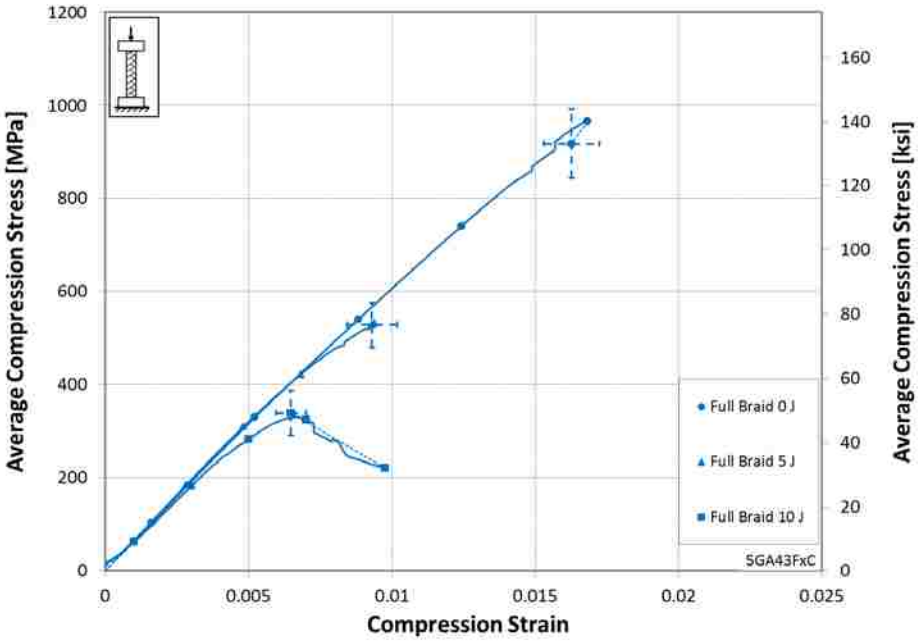

Figure 5.2: Average Stress-Strain Curves of Full Braid Fiberglass Configurations

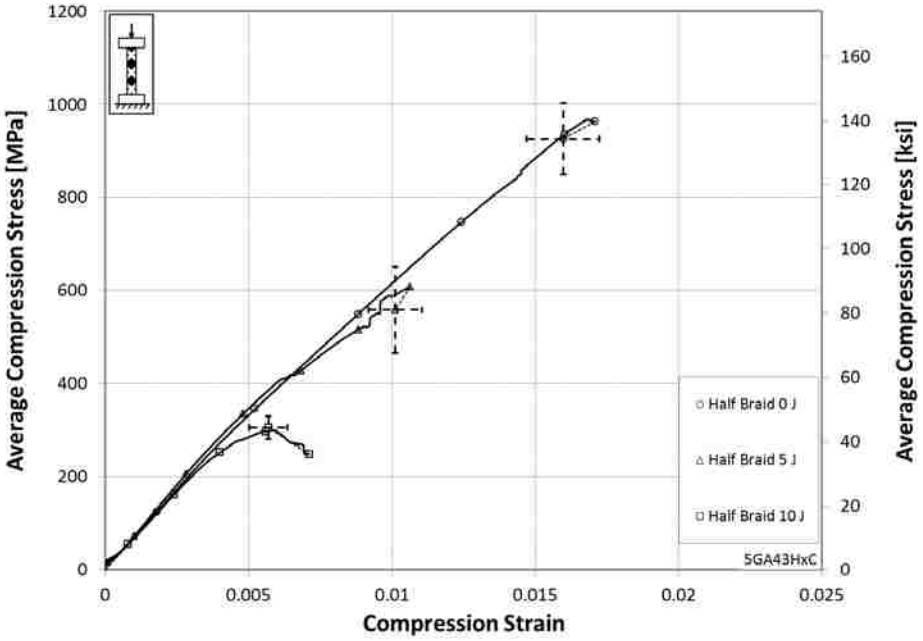

Figure 5.3: Average Stress-Strain Curves of Half Braid Fiberglass Configurations

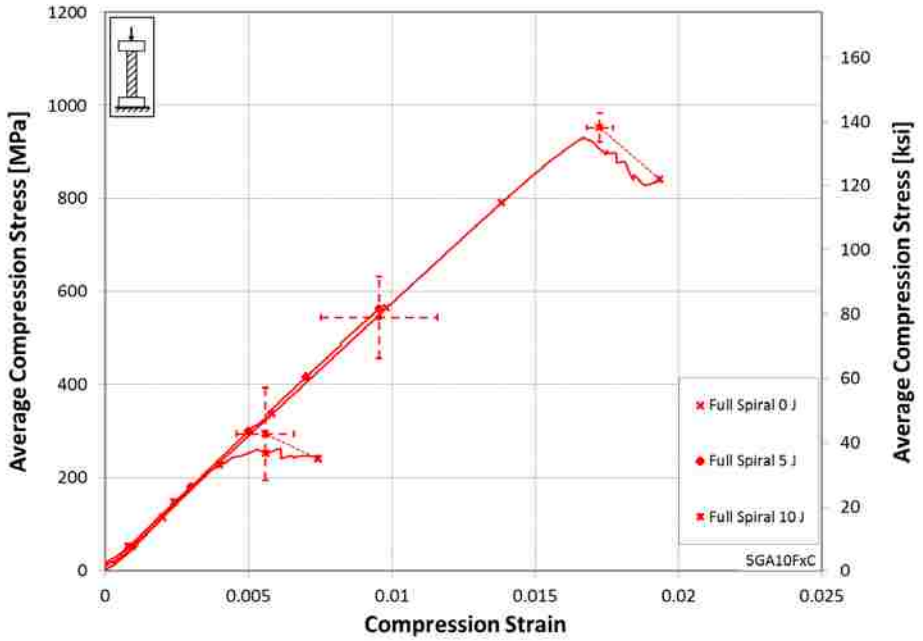

Figure 5.4: Average Stress-Strain Curves of Full Spiral Fiberglass Configurations

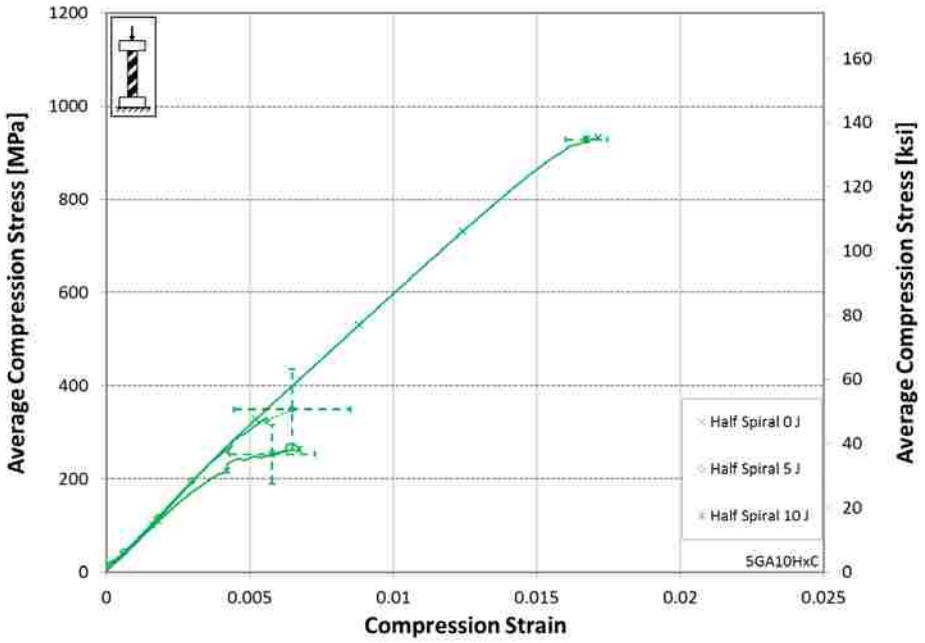

Figure 5.5: Average Stress-Strain Curves of Half Spiral Fiberglass Configurations

5.5 Influence of Impact Energy

A plot of the compression strength as a function of impact energy was prepared to illustrate the effect of impact energy on compression strength, as a function of sleeve type and coverage. Figure 5.6 compares trends of all sleeve configurations (full braid, full spiral, half braid, and half spiral) at each impact level (0 J, 5 J, 10 J). The dashed trend lines simply connect the averages of each sleeve configuration and should not be used for extrapolation. This plot shows that 5 J (3.7 ft-lbs) of impact energy significantly affects the ultimate strength of half spiral fiberglass configurations. Configurations impacted with 10 J (7.4 ft-lbs) of energy show that braided sleeves dominate the spiral sleeves.

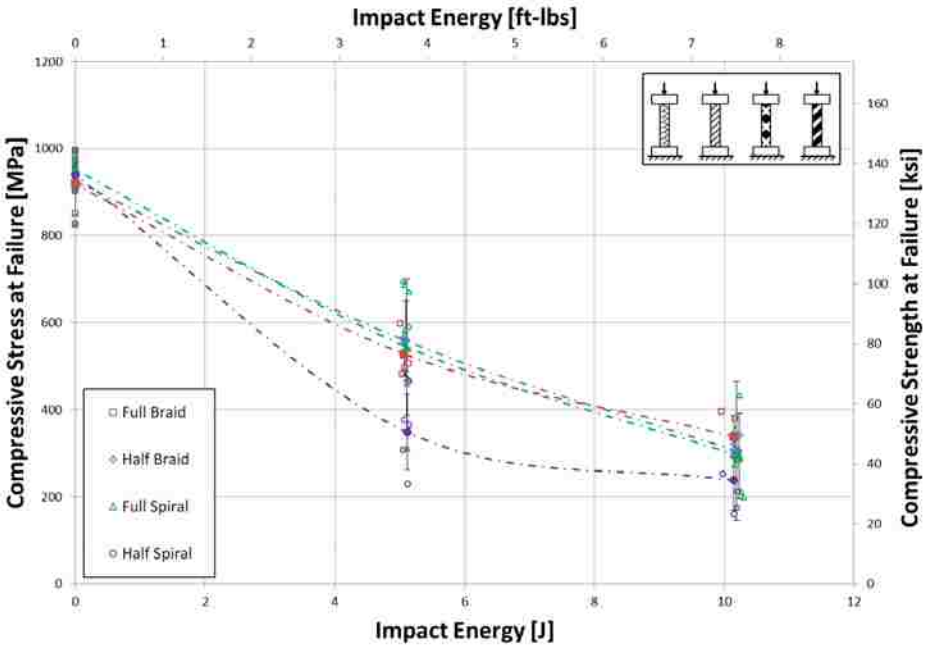

Figure 5.6: Compression Strength After Impact vs. Impact Energy for Fiberglass Configurations

5.6 Influence of Sleeve Type

In a similar manner conducted on carbon/epoxy specimens, Figure 5.7 and Figure 5.8 were to illustrate the effect of full braid vs. full spiral and half braid vs. half spiral, respectively, at each impact energy level. This approach allows comparison of results for full coverage braided and spiral samples, and half coverage braided and spiral sleeves. For all undamaged configurations, there exhibits virtually no difference (for modulus, or ultimate strength) between sleeve types. For full coverage (braid vs. spiral), there isn't a clear distinction in strength for fiberglass specimens with 5 J (3.7 ft-lbs). At 10 J (7.4 ft-lbs) of impact, braided sleeves performed better than spiral sleeves.

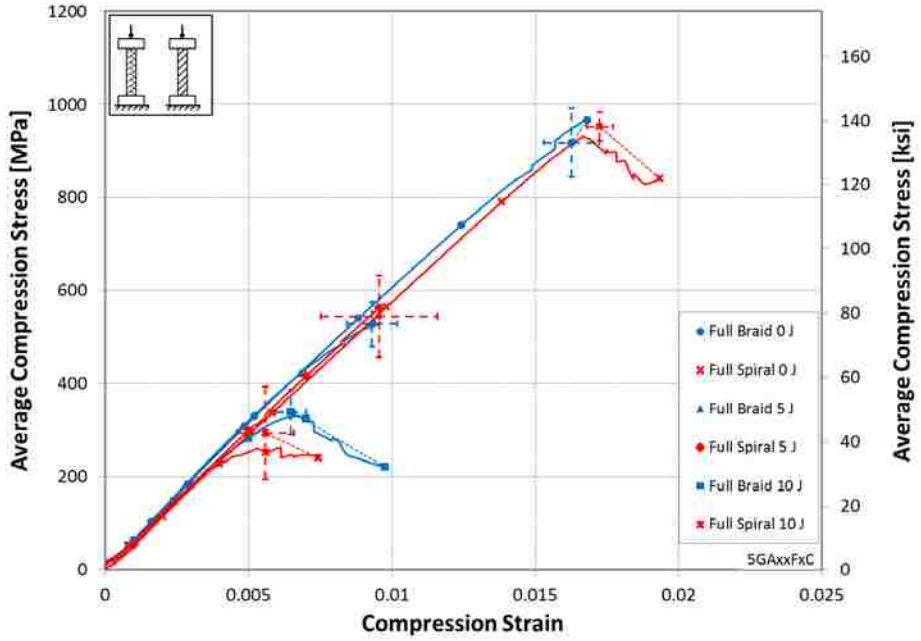

Figure 5.7: Average Stress-Strain Curves Comparing Full Coverage Braid vs. Spiral Fiberglass Configurations

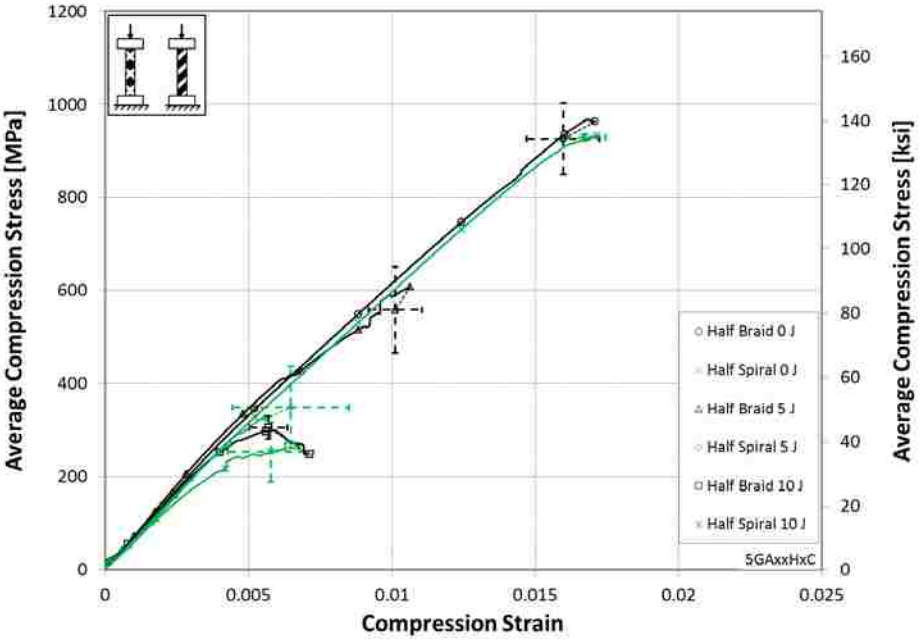

Figure 5.8: Average Stress-Strain Curves Comparing Half Coverage Braid vs. Spiral Fiberglass Configurations

5.7 Influence of Sleeve Coverage

An average stress-strain curves comparing full vs. half coverage braided sleeves for fiberglass configurations are shown in Figure 5.9. For undamaged and 5 J of impact specimens, there is essentially no difference in strength between full and half braided sleeves. With 10 J (7.4 ft-lbs) of impact, however, full coverage specimens perform slightly better than half coverage specimens.

An average stress-strain curves comparing full vs. half coverage spiral sleeves for fiberglass configurations are shown in Figure 5.10. Again, for undamaged specimens, there is essentially no difference in strength between full and half spiral sleeves. With both 5 and 10 J (3.7 and 7.4 ft-lbs) of impact, however, full coverage specimens perform better than half coverage specimens.

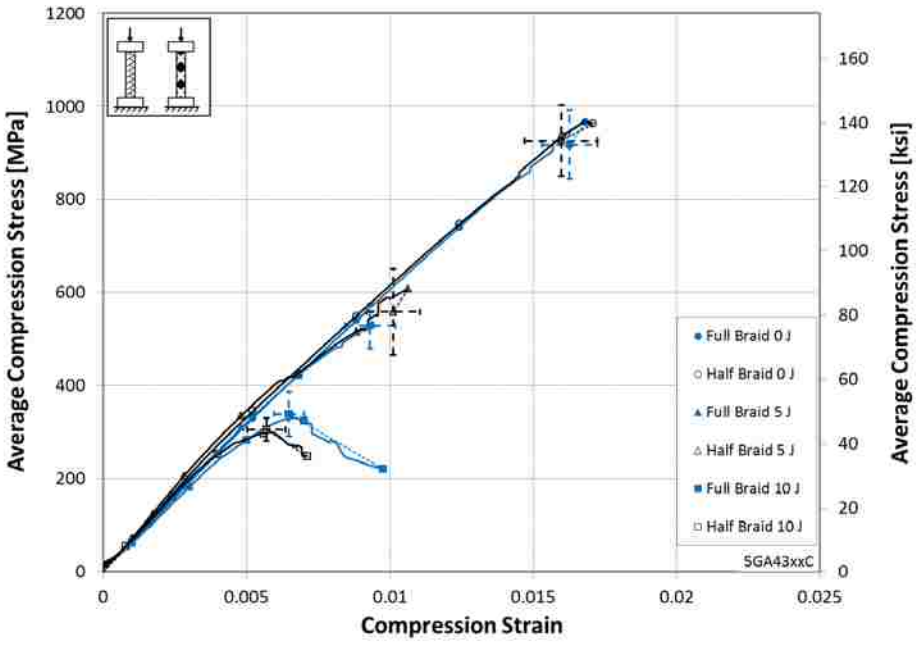

Figure 5.9: Average Stress-Strain Curves Comparing Full vs. Half Braid for Fiberglass Configurations

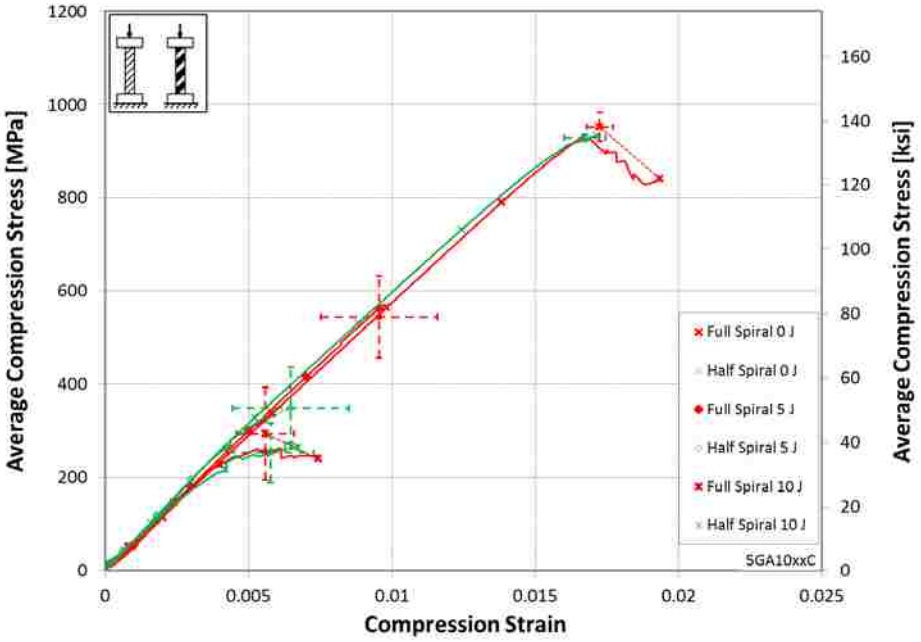

Figure 5.10: Average Stress-Strain Curves Comparing Full vs. Half Spiral for Fiberglass Configurations

6 DISCUSSION OF RESULTS

This chapter discusses the significance of the damage tolerance results for carbon/epoxy and fiberglass/epoxy composite configurations and compares them to the results of basalt/epoxy composites recently completed by Allen [2]. To illustrate the effect of sleeve type (braid vs. spiral) and coverage (full vs. half) for carbon/epoxy and fiberglass/epoxy composites, in a manner similar to Allen's research on basalt/epoxy composites [2], summary tables and figures are presented. In the tables, the differences in compression modulus and strength between configurations (in percentages) are normalized to the first row in the table. For example, -15% means that the performance of the configuration represented in that row exhibited 15% lower value than the previous row. In the figures, the error bars represent ±1 standard deviation. This chapter further compares the relative difference in modulus and ultimate strength of carbon, fiberglass, and basalt fiber/epoxy composites, with the intent to determine how the current results agree with the conclusions reached in Allen's parallel research [2].

In addition, an attempt to normalize the behavior of the various materials investigated, for comparative purposes, yielded a set of figures (Figure E.1– Figure E.12) that are included in Appendix E for future consideration.

6.1 Influence of Sleeve Type

To examine the influence of sleeve type, Figure 6.1 (for carbon/epoxy) and Figure 6.2 (for fiberglass/epoxy) were created by combining results of all braided sleeves (full and half), and all spiral sleeves (full and half), respectively. This approach allows comparison of just the sleeve type. The stress-strain curves for carbon/epoxy (Figure 6.1) indicate a very significant reduction in strength for damaged configurations. The plot also show a decreasing compression modulus with increasing impact energy, indicated by the shift of slopes to the right. On the other hand, slopes of the curves at each impact energy level remains unchanged, suggesting no effect of sleeve type on stiffness at each impact energy level. The stress-strain curves for fiberglass epoxy (Figure 6.2) yield a distinct difference in strength between configurations impacted with 5 J and 10 J. The plot for fiberglass epoxy also show consistent initial stiffness for all impact levels.

A summary of the relative difference between braided and spiral sleeves for carbon/epoxy composites is shown in Table 6.1. At no impact, there is essentially no difference in modulus and ultimate strength between the two sleeve types. Furthermore, for all damaged carbon/epoxy configurations, compression modulus and strength are virtually unaffected by sleeve type, as shown by less than 6% difference between braided and spiral sleeve types.

Similarly, a summary of the relative difference between braided and spiral sleeve for fiberglass/epoxy configurations is shown in Table 6.2. Again, at no impact, there is virtually no difference in modulus and ultimate strength between the two sleeve type configurations. In both 5 J and 10 J of impact cases, spiral sleeve type exhibited lower compression strength (18% lower) than braided sleeve type. Braided sleeve configurations also generally exhibited a slightly higher compression stiffness at both (5 J and 10 J) impact energy levels (9% and 4% higher,

respectively) than the comparable spiral sleeved configurations, although neither of these differences is significant given that it is not uncommon for composites to have a ±10% variation in mechanical properties [1] [12].

In summary, sleeve type does affect the compression strength of fiberglass/epoxy composites subjected to damage, as illustrated by an 18% lower strength for spiral sleeves. Carbon/epoxy composites, on the other hand, exhibited an insignificant difference in strength to justify manufacturing of braided over spiral sleeves.

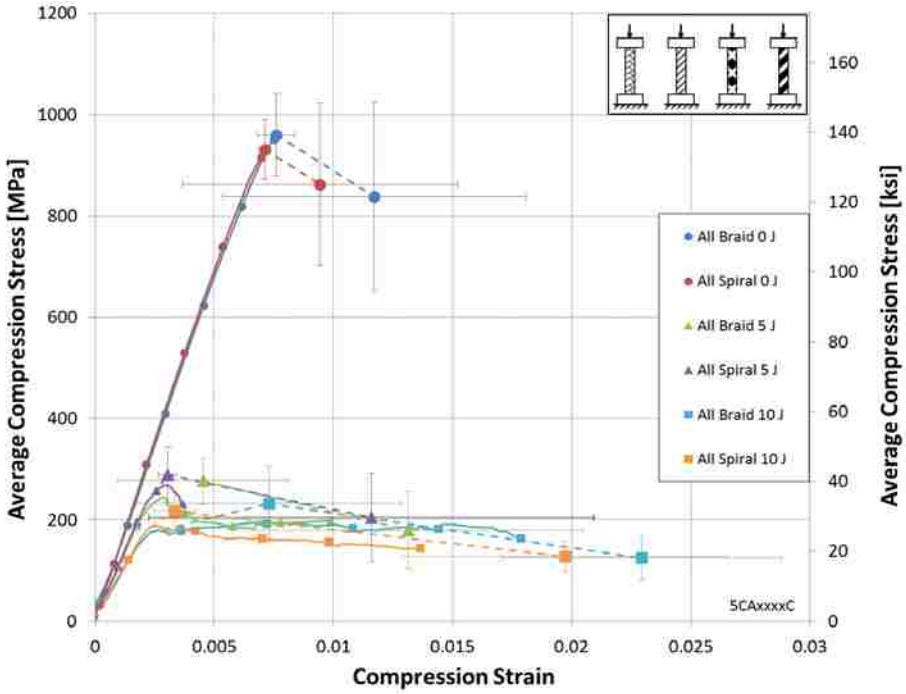

Figure 6.1: Average Stress-Strain Curves Comparing Braid vs. Spiral Carbon Composites, Independent of Coverage

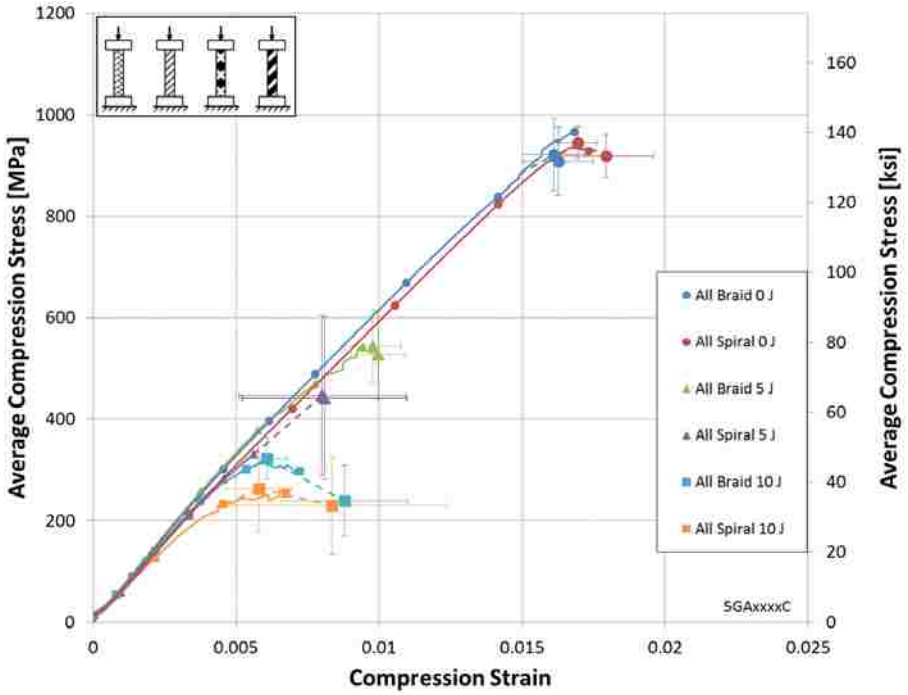

Figure 6.2: Average Stress-Strain Curves Comparing Braid vs. Spiral Fiberglass Composites, Independent of Coverage

Table 6.1: Compression Properties of Carbon Composites with Braided and Spiral Sleeves for Combined Full and Half Coverage

Specimen Configuration and Impact Energy		Average Compression Young's Modulus			Average Compression Strain at Ultimate Strength		Average Ultimate Compression Strength		
		[GPa	(10^6psi)]	Diff.	[10^3 με]	Diff.	[MPa	(ksi)]	Diff.
Undamaged	**All Braid**	136.4	(19.8)		7.6		960.2	(139.3)	
	All Spiral	141.5	(20.5)	+4%	7.1	-6%	931.1	(135.0)	-3%
5 J (3.7 ft-lbs)	**All Braid**	107.5	(15.6)		4.5		276.6	(40.1)	
	All Spiral	111.8	(16.2)	+4%	3.0	-33%	288.7	(41.9)	+4%
10 J (7.4 ft-lbs)	**All Braid**	88.3	(12.8)		7.3		231.7	(33.6)	
	All Spiral	83.9	(12.2)	-5%	3.3	-54%	217.2	(31.5)	-6%

Table 6.2: Compression Properties of Fiberglass Composites with Braided and Spiral Sleeves for Combined Full and Half Coverage

Specimen Configuration and Impact Energy		Average Compression Young's Modulus			Average Compression Strain at Ultimate Stress		Average Ultimate Compression Stress		
		[GPa (10^6psi)]		Diff.	[10^3 με]	Diff.	[MPa (ksi)]		Diff.
Undamaged	**All Braid**	59.2	(8.59)		16.1		921.8	(133.7)	
	All Spiral	56.8	(8.24)	-4%	17.0	+5%	945.2	(137.1)	+3%
5 J (3.7 ft-lbs)	**All Braid**	69.7	(10.11)		9.8		543.2	(78.8)	
	All Spiral	63.6	(9.22)	-9%	8.0	-18%	446.6	(64.8)	-18%
10 J (7.4 ft-lbs)	**All Braid**	64.3	(9.32)		6.1		322.0	(46.7)	
	All Spiral	61.4	(8.91)	-4%	5.8	-5%	263.0	(38.1)	-18%

6.2 Influence of Sleeve Coverage

To illustrate the effect of sleeve coverage (full vs. half), independent of the sleeve type, Figure 6.3 (for carbon/epoxy) and Figure 6.4 (for fiberglass/epoxy) were created by combining the results from full braid and spiral sleeve samples, and half braided and spiral sleeve samples for carbon/epoxy and fiberglass/epoxy samples, respectively. This combination of results approach allows comparison of just the sleeve coverage. The stress-strain curves for carbon/epoxy (Figure 6.3) indicate a very significant reduction in strength for damaged configurations, although there is no distinction between configurations impacted with 5 J and 10 J. The plot also show a decrease in compression modulus with increasing impact energy, indicated by the shift of slopes to the right. The stress-strain curves for fiberglass epoxy (Figure 6.4) yield a more distinct difference in strength between configurations impacted with 5 J and 10 J. The plot for fiberglass epoxy also show consistent initial stiffness for all impact levels.

A summary of the relative difference between full and half sleeve coverage for carbon/epoxy configurations is shown in Table 6.3. At no impact and 5 J (3.7 ft-lbs) impact,

there is virtually no difference in modulus, and ultimate strength between full and half sleeve coverage, as illustrated by the less than 8% difference. At 10 J (7.4 ft-lbs) of impact, however, half coverage exhibited lower compression stiffness (11% lower) and significantly lower compression strength (37% lower) than full coverage.

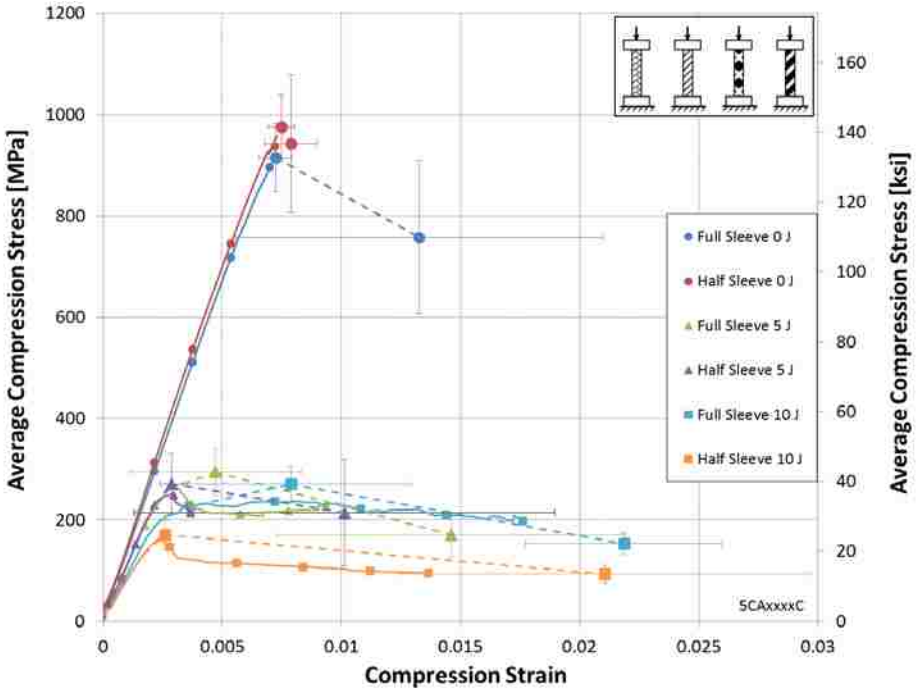

Figure 6.3: Average Stress-Strain Curves Comparing Full vs. Half Coverage for Carbon Configurations, Independent of Sleeve Type

Similarly, a summary of the relative difference between full and half coverage for fiberglass/epoxy configurations is shown in Table 6.4. Compression modulus is essentially unaffected by sleeve coverage, for undamaged and damaged configurations, as illustrated by less than 9% difference between sleeve coverage. In both 5 J and 10 J of impact energy levels, however, the half coverage exhibited lower compression strength (15% lower) than full coverage.

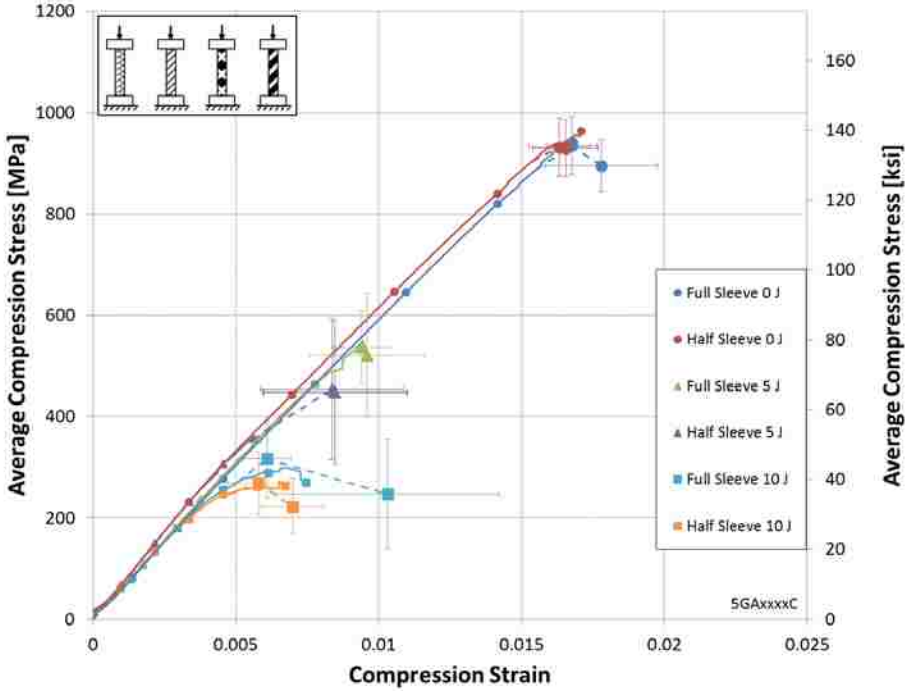

Figure 6.4: Average Stress-Strain Curves Comparing Full vs. Half Coverage for Fiberglass Configurations, Independent of Sleeve Type

Table 6.3: Compression Properties of Carbon Composites with Full and Half Coverage for Combined Braided and Spiral Sleeves

Impact Energy & Configuration		Average Compression Young's Modulus			Average Compression Strain at Ultimate Stress		Average Ultimate Compression Stress		
		[GPa (10^6psi)]		Diff.	[10^3 με]	Diff.	[MPa (ksi)]		Diff.
Undamaged	**Full**	136.5	(19.8)		7.2		915.2	(132.8)	
	Half	141.5	(20.5)	+4%	7.5	+3%	976.0	(141.6)	+7%
5 J (3.7 ft-lbs)	**Full**	108.2	(15.7)		4.7		294.2	(42.7)	
	Half	111.1	(16.1)	+3%	2.9	-39%	271.2	(39.3)	-8%
10 J (7.4 ft-lbs)	**Full**	90.9	(13.2)		7.9		270.0	(39.2)	
	Half	81.0	(11.8)	-11%	2.6	-67%	170.5	(24.8)	-37%

Table 6.4: Compression Properties of Fiberglass Composites with Full and Half Coverage for Combined Braided and Spiral Sleeves

Impact Energy & Configuration		Average Compression Young's Modulus			Average Compression Strain at Ultimate Stress		Average Ultimate Compression Stress		
		[GPa (10^6 psi)]		Diff.	[10^3 με]	Diff.	[MPa	(ksi)]	Diff.
Undamaged	**Full**	58.5	(8.48)		16.8		934.6	(135.6)	
	Half	57.6	(8.35)	-2%	16.3	-3%	932.6	(135.3)	0%
5 J (3.7 ft-lbs)	**Full**	63.7	(9.23)		9.4		536.1	(77.8)	
	Half	69.6	(10.09)	+9%	8.4	-11%	453.6	(65.8)	-15%
10 J (7.4 ft-lbs)	**Full**	60.8	(8.82)		6.1		316.4	(45.9)	
	Half	64.8	(9.39)	+7%	5.8	-5%	268.2	(38.9)	-15%

In summary, the amount of sleeve coverage shows an effect on the mechanical properties of both carbon fiber and fiberglass epoxy configurations subjected to damage. As mentioned above, carbon/epoxy configurations experienced a significant reduction of 37% in compression strength at 10 J (7.4 ft-lbs) of impact relative to undamaged configurations. Fiberglass/epoxy, however, exhibited a similar reduction in strength (15% lower for half coverage) at both 5 and 10 J (3.7 and 7.4 ft-lbs) of impact energy levels.

6.3 Influence of Impact Energy

The tables in this section compare the damage tolerance characteristics of carbon and fiberglass to basalt fiber/epoxy composites. The percentages in each row represent a percentage difference in strength of a particular configuration, relative to the corresponding undamaged configuration.

Table 6.5 compares the compression strength reduction of carbon, fiberglass and basalt fiber/epoxy configurations impacted with (5 J and 10 J) relative to undamaged configurations, isolating just the sleeve type (braid and spiral). Not surprisingly, the compression strength

decreases with increasing impact energy. At 5 J (3.7 ft-lbs) of impact, carbon/epoxy configurations exhibited a 70% reduction in strength compared to the undamaged configurations. Impacted fiberglass/epoxy configurations, on the other hand, exhibited about half of the undamaged strength. Basalt/epoxy configurations achieved about a third of the undamaged strength. For 10 J (7.4 ft-lbs) of impact, carbon/epoxy and fiberglass/epoxy composites decreased about two-thirds in strength compared to undamaged configurations, whereas basalt/epoxy exhibited just a little under one half the compression strength of undamaged configurations.

Table 6.5: Relative Difference in Compression Strength for Carbon, Fiberglass and Basalt Epoxy Composites, Braid vs. Spiral

Impact Energy & Configuration		Ultimate Compression Strength								
		Carbon			Fiberglass			Basalt		
		[MPa	(ksi)]	Diff.	[MPa	(ksi)]	Diff.	[MPa	(ksi)]	Diff.
Undamaged	**Braid**	960	(139.3)	--	921	(133.7)	--	762	(110.5)	--
	Spiral	931	(135.0)	--	945	(137.1)	--	704	(102.0)	--
5 J (3.7 ft-lbs)	**Braid**	276	(40.1)	-71%	543	(78.8)	-41%	459	(66.6)	-40%
	Spiral	288	(41.9)	-69%	446	(64.8)	-53%	528	(76.5)	-25%
10 J (7.4 ft-lbs)	**Braid**	231	(33.6)	-76%	322	(46.7)	-65%	338	(49.0)	-56%
	Spiral	217	(31.5)	-77%	263	(38.1)	-72%	309	(44.8)	-56%

Table 6.6 compares compression strength difference of impacted configurations (5 J and 10 J) relative to undamaged configurations by examining just the sleeve coverage (full and half). Similarly, compression strength decreases with increasing impact energy level. Carbon/epoxy configurations exhibited significant decrease in strength of approximately 70% and 75% for 5 J and 10 J of impact, respectively. Fiberglass/epoxy revealed a smaller reduction difference of 47% and 41% in strength at 5J and 10 J of impact, respectively. Basalt/epoxy showed similar reduction results compared to fiberglass configurations. For 10 J (7.4 ft-lbs) of impact, carbon

fiber and fiberglass epoxy configurations decreased about two-thirds in strength compared to undamaged configurations, whereas basalt/epoxy exhibited just a little under half in strength.

Table 6.6: Relative Difference in Compression Strength for Carbon, Fiberglass and Basalt Epoxy Composites, Full vs. Half

Impact Energy & Configuration		Ultimate Compression Strength								
		Carbon			Fiberglass			Basalt		
		[MPa	(ksi)]	Diff.	[MPa	(ksi)]	Diff.	[MPa	(ksi)]	Diff.
Undamaged	**Full**	915	(132.8)	--	934	(135.6)	--	743	(108)	--
	Half	976	(141.6)	--	932	(135.3)	--	723	(105)	--
5 J (3.7 ft-lbs)	**Full**	294	(42.7)	-68%	536	(77.8)	-43%	617	(89)	-17%
	Half	271	(39.3)	-72%	453	(65.8)	-51%	370	(54)	-49%
10 J (7.4 ft-lbs)	**Full**	270	(39.2)	-70%	316	(45.9)	-41%	416	(60)	-33%
	Half	170	(24.8)	-83%	268	(38.9)	-41%	230	(34)	-38%

6.4 Comparison of Carbon, Fiberglass and Basalt Core Fibers

This section compares the combined average compression Young's modulus and ultimate compression strength test results to illustrate the influence of sleeve type and coverage on carbon, fiberglass and basalt fiber/epoxy cores.

6.4.1 Compression Young's Modulus Comparison

The relative difference in compression Young's modulus between braided and spiral sleeves for carbon, fiberglass, and basalt fiber/epoxy configurations is summarized in Table 6.7. Compression stiffness is unaffected by sleeve type, as shown by very little difference in stiffness (less than 9% difference), comparing braided to spiral sleeves for all fiber/epoxy materials. Compression modulus for carbon/epoxy decreases with increasing impact energy. On the other hand, compression stiffness for fiberglass and basalt epoxy configurations remains unchanged with increasing impact energy.

Table 6.7: Compression Stiffness of Braided and Spiral Sleeves for Carbon, Fiberglass, and Basalt Configurations

Impact Energy & Configuration		Compression Stiffness								
		Carbon			Fiberglass			Basalt		
		[GPa (10^6 psi)]		Diff.	[GPa (10^6 psi)]		Diff.	[GPa (10^6 psi)]		Diff.
Undamaged	**Braid**	136	(19.8)		59.2	(8.59)		60.6	(8.79)	
	Spiral	141	(20.5)	+4%	56.8	(8.24)	-4%	58.5	(8.48)	-3%
5 J (3.7 ft-lbs)	**Braid**	107	(15.6)		69.7	(10.11)		58.9	(8.54)	
	Spiral	111	(16.2)	+4%	63.6	(9.22)	-9%	59.9	(8.69)	+2%
10 J (7.4 ft-lbs)	**Braid**	88.3	(12.8)		64.3	(9.32)		57.6	(8.35)	
	Spiral	83.9	(12.2)	-5%	61.4	(8.91)	-4%	53.6	(7.78)	-7%

The relative difference in compression Young's modulus between full and half coverage for carbon, fiberglass, and basalt fiber/epoxy configurations is summarized in Table 6.8. When undamaged and impacted with 5 J, there is very little difference in stiffness, comparing full to half coverage for all fiber/epoxy materials, as shown by less than 9% difference. At 10 J (7.4 ft-lbs) of impact, however, only carbon/epoxy configurations show an effect on stiffness; half coverage exhibit 11% lower modulus relative to full coverage. Again, compression stiffness decreases with increasing impact energy for carbon/epoxy configurations, while stiffness virtually remains unchanged with increasing impact energy.

Table 6.8: Compression Stiffness of Full and Half Coverage for Carbon, Fiberglass, and Basalt Configurations

Impact Energy & Configuration		Compression Stiffness								
		Carbon			Fiberglass			Basalt		
		[GPa (10^6 psi)]		Diff.	[GPa (10^6 psi)]		Diff.	[GPa (10^6 psi)]		Diff.
Undamaged	**Full**	136	(19.8)		58.5	(8.48)		58.9	(8.54)	
	Half	141	(20.5)	+4%	57.6	(8.35)	-2%	60.2	(8.73)	+2%
5 J (3.7 ft-lbs)	**Full**	108	(15.7)		63.7	(9.23)		61.1	(8.86)	
	Half	111	(16.1)	+3%	69.6	(10.09)	+9%	57.8	(8.38)	-5%
10 J (7.4 ft-lbs)	**Full**	90.9	(13.2)		60.8	(8.82)		58.5	(8.48)	
	Half	81.0	(11.8)	-11%	64.8	(9.39)	+7%	52.7	(7.64)	-10%

6.4.2 Ultimate Compression Strength Comparison

The relative difference in ultimate compression strength between braided and spiral sleeves for carbon, fiberglass, and basalt fiber/epoxy composites is summarized in Table 6.9. When undamaged, the ultimate compression strength of braided sleeve configurations is similar to spiral sleeve configurations for all core materials, as shown by less than 8% difference. Sleeve type significantly affects fiberglass and basalt fiber/epoxy configurations at the 5 J (3.7 ft-lbs) impact energy level; spiral sleeves exhibit 18% lower and 15% higher strength than braided sleeves, respectively. At 10 J (7.4 ft-lbs) of impact energy, only fiberglass epoxy configurations show significant effect; spiral sleeves exhibited 18% lower strength than braided sleeves.

Table 6.9: Ultimate Compression Strength of Braided and Spiral Sleeves for Carbon, Fiberglass, and Basalt Composites

Impact Energy & Configuration		Ultimate Compression Strength								
		Carbon			Fiberglass			Basalt		
		[MPa	(ksi)]	Diff.	[MPa	(ksi)]	Diff.	[MPa	(ksi)]	Diff.
Undamaged	**Braid**	960	(139.3)		921	(133.7)		762	(110.5)	
	Spiral	931	(135.0)	-3%	945	(137.1)	+3%	704	(102.0)	-8%
5 J (3.7 ft-lbs)	**Braid**	276	(40.1)		543	(78.8)		459	(66.6)	
	Spiral	288	(41.9)	+4%	446	(64.8)	-18%	528	(76.5)	+15%
10 J (7.4 ft-lbs)	**Braid**	231	(33.6)		322	(46.7)		338	(49.0)	
	Spiral	217	(31.5)	-6%	263	(38.1)	-18%	309	(44.8)	-9%

The relative difference in ultimate compression strength between full and half coverage for carbon, fiberglass, and basalt fiber/epoxy configurations is summarized in Table 6.10. When undamaged, sleeve coverage virtually has no effect on the ultimate strength of either fiber/epoxy material. At 5 J (3.7 ft-lbs) of impact, however, all core materials exhibit a similar trend, revealing that full coverage performs better than half coverage, particularly fiberglass and basalt fiber/epoxy configurations, illustrated with 15% and 40% reduction in strength, respectively.

For all three core materials, at 10 J (7.4 ft-lbs) of impact, the ultimate strengths are significantly affected by the amount of sleeve coverage; i.e., full coverage exhibited 37%, 15%, and 45% higher strengths than half coverage for carbon, fiberglass, and basalt fiber/epoxy composites, respectively.

Table 6.10: Ultimate Compression Strength of Full and Half Coverage for Carbon, Fiberglass, and Basalt Composites

Impact Energy & Configuration		Ultimate Compression Strength								
		Carbon			Fiberglass			Basalt		
		[MPa	(ksi)]	Diff.	[MPa	(ksi)]	Diff.	[MPa	(ksi)]	Diff.
Undamaged	**Full**	915	(132.8)		934	(135.6)		743	(108)	
	Half	976	(141.6)	+7%	932	(135.3)	0%	723	(105)	-3%
5 J (3.7 ft-lbs)	**Full**	294	(42.7)		536	(77.8)		617	(89)	
	Half	271	(39.3)	-8%	453	(65.8)	-15%	370	(54)	-40%
10 J (7.4 ft-lbs)	**Full**	270	(39.2)		316	(45.9)		416	(60)	
	Half	170	(24.8)	-37%	268	(38.9)	-15%	230	(34)	-45%

6.5 Summary of Results

In summary, braided sleeves yielded higher compression strength for fiberglass/epoxy composites subjected to damage, and contrarily yielded insignificant difference in strength for carbon/epoxy composites. Therefore braided sleeves on fiberglass/epoxy composites yielded sufficiently higher CSAI than spiral sleeves to justify the increased manufacturing complexity.

Full coverage exhibited higher CSAI than half coverage on both carbon fiber and fiberglass epoxy configurations. Carbon/epoxy configurations experienced up to 37% reduction in strength on damaged relative to undamaged configurations. Fiberglass/epoxy configurations also exhibited a similar reduction in strength (18% reduction). Not surprisingly, the compression strength decreases with increasing impact energy for both carbon fiber and fiberglass epoxy composites. Therefore, full coverage sleeves on carbon fiber and fiberglass epoxy composites

yielded sufficiently higher CSAI than half coverage sleeves to justify the increased manufacturing complexity.

The results of all fiber/epoxy composites yielded very little difference in compression stiffness between braided and spiral sleeves, and between full and half coverage. The compression modulus of carbon/epoxy composites decreases with increasing impact energy. On the other hand, the compression stiffness of fiberglass and basalt fiber/epoxy configurations virtually remains unchanged with increasing impact energy. Carbon/epoxy composites are about twice as stiff as fiberglass and basalt fiber/epoxy composites. Carbon fiber and fiberglass epoxy composites exhibited similar damage tolerance characteristics (compression stiffness) to basalt/epoxy composites with respect to sleeve type and coverage.

For all three core materials, the ultimate strengths are significantly affected by sleeve coverage; i.e., full coverage exhibited 37%, 15%, and 45% higher strengths than half coverage for carbon fiber, fiberglass, and basalt fiber epoxy composites, respectively. Fiberglass/epoxy is about as strong as carbon/epoxy and about 20% stronger than basalt/epoxy composites. Both fiberglass and basalt fiber epoxy composites retained about half the strength when impacted with 5 J (3.7 ft-lbs), whereas carbon/epoxy composites retained only a third of the strength at 5 J (3.7 ft-lbs) of impact. Carbon fiber and fiberglass epoxy composites exhibited similar damage tolerance characteristics (compression strength) to basalt/epoxy composites with respect to sleeve coverage.

In terms of impact energy, all fiber/epoxy composites yielded a reduction in compression strength with increasing impact energy. And therefore, carbon fiber and fiberglass epoxy composites exhibited similar damage tolerance characteristics to basalt epoxy composites as a function of impact energy, i.e., compression strength decreases with increasing impact energy.

7 CONCLUSIONS

This chapter presents general conclusions reached in the current research, and describes recommendations for future research. Compression tests were conducted to quantify the damage tolerance of unidirectional carbon fiber and fiberglass epoxy composite rods consolidated with various aramid sleeve configurations. The rod elements represent individual members of IsoTruss structures. Test variables include core materials, impact energy levels, sleeve type, and sleeve coverage.

7.1 General Conclusions for Carbon/Epoxy and Fiberglass/Epoxy Composites

1. Co-curing dry fiber over unidirectional fiber/epoxy composites effectively consolidates the core materials.
2. When undamaged, the ultimate compression strength and compression stiffness are virtually unaffected by sleeve type (braid or spiral) and coverage (half or full), as demonstrated by Hansen [5], for carbon/epoxy composites with carbon/epoxy braided sleeves.
3. Increasing aramid sleeve coverage increases the damage tolerance of carbon fiber and fiberglass epoxy composite elements.
4. Not surprisingly, ultimate compression strength and compression stiffness after impact decrease with increasing impact energy levels.

7.2 Conclusions Drawn from Comparison to Basalt/Epoxy Results

In general, the conclusions from related research by Allen [2] [3] on basalt/epoxy composites are equally applicable to carbon fiber and/or fiberglass epoxy composites. The comparison of conclusions drawn in the current research are as follows:

1. Braided sleeves on fiberglass/epoxy composites yield sufficiently higher CSAI than spiral sleeves to justify the increased manufacturing complexity.
2. Full coverage sleeves on carbon fiber and fiberglass epoxy composites yield sufficiently higher CSAI than half coverage sleeves to justify the increased manufacturing complexity.
3. Carbon fiber and fiberglass epoxy composites exhibit similar damage tolerance characteristics (compression stiffness) to basalt/epoxy composites with respect to sleeve type and coverage.
4. Carbon fiber and fiberglass epoxy composites exhibit similar damage tolerance characteristics (compression strength) to basalt/epoxy composites with respect to sleeve coverage.
5. Carbon fiber and fiberglass epoxy composites exhibit similar damage tolerance characteristics to basalt epoxy composites as a function of impact energy; i.e., compression strength decreases with increasing impact energy.

7.3 Recommendations

1. Perform compression strength after impact tests on carbon/epoxy composites consolidated and co-cured with sleeves at impact energy levels ranging from 1-4 J (0.7-3.0 ft-lbs) to see if carbon/epoxy retains any strength after impact.

2. Investigate internal damages inflicted on specimens under impact to further understand the scatter in test results.

REFERENCES

[1] Strong, A. and Jensen, D., (2002), "The Ultimate Composite Structure," *Composites Fabrication*, pp. 22–27, Aug. 2002.

[2] Allen, D. (2011), "Damage Tolerance of Unidirectional Basalt Composites Encased in an Aramid Sleeve," M.S. Thesis, Brigham Young University, Provo, Utah.

[3] Allen, D. (2011), "Compression Strength After Impact of Basalt Fiber Members in an Aramid Sleeve," presented at *SAMPE Tech Conference*, Fort Worth Texas, Oct. 2011.

[4] Stoutis, C. (2000), "Compression Testing of Pultruded Carbon Fibre-Epoxy Cylindrical Rods," *Journal of Materials Science*, Vol. 34, pp. 3441-3446.

[5] Hansen, S. (2004), "Influence of Consolidation and Interweaving on Compression Behavior of IsoTruss® Structures," M.S. Thesis, Brigham Young University, Provo, Utah.

[6] Wisnom, M. (1999), "Suppression of Splitting and Impact Sensitivity of Unidirectional Carbon-Fibre Composite Rods Using Tensioned Overwind," *Composites Part A: Applied Science and Manufacturing*, Vol. 30, No. 5, pp. 661-665.

[7] Allen, D. (2011), "Influence of Braid Sleeves on the Impact Damage of Cylindrical Unidirectional Elements," presented *at The 18th International Conference on Composite Materials*, Aug. 2011.

[8] Jensen, M., and Jensen, D., (2010), "Continuous Manufacturing of Cylindrical Composite Lattice Structures," presented at the *International Conference on Textile Composites* (TEXCOMP10), Oct. 26-28, 2010.

[9] Kesler, S. (2006), "Consolidation and Interweaving of Composite Members by a Continuous Manufacturing Process," M.S. Thesis, Brigham Young University, Provo, Utah.

[10] Kesler, S. L. and Jensen D. W., "Consolidation and Interweaving of Composite Members by a Continuous Manufacturing Process," Digital Proceedings of the Sixth International Conference on Composite Science and Technology, Durban, South Africa, ISBN: 1-86840-642-3, 15 pp., Jan. 22-24, 2007.

[11] Jensen, D. W. and Rackliffe M. E., "Ultra-Lightweight IsoTruss™ Grid Structures," Experimental Techniques and Design in Composite Materials 6, University of Padova, Vicenza, Italy, p. 53, June 18–20, 2003.

[12] Jensen, D. W., "A Glimpse Into the World of Innovative Composite IsoTruss™ Grid Structures," *SAMPE Journal,* Vol. 36, No. 5, pp. 8–16, Sep./Oct. 2000.

[13] Jensen, D. (2010), "Using External Robots Instead of Internal Mandrels to Produce Composite Lattice Structures," presented at *The International Conference on Textile Composites (TEXCOMP10),* Oct. 26-28, 2010.

[14] Winkel, L. (2001), "Parametric Investigation of IsoTruss™ Geometry Using Linear Finite Element Analysis," M.S. Thesis, Brigham Young University, Provo, Utah.

[15] Scoresby, B. (2003), "Low Velocity Longitudinal and Radial Impact of IsoTruss™ Grid Structures," M.S. Thesis, Brigham Young University, Provo, Utah.

[16] McCune, A. (2001), "Tension and Compression of Carbon/Epoxy IsoTruss™ Grid Structures," M.S. Thesis, Brigham Young University, Provo, Utah.

[17] Embley, M. (2011), "Damage Tolerance of Buckling-Critical Unidirectional Carbon, Fiberglass, and Basalt Fiber Composites in Co-Cured Aramid Sleeves," M.S. Thesis, Brigham Young University, Provo, Utah.

[18] Embley, M. (2011), "Buckling Strength of Damaged Unidirectional Basalt Composite Rods with Braid Sleeves," presented at *SAMPE Tech Conference,* Fort Worth Texas, Oct. 2011.

[19] Jensen, D. W., "Manufacturing Small Diameter IsoTruss® Lattice Structures for Mountain Bike Frames," *The 15th SICOMP Conference on Manufacturing and Design of Composites,* Sarohus, Gothenburg, Sweden, Sep. 27–28, 2004.

[20] Toho Tenax America, Inc., (2011) "Continuous Filament Carbon Fiber Lot Average Properties" http://www.tohotenaxamerica.com/contfil.php

[21] Owens Corning (2011) "OVC Reinforcements Properties Summary" http://www.ocvreinforcements.com/hp/index.aspx

[22] Kamenny Vek KV 11 Series Data Sheet (2011) http://www.basfiber.com/Sites/basfiber/Uploads/BCF%20KV11%20assembled_TDS_eng.202CB9D826F74BC685B3910192BB01FF.pdf

[23] TCR Composites (2007) "UF3325 TCR™ Resin Data Sheet," Revision 10. http://www.tcrcomposites.com/pdfs/resindata/

[24] Dupont, "Section II: Properties of Kevlar®," *Technical Guide Kevlar Aramid Fiber,* http://www2.dupont.com/Kevlar/en_US/assets/downloads/KEVLAR_Technical_Guide.pdf

[25] Harthness, J., Sjoblom, P., Cordell, T., "On Low-Velocity Impact Testing of Composite Materials," *Journal of Composite Materials,* Vol. 22, No. 1, pp. 30-52, 1988.

[26] Sika, C. (2012), "Compression Strength After Impact of Unidirectional Fiberglass Rods Consolidated with Aramid Sleeves," to present at *AIAA SDM Conference,* Honolulu, Hawaii, Apr. 2012.

APPENDIX A: MICROSCOPE MEASUREMENTS

Appendix A contains cross-sectional area, offset angle, and sleeve coverage microscopic measurements for carbon fiber and fiberglass epoxy composite elements used in this research. Cross-sectional areas for carbon fiber and fiberglass epoxy are shown in Table A.1-Table A.4. Offset angle measurements for carbon and fiberglass specimens are summarized in Table A.5-Table A.8. Table A.9 and Table A.10 summarize sleeve coverage measurements for carbon and fiberglass specimens, respectively.

Table A.1: Cross-Sectional Area Measurements for Carbon Specimens with Braided Sleeves

Specimen Configuration		Cross-sectional Area [mm^2]			
		End 1	End 2	Average	Std. Dev.
5CA43FNC	1	50.66	50.33	50.50	0.23
	2	48.41	48.81	48.61	0.28
	3	48.85	48.96	48.90	0.08
	4	48.74	48.42	48.58	0.23
	5	49.68	49.12	49.40	0.40
	Average			49.20	0.24
5CA43FLC	1	48.74	49.17	48.95	0.30
	2	49.34	48.88	49.11	0.32
	3	50.17	50.90	50.54	0.52
	4	50.36	49.81	50.09	0.39
	5	49.34	48.88	49.11	0.32
	Average			49.56	0.37
5CA43FSC	1	49.31	51.21	50.26	1.35
	2	50.21	49.85	50.03	0.26
	3	50.55	49.72	50.14	0.59
	4	50.00	50.02	50.01	0.02
	5	49.41	50.14	49.78	0.52
	Average			49.98	0.46
5CA43HNC	1	48.22	48.05	48.13	0.12
	2	45.63	47.54	46.59	1.35
	3	49.37	48.82	49.10	0.39
	4	47.34	47.76	47.55	0.30
	5	47.53	47.19	47.36	0.24
	Average			47.75	0.48
5CA43HLC	1	46.60	49.01	47.81	1.71
	2	48.34	48.59	48.46	0.18
	3	48.04	49.47	48.75	1.01
	4	49.23	48.88	49.06	0.25
	5	48.27	48.05	48.16	0.15
	Average			48.45	0.66
5CA43HSC	1	47.95	48.14	48.04	0.13
	2	47.19	47.86	47.52	0.47
	3	48.50	47.41	47.95	0.77
	4	48.70	50.00	49.35	0.92
	5	47.91	49.11	48.51	0.85
	Average			48.23	0.55

Table A.2: Cross-Sectional Area Measurements for Carbon Specimens with Spiral Sleeves

Specimen Configuration		Cross-Sectional Area [mm^2]			
		End 1	End 2	Average	Std. Dev.
5CA10FNC	1	48.32	48.36	48.34	0.03
	2	50.10	50.71	50.40	0.43
	3	49.77	50.26	50.01	0.34
	4	49.60	49.79	49.69	0.13
	5	49.82	49.68	49.75	0.10
	6	49.84	49.84	49.84	0.00
	Average			49.67	0.17
5CA10FLC	1	48.77	49.93	49.35	0.82
	2	48.98	48.45	48.71	0.37
	3	47.97	48.81	48.39	0.60
	4	47.99	48.34	48.17	0.25
	5	50.22	48.91	49.57	0.93
	6	51.09	52.34	51.72	0.88
	Average			49.32	0.64
5CA10FSC	1	47.32	48.45	47.89	0.80
	2	49.48	49.12	49.30	0.25
	3	48.90	49.90	49.40	0.71
	4	48.88	49.40	49.14	0.37
	5	50.17	49.98	50.07	0.13
	6	49.70	49.68	49.69	0.01
	Average			49.25	0.38
5CA10HNC	1	50.18	49.36	49.77	0.58
	2	48.30	46.90	47.60	0.99
	3	50.72	50.69	50.70	0.02
	4	47.66	47.25	47.45	0.29
	5	47.35	48.74	48.04	0.98
	Average			48.38	0.51
5CA10HLC	1	49.79	50.19	49.99	0.28
	2	49.98	49.39	49.69	0.42
	3	46.30	48.54	47.42	1.58
	4	49.38	49.68	49.53	0.21
	5	49.08	49.84	49.46	0.54
	Average			49.22	0.61
5CA10HSC	1	49.23	50.72	49.97	1.06
	2	47.05	46.77	46.91	0.20
	3	48.18	46.07	47.13	1.50
	4	49.02	49.21	49.11	0.14
	5	45.20	46.08	45.64	0.62
	Average			48.10	0.75

Table A.3: Cross-Sectional Area Measurements for Fiberglass Specimens with Braided Sleeves

Specimen Configuration		Cross-Sectional Area [mm^2]			
		End 1	End 2	Average	Std. Dev.
5GA43FNC	1	43.24	43.29	43.27	0.04
	2	42.85	44.45	43.65	1.13
	3	43.62	43.58	43.60	0.03
	4	42.50	42.72	42.61	0.15
	5	40.90	40.78	40.84	0.09
	Average			42.90	0.36
5GA43FLC	1	43.71	43.85	43.78	0.10
	2	43.05	43.70	43.38	0.46
	3	44.62	42.80	43.71	1.29
	4	43.16	43.17	43.17	0.00
	5	43.73	43.68	43.71	0.04
	6	42.04	41.55	41.80	0.35
	Average			43.26	0.37
5GA43FSC	1	42.94	42.80	42.87	0.10
	2	42.94	43.37	43.15	0.30
	3	44.24	43.13	43.68	0.79
	4	43.76	43.19	43.48	0.40
	5	43.04	44.42	43.73	0.98
	6	42.18	42.32	42.25	0.10
	Average			43.19	0.45
5GA43HNC	1	44.29	44.26	44.27	0.03
	2	43.76	44.45	44.11	0.49
	3	40.82	43.61	42.21	1.98
	4	44.89	43.99	44.44	0.64
	5	45.40	44.61	45.01	0.56
	Average			43.97	0.62
5GA43HLC	1	43.76	44.03	43.89	0.20
	2	44.00	44.18	44.09	0.12
	3	44.78	44.02	44.40	0.54
	4	45.32	45.16	45.24	0.11
	5	44.42	43.88	44.15	0.38
	6	43.95	43.81	43.88	0.10
	Average			44.28	0.24
5GA43HSC	1	44.36	44.22	44.29	0.10
	2	44.47	44.22	44.34	0.17
	3	44.52	44.77	44.64	0.18
	4	44.28	44.74	44.51	0.32
	5	43.75	43.73	43.74	0.01
	Average			44.28	0.13

Table A.4: Cross-Sectional Area Measurements for Fiberglass Specimens with Spiral Sleeves

Specimen Configuration		Cross-Sectional Area [mm^2]			
		End 1	End 2	Average	Std. Dev.
5GA10FNC	1	44.85	44.76	44.80	0.06
	2	44.29	44.59	44.44	0.21
	3	43.87	44.06	43.97	0.13
	4	45.18	43.88	44.53	0.92
	5	44.58	44.20	44.39	0.26
	Average			44.39	0.36
5GA10FLC	1	43.58	43.19	43.39	0.27
	2	43.69	44.42	44.05	0.52
	3	44.87	44.20	44.53	0.47
	4	43.73	43.36	43.55	0.26
	5	45.12	44.00	44.56	0.80
	6				
	Average			44.02	0.46
5GA10FSC	1	44.73	45.15	44.94	0.29
	2	44.29	45.00	44.64	0.50
	3	44.00	43.62	43.81	0.27
	4	42.28	43.10	42.69	0.58
	5	44.25	43.77	44.01	0.34
	Average			43.94	0.40
5GA10HNC	1	45.31	43.82	44.57	1.06
	2	45.57	44.87	45.22	0.50
	3	44.86	45.20	45.03	0.24
	4	44.73	45.32	45.02	0.42
	5	45.32	45.21	45.27	0.07
	Average			45.19	0.41
5GA10HLC	1	44.80	43.25	44.03	1.09
	2	44.21	44.36	44.28	0.10
	3	44.19	45.31	44.75	0.79
	4	43.83	44.79	44.31	0.68
	5	44.15	43.88	44.02	0.19
	6	43.06	45.66	44.36	1.84
	Average			44.29	0.78
5GA10HSC	1	44.92	44.50	44.71	0.29
	2	44.76	43.73	44.25	0.73
	3	45.22	45.44	45.33	0.16
	4	44.19	45.38	44.79	0.84
	5	45.42	45.24	45.33	0.13
	Average			44.95	0.37

Table A.5: Offset Measurements for Carbon Specimens with Braided Sleeves

Specimen Configuration		Offset					
		Top		Bottom		Total	Angle
		X	Y	X	Y		
		[mm]					[Deg.]
5CA43FNC	1	-0.238	-0.429	0.357	-0.190	0.6411	0.4132
	2	0.071	-0.595	0.429	0.333	0.9949	0.6412
	3	0.119	0.048	-0.357	0.286	0.5324	0.3431
	4	0.905	0.405	0.500	-0.095	0.6433	0.4146
	5	-0.500	-0.571	-0.071	0.429	1.0880	0.7012
	Average					0.7799	0.5026
	St Dev.					0.2451	0.1580
5CA43FLC	1	0.024	-0.333	0.071	0.190	0.5260	0.3390
	2	0.048	-0.548	-0.357	-0.286	0.4821	0.3107
	3	-0.071	-0.595	-0.119	-0.071	0.5260	0.3390
	4	0.381	0.333	0.000	0.167	0.4158	0.2680
	5	0.500	-0.286	-0.095	-0.357	0.5995	0.3864
	Average					0.5099	0.3286
	St Dev.					0.0674	0.0434
5CA43FSC	1	0.476	0.619	0.667	-0.619	1.2527	0.8073
	2	-0.238	-0.310	-0.333	0.214	0.5324	0.3431
	3	-0.071	-0.048	0.000	-0.524	0.4815	0.3103
	4	0.048	-0.238	0.119	-0.190	0.0858	0.0553
	5						
	6	-0.643	0.048	-0.762	0.071	0.1214	0.0782
	Average					0.4948	0.3189
	St Dev.					0.2342	0.1510
5CA43HNC	1	-0.167	-0.286	-0.167	0.167	0.4524	0.2916
	2	-0.143	-0.262	-0.167	0.429	0.6909	0.4453
	3	0.238	0.048	-0.214	0.000	0.4549	0.2932
	4	0.262	0.333	-0.119	0.214	0.3991	0.2572
	5	-0.286	0.262	-0.167	0.167	0.1524	0.0982
	Average					0.4299	0.2771
	St Dev.					0.1918	0.1236
5CA43HLC	1	-0.381	0.048	-0.167	-0.119	0.0532	0.0343
	2	0.048	0.048	0.024	0.000	0.1448	0.0933
	3	0.048	-0.071	-0.095	-0.048	0.9246	0.5959
	4	1.357	-0.119	0.452	0.071	0.3941	0.2540
	5						
	6	-0.143	-0.071	0.024	-0.429	0.7619	0.4910
	Average					0.4557	0.2937
	St Dev.					0.3794	0.2446
5CA43HSC	1	0.143	0.190	-0.095	0.548	0.4292	0.2766
	2	0.048	0.310	0.000	0.048	0.2662	0.1716
	3	0.024	0.095	0.214	0.357	0.3238	0.2087
	4	0.357	-0.286	-0.429	-0.500	0.8144	0.5249
	5	0.524	0.214	0.000	0.286	0.5287	0.3407
	Average					0.4725	0.3045
	St Dev.					0.2159	0.1392

Table A.6: Offset Measurements for Carbon Specimens with Spiral Sleeves

Specimen Configuration		Offset					
		Top		Bottom		Total	Angle
		X	Y	X	Y		
		[mm]					[Deg.]
5CA10FNC	1	0.143	0.119	0.452	-0.095	0.3765	0.2426
	2	0.476	0.310	-0.286	0.000	0.8224	0.5300
	3	-0.310	-0.095	-0.095	0.119	0.3030	0.1953
	4	-0.714	-0.071	-0.643	0.286	0.3642	0.2347
	5	-0.119	-0.357	-0.238	0.310	0.6772	0.4364
	6	0.000	-0.429	0.119	-0.214	0.2451	0.1580
	Average					0.4647	0.2995
	St Dev.					0.2303	0.1485
5CA10FLC	1	0.262	0.048	-0.071	0.524	0.5813	0.3746
	2	-0.119	-0.048	-0.071	-0.071	0.0532	0.0343
	3	0.071	-0.619	0.405	0.310	0.9866	0.6358
	4	-0.167	0.048	-0.167	-0.262	0.3095	0.1995
	5	-0.214	0.262	0.000	0.119	0.2575	0.1660
	6	0.476	0.214	0.167	0.119	0.3238	0.2087
	Average					0.4187	0.2698
	St Dev.					0.3253	0.2097
5CA10FSC	1						
	2	-0.048	-0.119	0.310	-0.071	0.3603	0.2322
	3	0.119	0.000	-0.119	0.071	0.2486	0.1602
	4	0.881	-0.500	0.524	0.286	0.8631	0.5562
	5	0.190	0.048	0.119	-0.119	0.1813	0.1169
	6	0.095	0.095	-0.500	0.190	0.6028	0.3885
	Average					0.4512	0.2908
	St Dev.					0.2805	0.1808
5CA10HNC	1	0.262	0.190	-0.595	-0.071	0.8963	0.5776
	2	0.357	-0.119	0.143	-0.167	0.2195	0.1415
	3	-0.167	0.048	-0.095	-0.071	0.1388	0.0895
	4	-0.286	-0.333	0.000	-0.119	0.3571	0.2302
	5	-0.024	0.167	-0.286	0.143	0.2630	0.1695
	Average					0.3749	0.2416
	St Dev.					0.3018	0.1946
5CA10HLC	1	-0.524	-0.476	-0.119	-0.405	0.4110	0.2649
	2	-0.143	0.262	-0.143	0.119	0.1429	0.0921
	3	0.500	-0.143	-0.524	-0.429	1.0629	0.6850
	4	-0.214	-0.071	0.119	-0.071	0.3333	0.2148
	5						
	6	-0.071	0.262	0.000	0.167	0.1190	0.0767
	Average					0.3449	0.2223
	St Dev.	-0.143	0.190	0.000	0.405	0.3823	0.2464
5CA10HSC	1	0.143	0.190	-0.095	0.548	0.2130	0.1373
	2	0.048	0.310	0.000	0.048	0.6709	0.4324
	3	0.024	0.095	0.214	0.357	0.4580	0.2952
	4	0.357	-0.286	-0.429	-0.500	0.1065	0.0686
	5	0.524	0.214	0.000	0.286	0.3839	0.2474
	Average					0.3562	0.2296
	St Dev.					0.1978	0.1275

Table A.7: Offset Measurements for Fiberglass Specimens with Braided Sleeves

Specimen Configuration		Offset					
		Top		Bottom		Total	Angle
		X	Y	X	Y		
		[mm]					[Deg.]
5GA43FNC	1	-0.595	0.119	0.333	0.095	0.9289	0.5986
	2	-0.095	-0.048	-0.071	-0.095	0.0528	0.0340
	3	0.190	-0.452	0.071	0.214	0.6772	0.4365
	4	0.024	-0.238	-0.619	-0.095	0.6585	0.4244
	5	0.833	-0.429	-0.548	-0.262	1.3910	0.8964
	Average					0.7417	0.4780
	St Dev.					0.4853	0.3128
5GA43FLC	1	0.738	-0.357	-0.381	-0.190	1.1314	0.7291
	2	0.071	-0.452	0.238	-0.143	0.3515	0.2266
	3	-0.476	0.262	1.262	0.714	1.7960	1.1574
	4						
	5	0.119	0.357	-0.119	-0.143	0.5538	0.3569
	6	0.262	-0.405	0.095	-0.429	0.1684	0.1085
	Average					0.8002	0.5157
	St Dev.					0.6638	0.4278
5GA43FSC	1	-0.119	-0.167	0.310	-0.452	0.5151	0.3320
	2	0.095	0.167	0.095	-0.071	0.2381	0.1535
	3	-0.286	0.071	0.762	-0.905		
	4	0.214	-0.071	0.262	-0.119	0.0673	0.0434
	5	1.095	0.524	-1.619	0.024	2.7600	1.7782
	6	-1.071	0.286	0.310	-0.238	1.4769	0.9518
	Average					1.0115	0.6519
	St Dev.					1.1191	0.7212
5GA43HNC	1	-0.238	-0.119	0.262	0.095	0.1024	0.0660
	2	0.095	0.095	0.214	-0.095	0.2867	0.1848
	3	0.190	0.143	-0.429	0.071	0.0957	0.0617
	4	-0.429	0.119	-0.286	-0.095	0.2575	0.1660
	5	0.286	0.000	-0.286	-0.048	0.5734	0.3695
	Average					0.2632	0.1696
	St Dev.					0.1941	0.1251
5GA43HLC	1	-0.119	-0.095	0.214	-0.024	0.3409	0.2197
	2	-0.238	-0.119	0.262	0.095	0.5440	0.3506
	3	0.095	0.095	0.214	-0.095	0.2246	0.1448
	4	0.190	-0.238	0.095	-0.262	0.0982	0.0633
	5	-0.286	-0.095	-0.071	-0.190	0.2345	0.1511
	6	-0.048	0.143	0.167	-0.048	0.2867	0.1848
	Average					0.2881	0.1857
	St Dev.					0.1491	0.0961
5GA43HSC	1	0.095	0.000	-0.024	-0.167	0.2048	0.1320
	2	0.119	-0.143	-0.238	-0.262	0.3765	0.2426
	3	-0.143	-0.333	0.381	-0.190	0.5429	0.3499
	4	0.119	0.000	0.095	-0.214	0.2156	0.1390
	5	-0.095	-0.048	-0.071	-0.095	0.0532	0.0343
	Average					0.2786	0.1796
	St Dev.					0.1868	0.1204

Table A.8: Offset Measurements for Fiberglass Specimens with Spiral Sleeves

Specimen Configuration		Offset					
		Top		Bottom		Total	Angle
		X	Y	X	Y		
		[mm]					[Deg.]
5GA10FNC	1	-0.071	0.167	-0.095	-0.190	0.3579	0.2307
	2	-0.048	0.238	0.333	-0.071	0.4908	0.3163
	3	-0.143	-0.486	0.095	0.024	0.5624	0.3625
	4	-0.452	0.238	-0.119	0.071	0.3727	0.2402
	5	-0.190	0.214	-0.095	0.000	0.2345	0.1511
	Average					0.4037	0.2602
	St Dev.					0.1269	0.0818
5GA10FLC	1	0.286	0.500	0.452	-0.524	1.0373	0.6685
	2	-0.143	-0.486	-0.195	-0.164	0.3261	0.2102
	3	-0.152	0.238	-0.119	0.271	0.0471	0.0304
	4	0.190	0.190	0.524	-0.048	0.4096	0.2640
	5	0.352	0.119	-0.071	0.262	0.4472	0.2882
	6						
	Average					0.4535	0.2923
	St Dev.					0.3619	0.2333
5GA10FSC	1	0.119	-0.952	-0.214	0.024	1.0316	0.6648
	2						
	3	-0.405	-0.333	-0.262	-0.452	0.1860	0.1199
	4	-0.119	0.357	-0.143	0.095	0.2630	0.1695
	5	0.143	-0.071	0.024	-0.190	0.1684	0.1085
	6	0.452	0.119	-0.071	0.262	0.5429	0.3499
	Average					0.4384	0.2825
	St Dev.					0.36406	0.2346
5GA10HNC	1	-0.214	0.548	0.000	0.333	0.3031	0.1953
	2	-0.405	-0.095	-0.524	0.024	0.1684	0.1085
	3	-0.024	0.000	0.310	0.333	0.4714	0.3038
	4	0.190	-0.238	0.095	-0.262	0.0980	0.0632
	5	-0.286	-0.095	-0.071	-0.190	0.2351	0.1515
	Average					0.2552	0.1645
	St Dev.					0.1429	0.0921
5GA10HLC	1	-0.119	-0.095	0.214	-0.024	0.3409	0.2197
	2	-0.238	-0.119	0.262	0.095	0.5440	0.3506
	3	0.095	0.095	0.214	-0.095	0.2246	0.1448
	4	0.190	-0.238	0.095	-0.262	0.0982	0.0633
	5	-0.286	-0.095	-0.071	-0.190	0.2345	0.1511
	6	-0.048	0.143	0.167	-0.048	0.2867	0.1848
	Average					0.2881	0.1857
	St Dev.					0.1491	0.0961
5GA10HSC	1	-0.048	0.238	0.143	0.000	0.3049	0.1965
	2	0.071	-0.071	-0.119	0.024	0.2130	0.1373
	3	0.095	-0.095	0.405	0.500	0.6709	0.4324
	4	-0.071	-0.167	0.381	-0.095	0.4580	0.2952
	5	0.143	-0.310	0.048	-0.262	0.1065	0.0686
	Average					0.3507	0.2260
	St Dev.					0.2206	0.1422

Table A.9: Sleeve Coverage Measurements for Half Coverage Carbon Specimens

Specimen Configuration		Not Covered [%]						Average Coverage
		1	2	3	4	Avg.	St. Dev.	[%]
5CA43HNC	1	34.91	11.75	11.94	18.72	19.33	10.88	80.7
	2	13.47	11.65	14.61	26.82	16.64	6.89	83.4
	3	20.51	48.19	15.76	8.02	23.12	17.49	76.9
	4	9.10	25.69	43.04	13.37	22.80	15.22	77.2
	5	26.10	9.79	25.23	7.57	17.17	9.86	82.8
	Average							80.2
	St Dev.							3.0
5CA43HLC	1	50.62	3.34	4.23	34.07	23.06	23.27	76.9
	2	28.37	18.71	51.15	27.23	31.36	13.88	68.6
	3	21.81	17.82	11.94	26.92	19.62	6.33	80.4
	4	30.46	0.36	14.89	58.91	26.15	25.06	73.8
	5	21.26	8.95	22.71	3.96	14.22	9.21	85.8
	6							
	Average							74.6
	St Dev.							9.7
5CA10HSC	1	22.81	15.35	24.17	10.08	18.10	6.61	81.9
	2	5.55	34.83	31.06	4.15	18.90	16.31	81.1
	3	33.66	5.57	37.02	37.95	28.55	15.43	71.5
	4	11.31	23.84	7.44	35.00	19.40	12.54	80.6
	5	34.19	83.22	11.00	1.12	32.38	36.62	67.6
	Average							75.2
	St Dev.							6.7
5CA10HNC	1	63.89	54.54	58.64	46.72	55.95	7.25	44.1
	2	60.98	54.04	59.01	64.01	59.51	4.18	40.5
	3	44.43	52.55	51.88	45.76	48.66	4.16	51.3
	4	54.30	67.57	66.81	54.50	60.79	7.39	39.2
	5	56.62	52.56	47.51	46.67	50.84	4.65	49.2
	Average							44.3
	St Dev.							4.9
5CA10HLC	1	49.39	48.42	52.45	48.03	49.58	2.00	50.4
	2	51.75	57.25	53.68	47.64	52.58	4.00	47.4
	3	73.28	71.84	73.53	78.26	74.23	2.79	25.8
	4	44.52	35.99	27.88	32.92	35.33	6.98	64.7
	5	38.32	47.82	48.68	46.67	45.37	4.77	54.6
	6							
	Average							48.6
	St Dev.							14.3
5CA10HSC	1	53.47	53.88	54.93	61.22	55.88	3.62	44.1
	2	45.02	31.84	35.36	43.36	38.90	6.32	61.1
	3	64.81	72.92	58.36	65.88	65.49	5.96	34.5
	4	61.95	53.67	49.63	52.16	54.35	5.33	45.6
	5	54.10	44.24	41.83	53.25	48.35	6.23	51.6
	Average							45.2
	St Dev.							10.4

Table A.10: Sleeve Coverage Measurements for Half Coverage Fiberglass Specimens

Specimen Configuration		Not Covered [%]						Average Coverage
		1	2	3	4	Avg.	St. Dev.	[%]
5GA43HNC	1	34.91	11.75	11.94	18.72	19.33	10.88	80.7
	2	13.47	11.65	14.61	26.82	16.64	6.89	83.4
	3	20.51	48.19	15.76	8.02	23.12	17.49	76.9
	4	9.10	25.69	43.04	13.37	22.80	15.22	77.2
	5	26.10	9.79	25.23	7.57	17.17	9.86	82.8
	Average							80.2
	St Dev.							3.0
5GA43HLC	1	50.62	3.34	4.23	34.07	23.06	23.27	76.9
	2	28.37	18.71	51.15	27.23	31.36	13.88	68.6
	3	21.81	17.82	11.94	26.92	19.62	6.33	80.4
	4	30.46	0.36	14.89	58.91	26.15	25.06	73.8
	5	21.26	8.95	22.71	3.96	14.22	9.21	85.8
	6							
	Average							74.6
	St Dev.							9.7
5GA43HSC	1	22.81	15.35	24.17	10.08	18.10	6.61	81.9
	2	5.55	34.83	31.06	4.15	18.90	16.31	81.1
	3	33.66	5.57	37.02	37.95	28.55	15.43	71.5
	4	11.31	23.84	7.44	35.00	19.40	12.54	80.6
	5	34.19	83.22	11.00	1.12	32.38	36.62	67.6
	Average							75.2
	St Dev.							6.7
5GA10HNC	1	63.89	54.54	58.64	46.72	55.95	7.25	44.1
	2	60.98	54.04	59.01	64.01	59.51	4.18	40.5
	3	44.43	52.55	51.88	45.76	48.66	4.16	51.3
	4	54.30	67.57	66.81	54.50	60.79	7.39	39.2
	5	56.62	52.56	47.51	46.67	50.84	4.65	49.2
	Average							44.3
	St Dev.							4.9
5GA10HLC	1	49.39	48.42	52.45	48.03	49.58	2.00	50.4
	2	51.75	57.25	53.68	47.64	52.58	4.00	47.4
	3	73.28	71.84	73.53	78.26	74.23	2.79	25.8
	4	44.52	35.99	27.88	32.92	35.33	6.98	64.7
	5	38.32	47.82	48.68	46.67	45.37	4.77	54.6
	6							
	Average							48.6
	St Dev.							14.3
5GA10HSC	1	53.47	53.88	54.93	61.22	55.88	3.62	44.1
	2	45.02	31.84	35.36	43.36	38.90	6.32	61.1
	3	64.81	72.92	58.36	65.88	65.49	5.96	34.5
	4	61.95	53.67	49.63	52.16	54.35	5.33	45.6
	5	54.10	44.24	41.83	53.25	48.35	6.23	51.6
	Average							45.2
	St Dev.							10.4

APPENDIX B: PICTURES OF SPECIMENS AT FAILURE

Appendix B contains failure pictures of all tested specimens investigated in this research. Figure B.1 and Figure B.2 show full braided and half braided sleeves of carbon/epoxy elements, respectively. Full and half spiral carbon specimens are shown in Figure B.3 and Figure B.4, respectively. Figure B.5 and Figure B.6 show full braided and half braided sleeves of fiberglass/epoxy elements, respectively. Full and half spiral fiberglass specimens are shown in Figure B.7 and Figure B.8, respectively.

Figure B.1: Pictures of Full Braid Carbon Specimens After Failure

Figure B.2: Pictures of Half Braid Carbon Specimens After Failure

Figure B.3: Pictures of Full Spiral Carbon Specimens After Failure

Figure B.4: Pictures of Half Spiral Carbon Specimens After Failure

Figure B.5: Pictures of Full Braid Fiberglass Specimens After Failure

Figure B.6: Pictures of Half Braid Fiberglass Specimens After Failure

Figure B.7: Pictures of Full Spiral Fiberglass Specimens After Failure

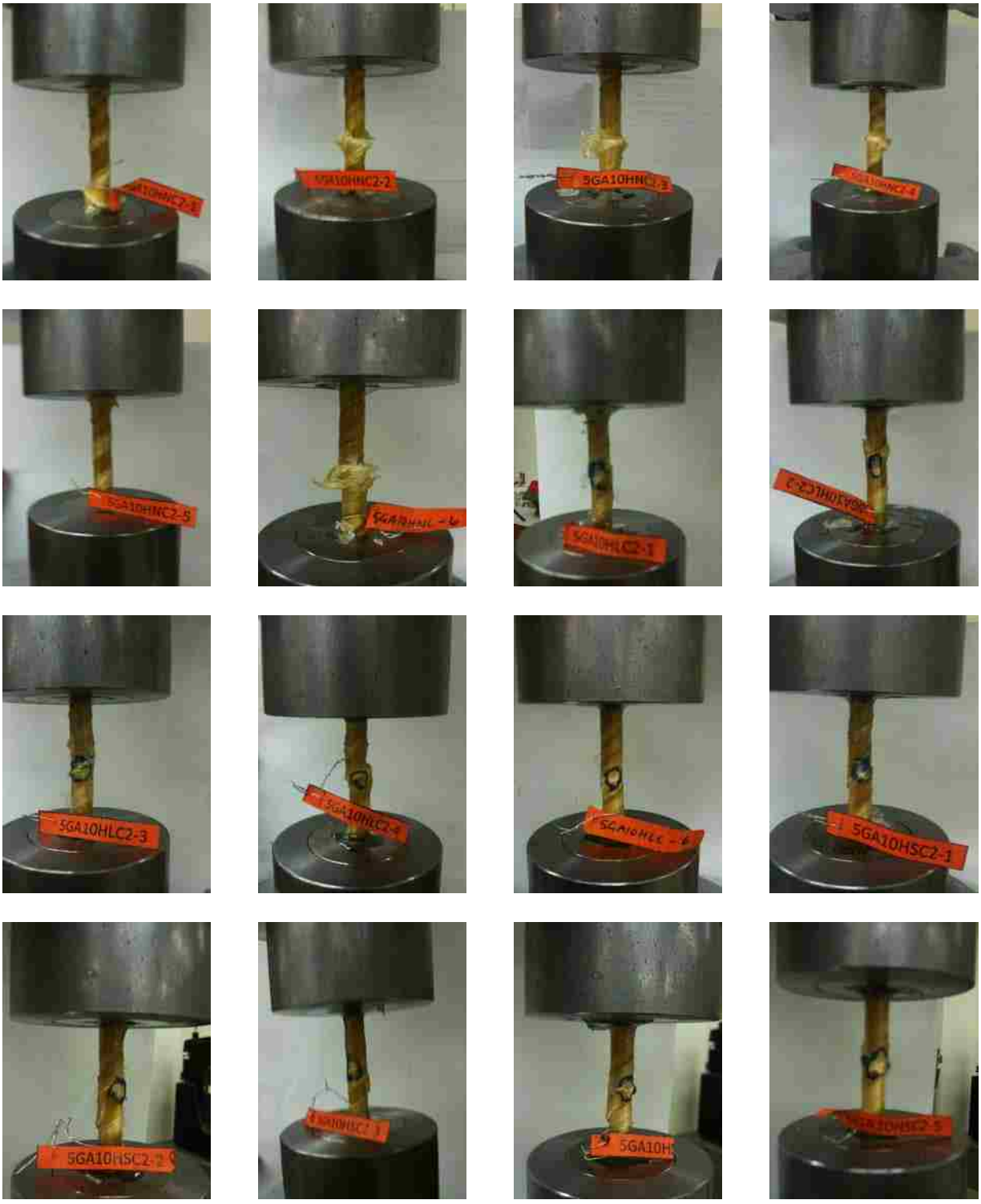

Figure B.8: Pictures of Half Spiral Fiberglass Specimens After Failure

APPENDIX C: JUSTIFICATION FOR DISCARDED OUTLIERS

This section demonstrates stress-strain curves with Chauvenet's envelope that justifies specimens that were considered outliers and were not included in the final data results. Specimens that were excluded from the final data results are color coded and shown in dotted line.

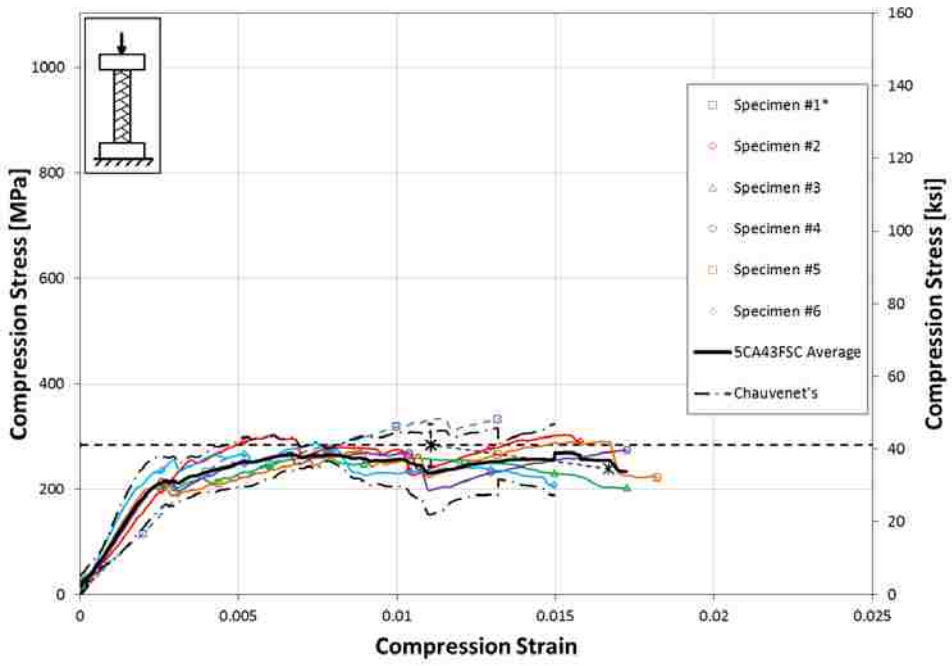

Figure C.1: Chauvenet's Envelope and Stress-Strain Curves for Full Braid, 10 J (7.4 ft-lbs) Impact, Carbon Specimens (5CA43FSC)

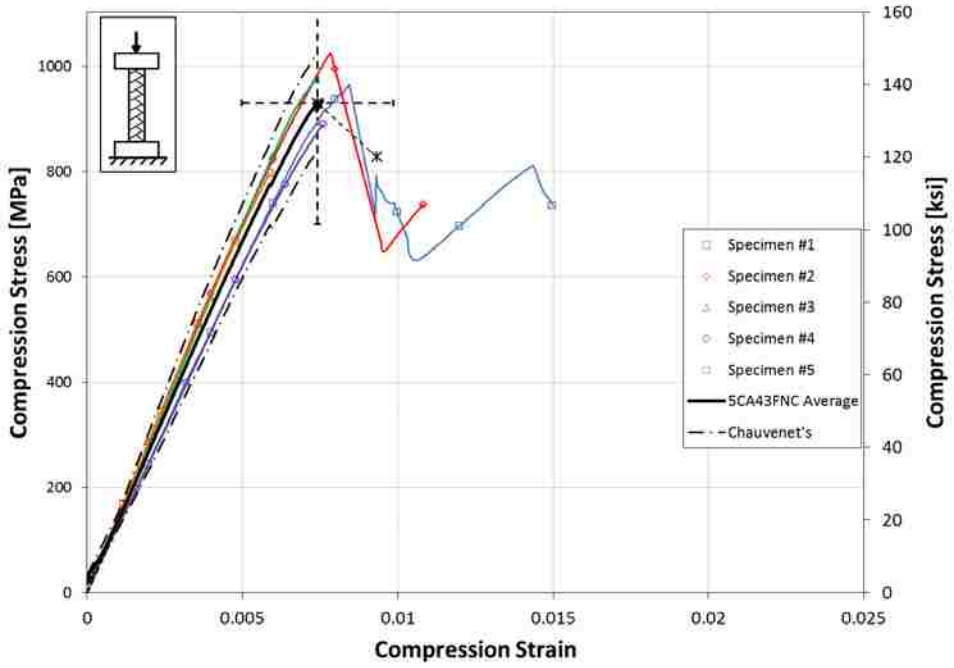

Figure C.2: Chauvenet's Envelope and Stress-Strain Curves for Full Braid, Undamaged, Carbon Specimens (5CA43FNC)

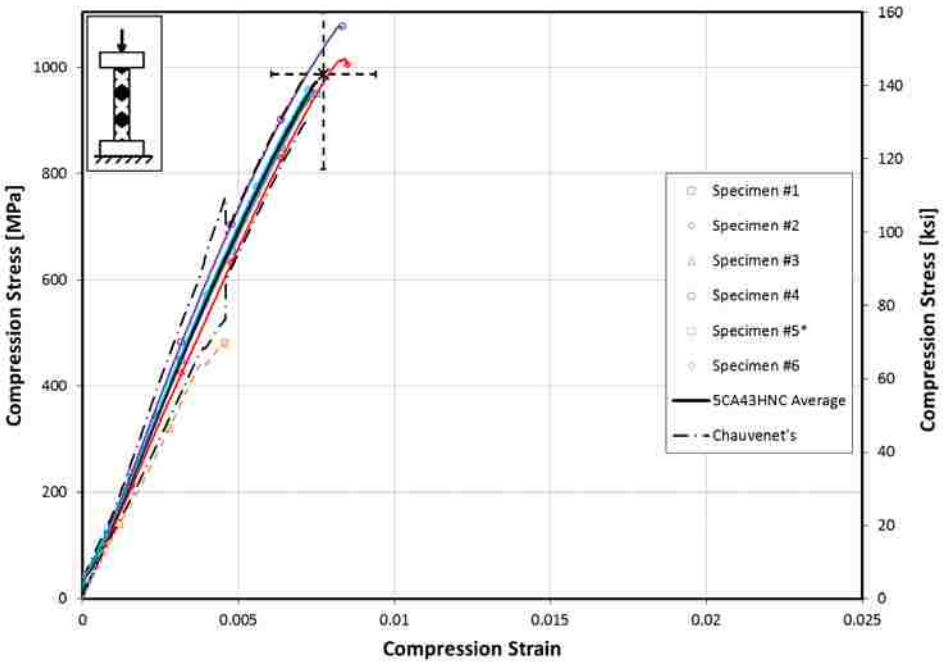

Figure C.3: Chauvenet's Envelope and Stress-Strain Curves for Half Braid, Undamaged, Carbon Specimens (5CA43HNC)

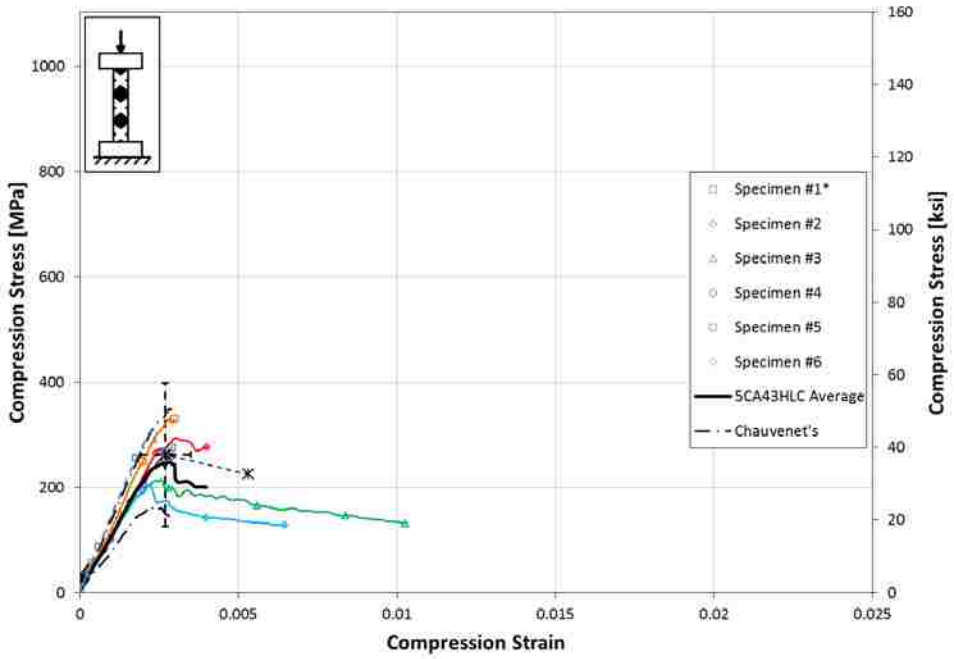

Figure C.4: Chauvenet's Envelope and Stress-Strain Curves for Half Braid, 5 J (3.7 ft-lbs) Impact, Carbon Specimens (5CA43HLC)

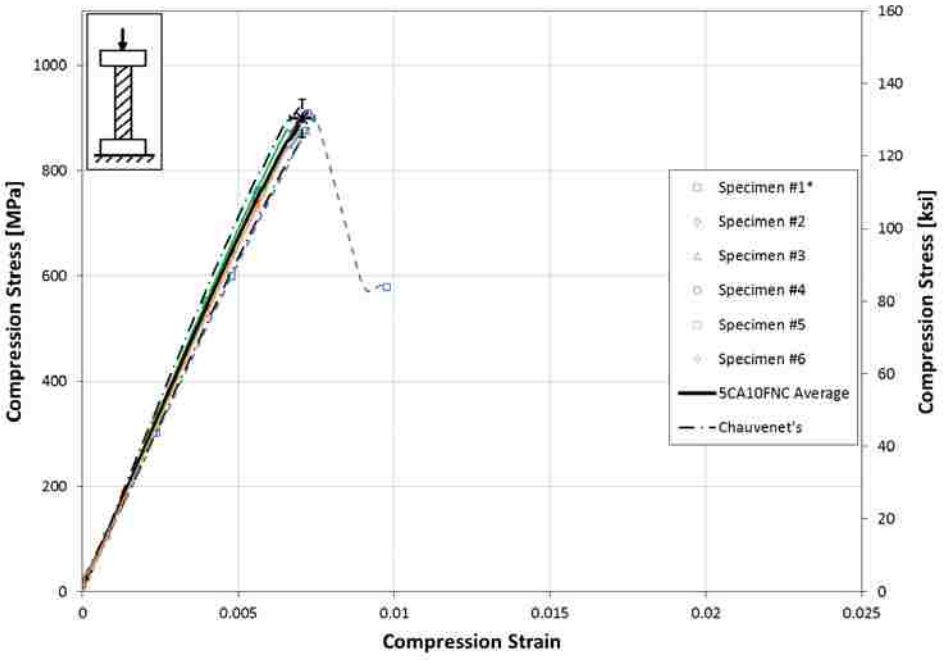

Figure C.5: Chauvenet's Envelope and Stress-Strain Curves for Full Spiral, Undamaged, Carbon Specimens (5CA10FNC)

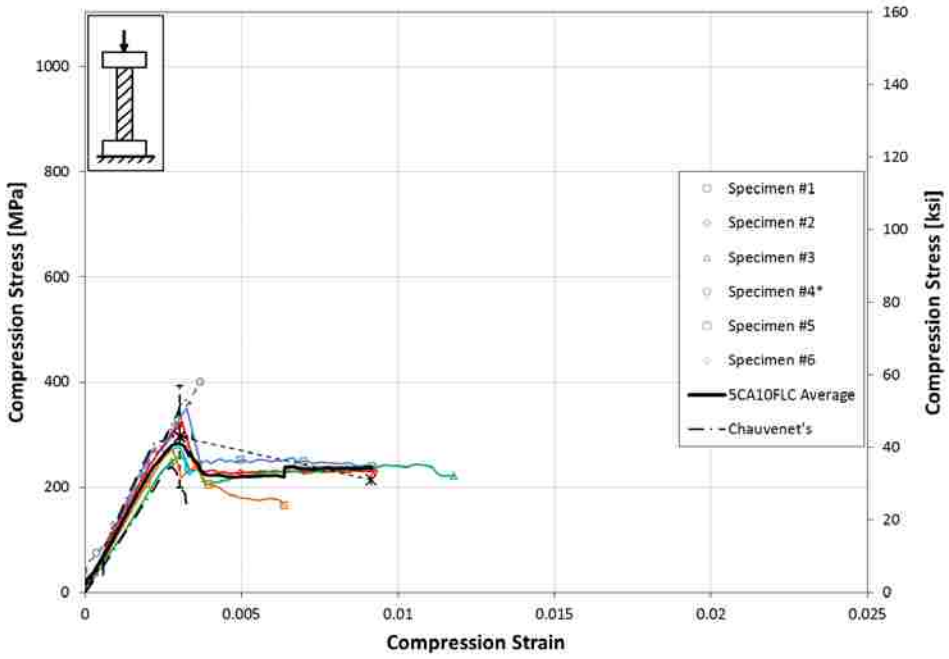

Figure C.6: Chauvenet's Envelope and Stress-Strain Curves for Full Spiral, 5 J (3.7 ft-lbs) Impact, Carbon Specimens (5CA10FLC)

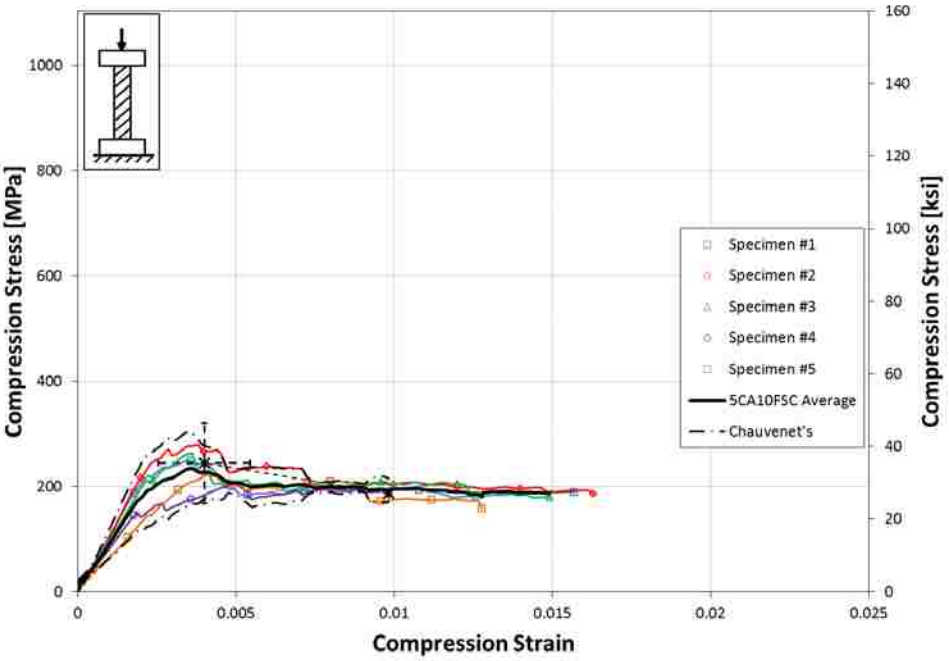

Figure C.7: Chauvenet's Envelope and Stress-Strain Curves for Full Spiral,10 J (7.4 ft-lbs) Impact, Carbon Specimens (5CA43HNC)

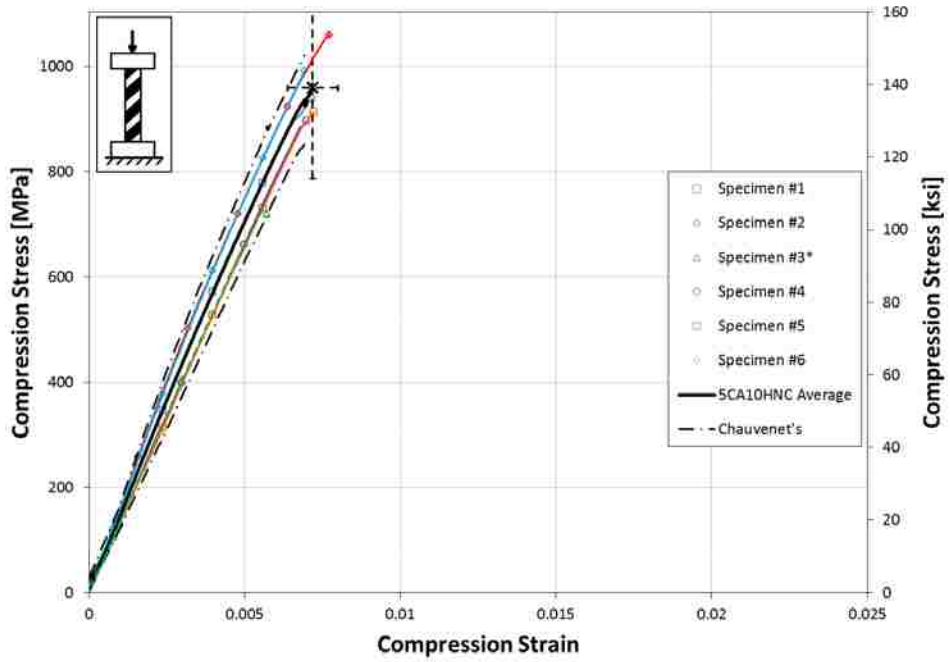

Figure C.8: Chauvenet's Envelope and Stress-Strain Curves for Half Spiral, Undamaged, Carbon Specimens (5CA10HNC)

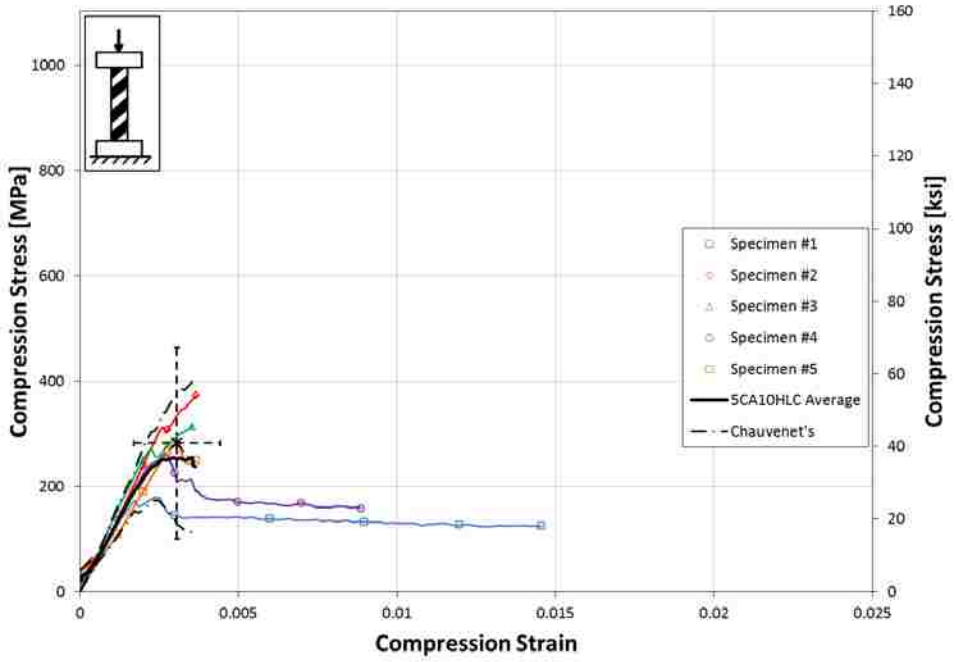

Figure C.9: Chauvenet's Envelope and Stress-Strain Curves for Half Spiral,5 J (3.7 ft-lbs) Impact, Carbon Specimens (5CA10HLC)

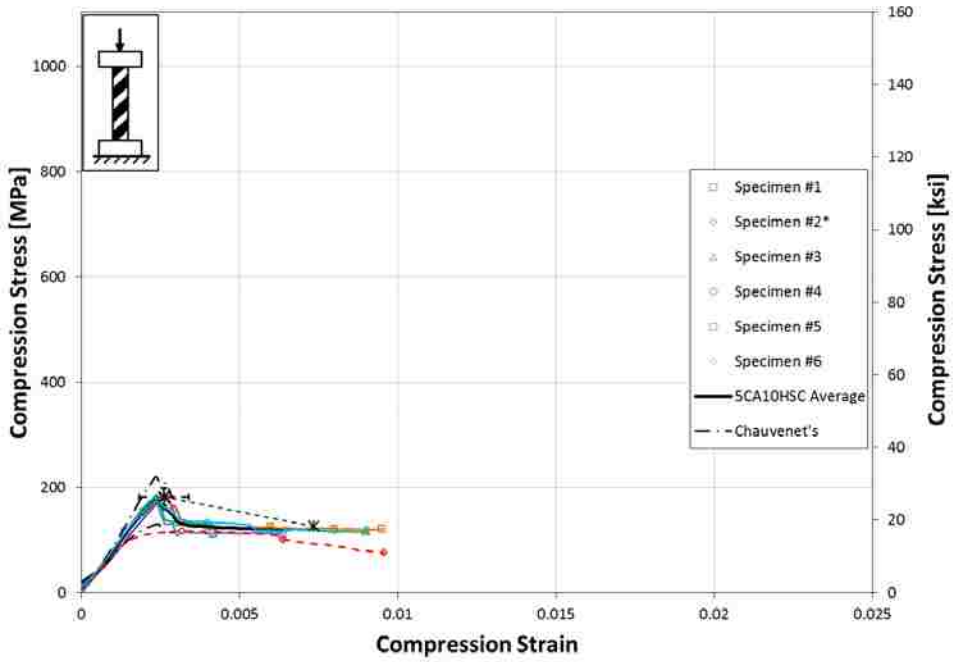

Figure C.10: Chauvenet's Envelope and Stress-Strain Curves for Half Spiral, 10 J (7.4 ft-lbs) Impact, Carbon Specimens (5CA43HNC)

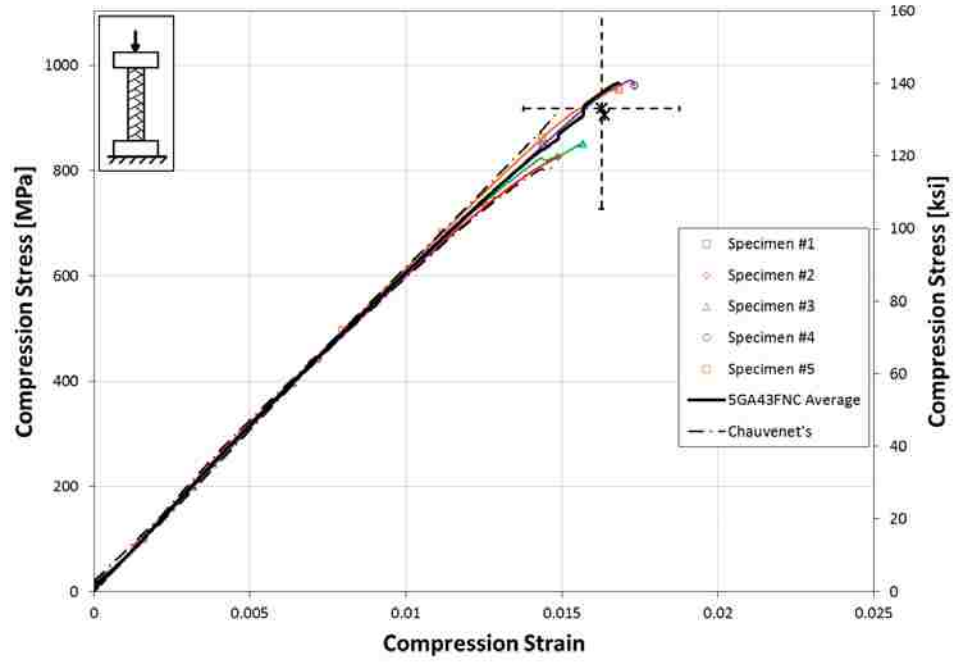

Figure C.11: Chauvenet's Envelope and Stress-Strain Curves for Full Braid, Undamaged, Fiberglass Specimens (5GA43FNC)

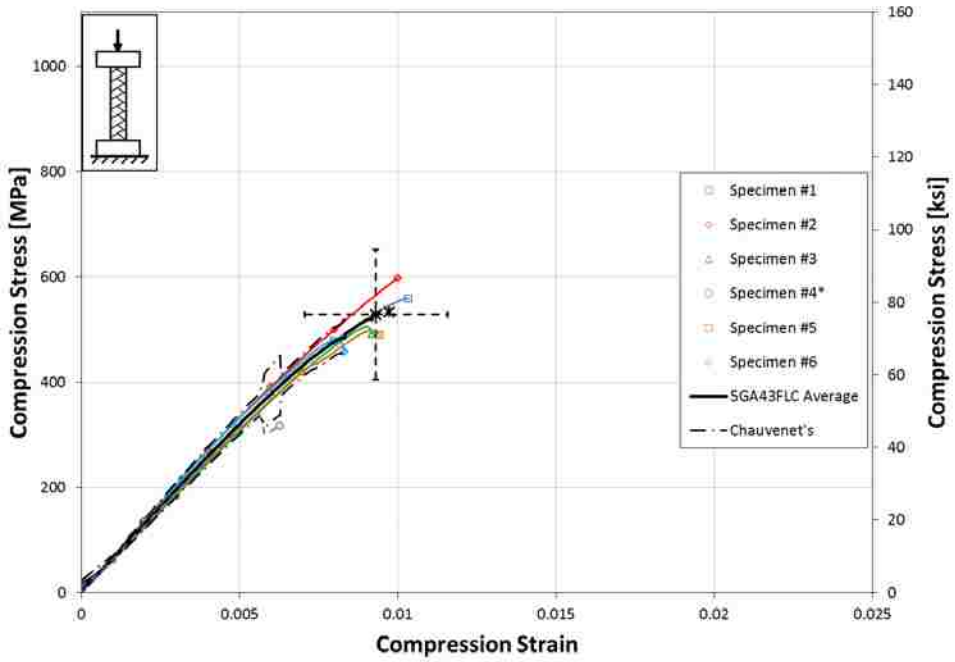

Figure C.12: Chauvenet's Envelope and Stress-Strain Curves for Full Braid, 5 J (3.7 ft-lbs) Impact, Fiberglass Specimens (5GA43FLC)

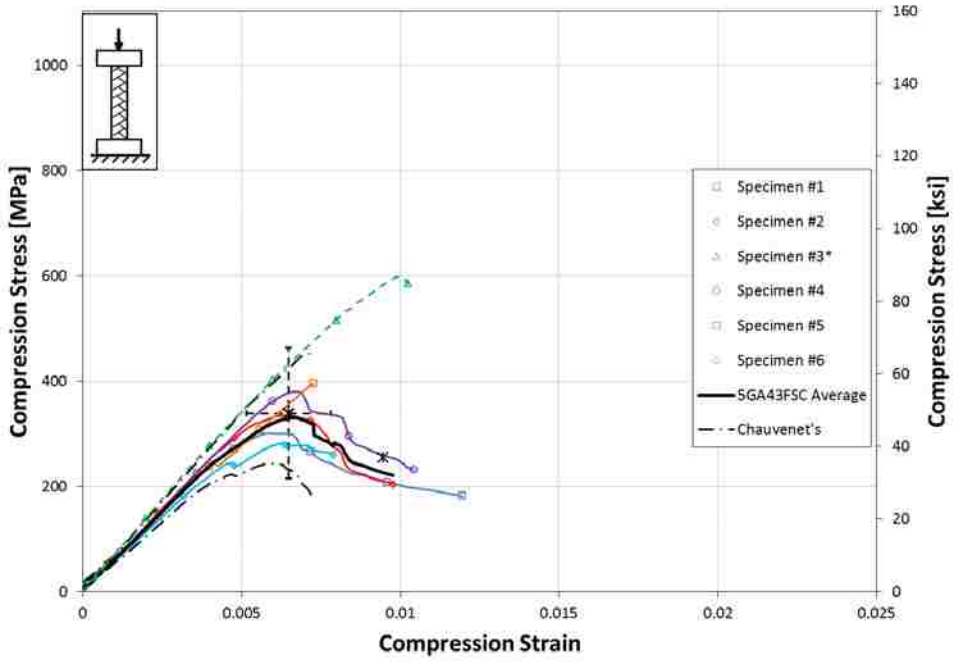

Figure C.13: Chauvenet's Envelope and Stress-Strain Curves for Full Braid, 10 J (7.4 ft-lbs) Impact, Fiberglass Specimens (5GA43FSC)

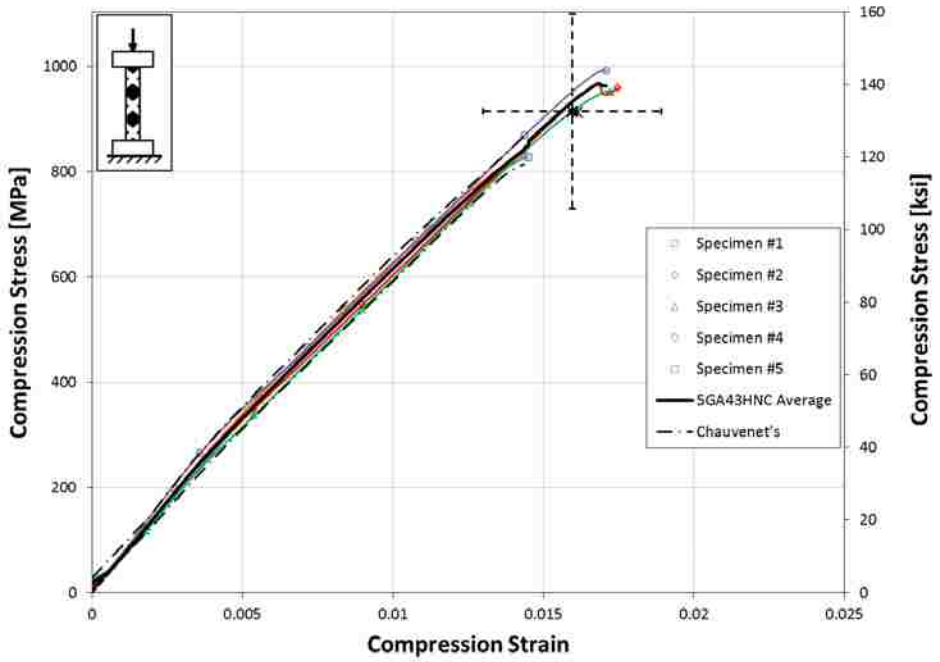

Figure C.14: Chauvenet's Envelope and Stress-Strain Curves for Half Braid, Undamaged, Fiberglass Specimens (5GA43HNC)

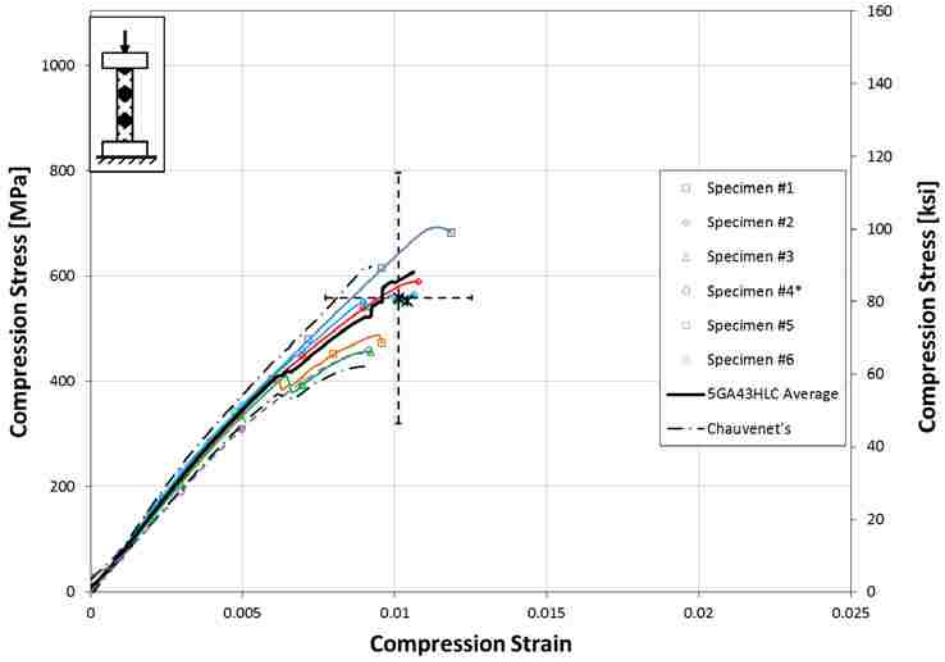

Figure C.15: Chauvenet's Envelope and Stress-Strain Curves for Half Braid, 5 J (3.7 ft-lbs) Impact, Fiberglass Specimens (5GA43HLC)

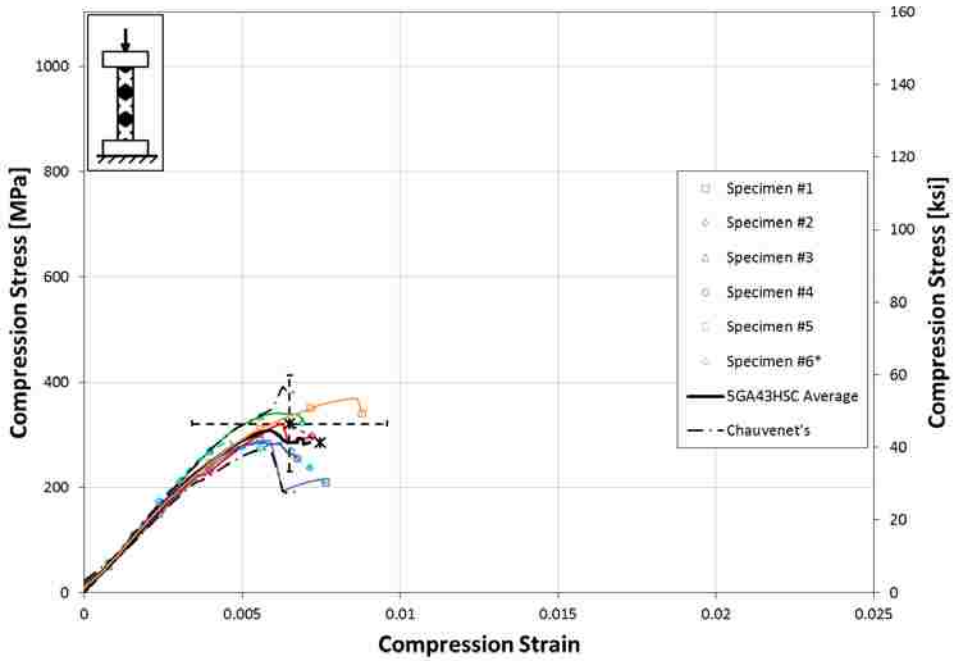

Figure C.16: Chauvenet's Envelope and Stress-Strain Curves for Half Braid, 10 J (7.4 ft-lbs) Impact, Fiberglass Specimens (5GA43HSC)

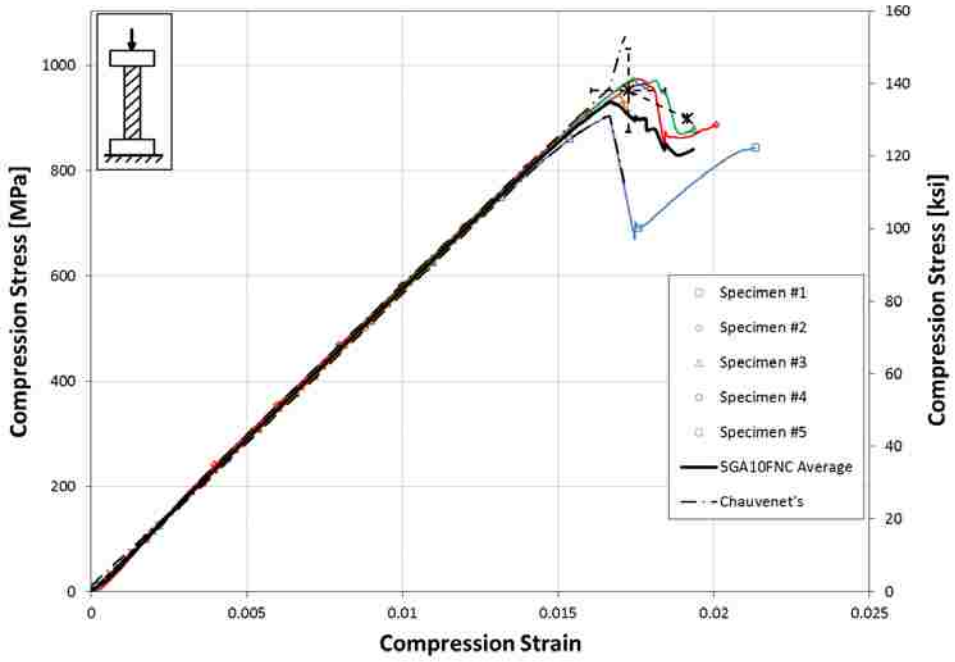

Figure C.17: Chauvenet's Envelope and Stress-Strain Curves for Full Spiral, Undamaged, Fiberglass Specimens (5GA10FNC)

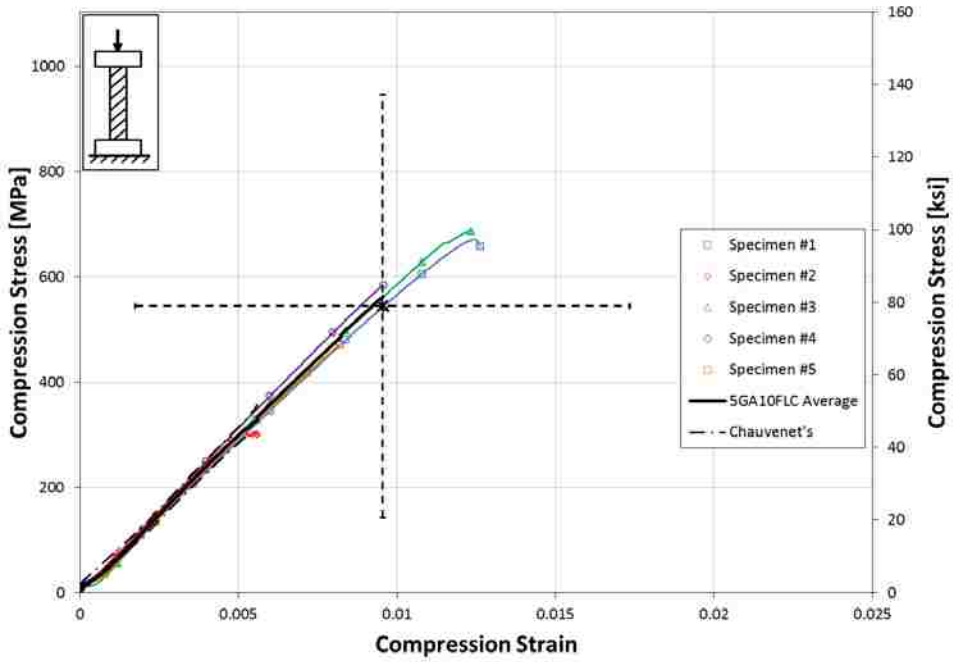

Figure C.18: Chauvenet's Envelope and Stress-Strain Curves for Full Spiral, 5 J (3.7 ft-lbs) Impact, Fiberglass Specimens (5GA10FLC)

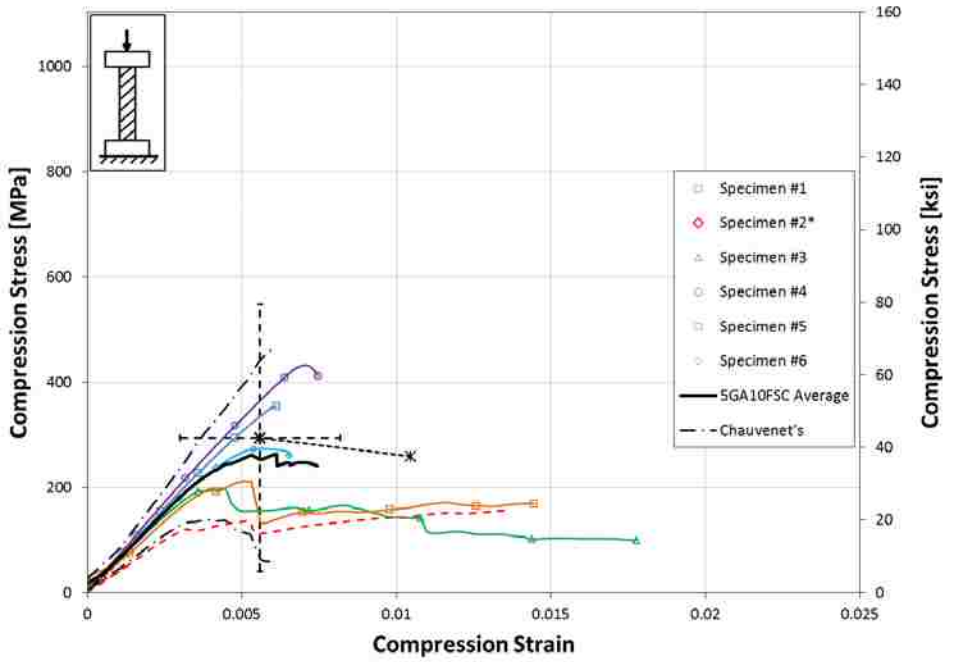

Figure C.19: Chauvenet's Envelope and Stress-Strain Curves for Full Spiral, 10 J (7.4 ft-lbs) Impact, Fiberglass Specimens (5GA10FSC)

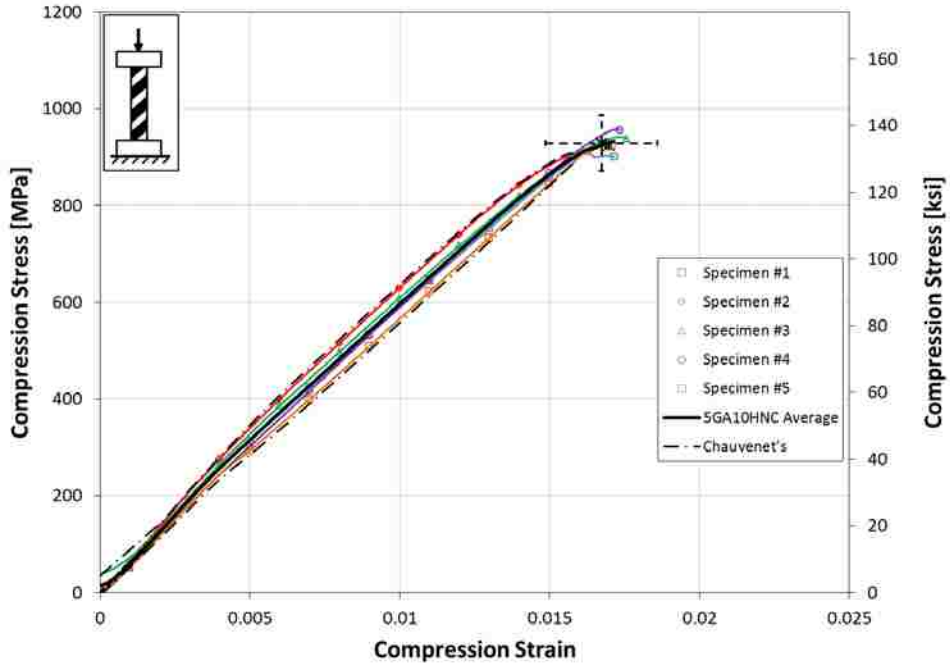

Figure C.20: Chauvenet's Envelope and Stress-Strain Curves for Half Spiral, Undamaged, Fiberglass Specimens (5GA10HNC)

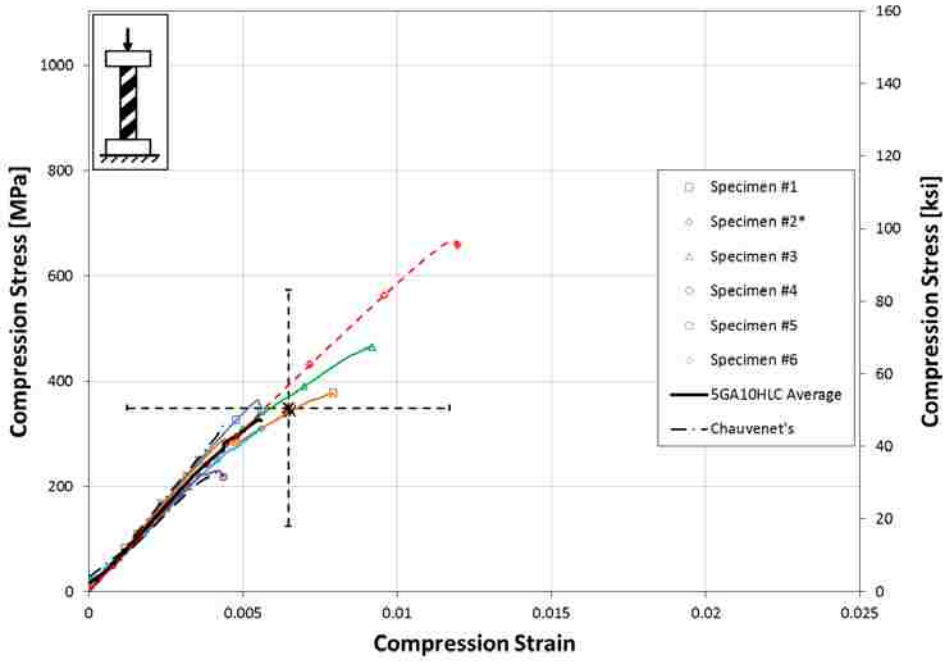

Figure C.21: Chauvenet's Envelope and Stress-Strain Curves for Half Spiral, 5 J (3.7 ft-lbs) Impact, Fiberglass Specimens (5GA10HLC)

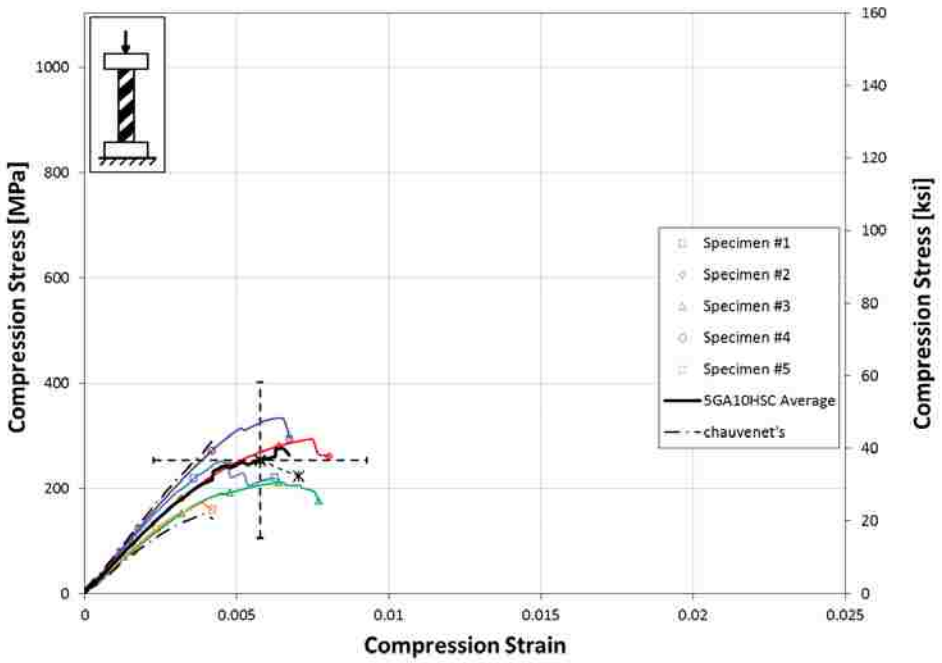

Figure C.22: Chauvenet's Envelope and Stress-Strain Curves for Half Spiral, 10 J (7.4 ft-lbs) Impact, Fiberglass Specimens (5GA10HSC)

APPENDIX D: OFFSET PLOTS

This section illustrates CSAI vs. offset angle plots that were used in this research. As previously described, offset angles had insignificant effect on the CSAI of specimens. Offset angles were therefore not incorporated in the adjustment of the final data results. Figure D.1 and Figure D.2 summarize misalignment results for carbon fiber and fiberglass epoxy composites, respectively.

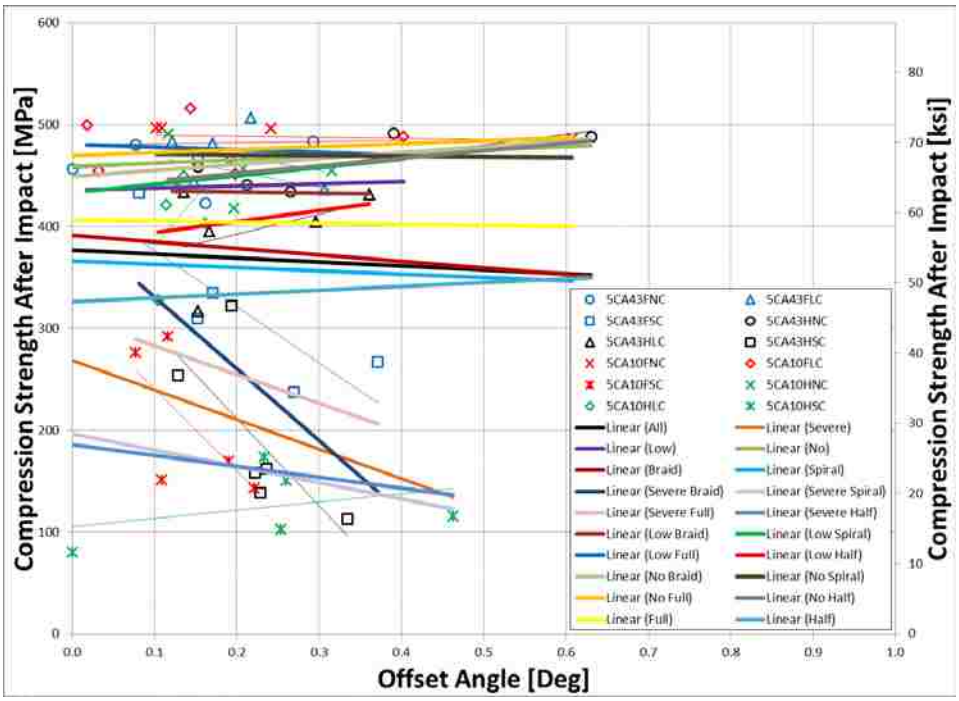

Figure D.1: Offset Angle vs. CSAI for Carbon Specimens

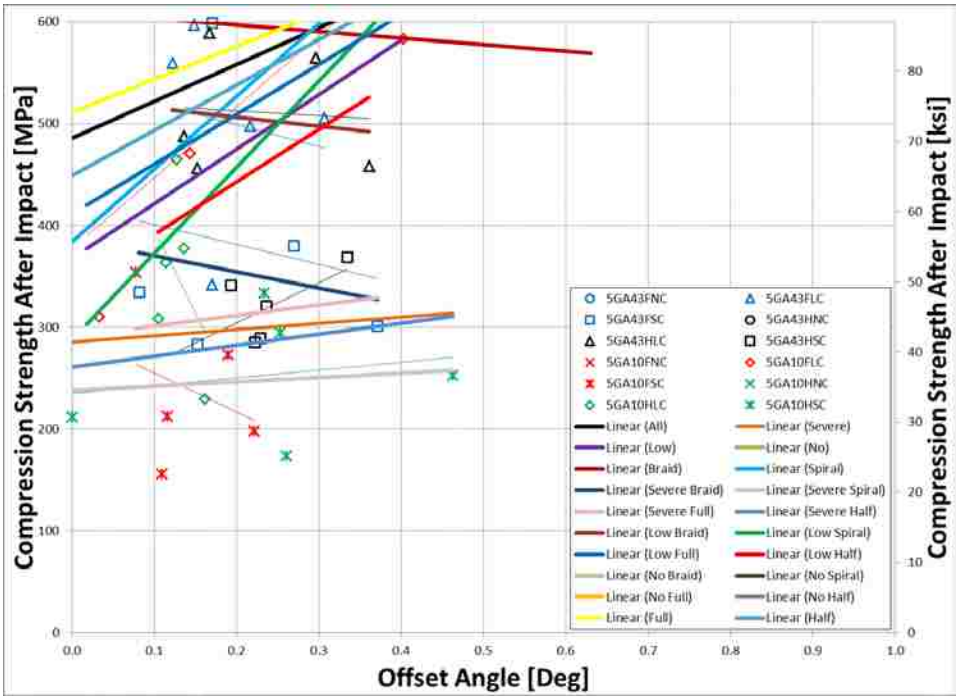

Figure D.2: Offset Angle vs. CSAI for Fiberglass Specimens

APPENDIX E: NORMALIZED AVERAGE CURVES

To investigate the mechanical behavior of carbon, fiberglass, and basalt fiber/epoxy composites, normalized average compression stress and deformation curves were prepared. These curves were obtained by normalizing compression stress-strain curves of impacted configurations to their corresponding undamaged maximum compression stress and strain. Subsequently, normalized stress and deformation plots of all fiber/epoxy core materials examining braided and spiral sleeve, and full and half coverage are presented in this section, respectively.

E.1 Normalized Average Curves for Braided and Spiral Sleeve Configurations

Figure E.1 contains all 18 normalized configurations. Figure E.2– Figure E.4 compares the normalized compression stresses as a function of impact energy levels.

Figure E.5 and Figure E.6 compare the normalized compression stresses as a function of sleeve coverage (full and half), respectively.

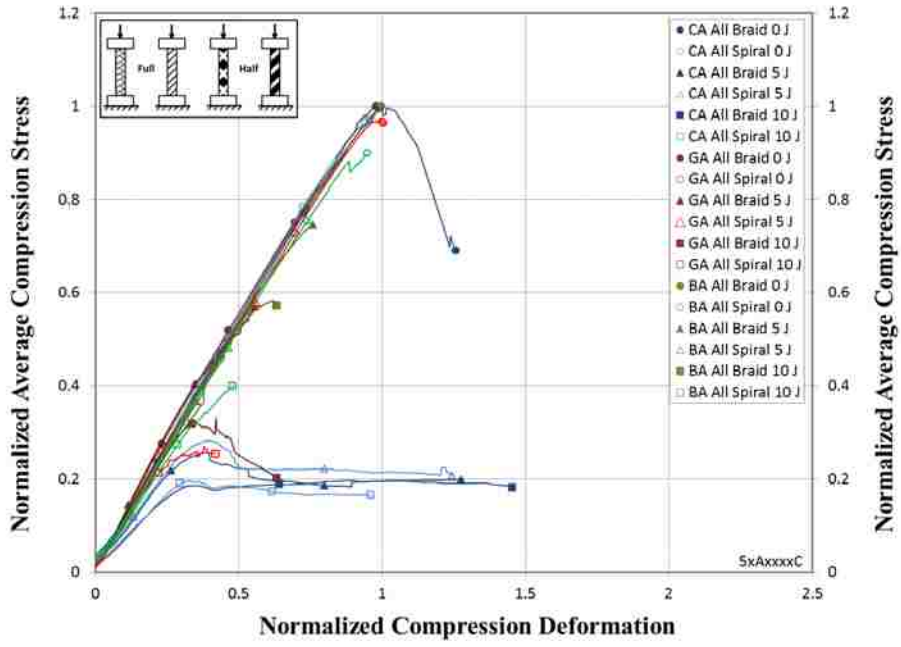

Figure E.1: Normalized Compression Stress-Deformation Plot, Braid vs. Spiral Sleeves

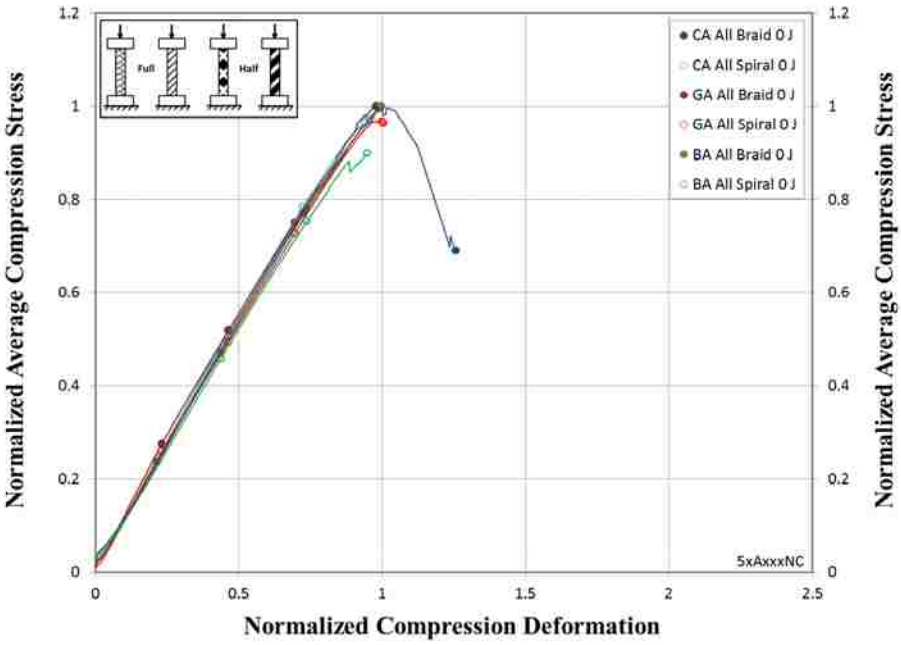

Figure E.2: Normalized Compression Stress-Deformation Curves, Undamaged, Braid vs. Spiral Sleeve Configurations

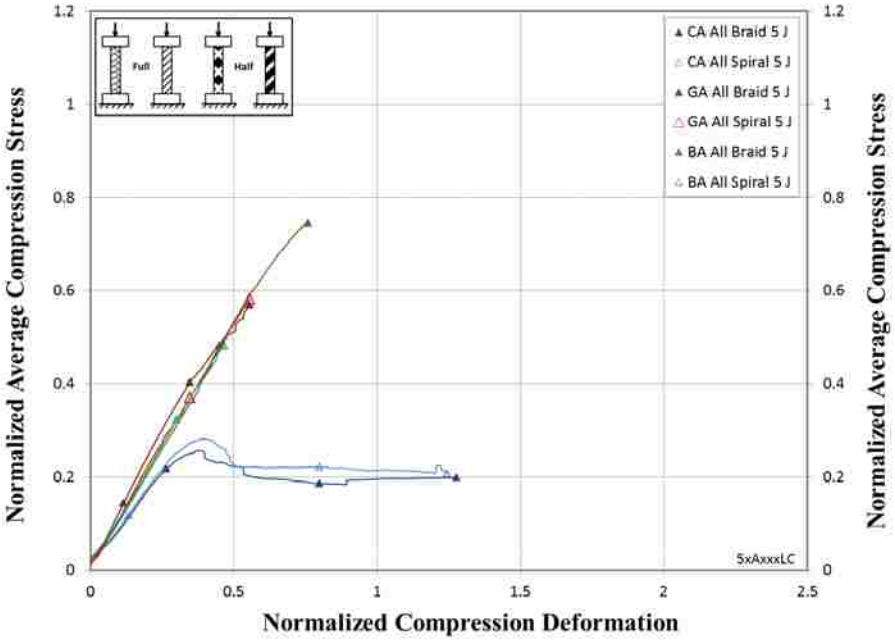

Figure E.3: Normalized Compression Stress-Deformation Curves, 5 J of Impact, Braid vs. Spiral Sleeve Configurations

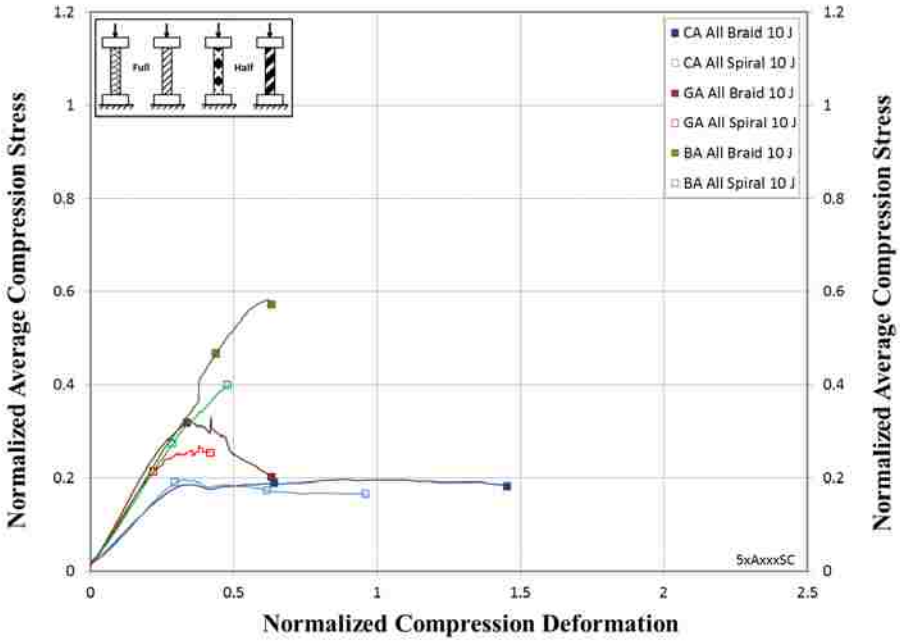

Figure E.4: Normalized Compression Stress-Deformation Curves, 10 J of Impact, Braid vs. Spiral Sleeve Configurations

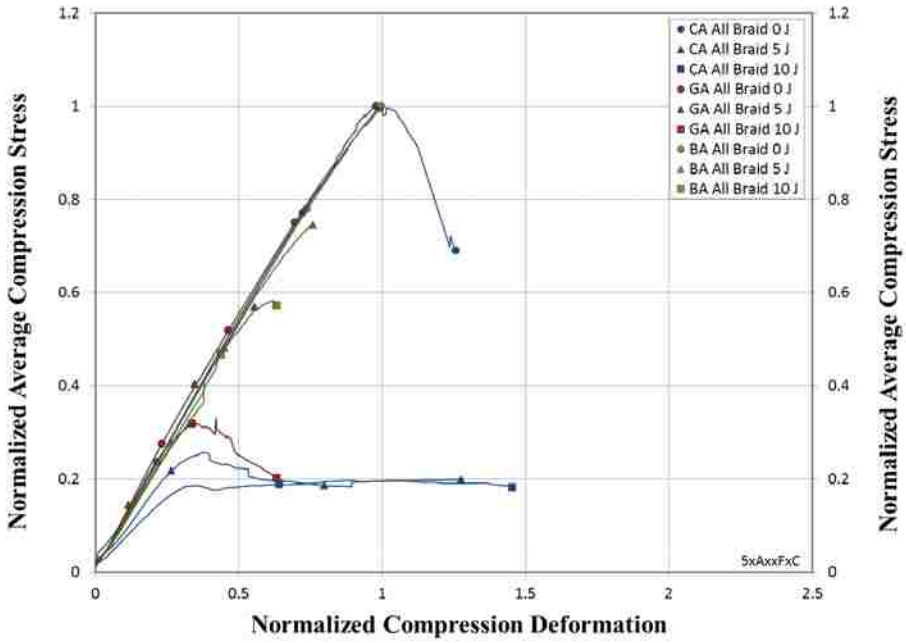

Figure E.5: Normalized Compression Stress-Deformation Curves of All Braided Sleeve Configurations

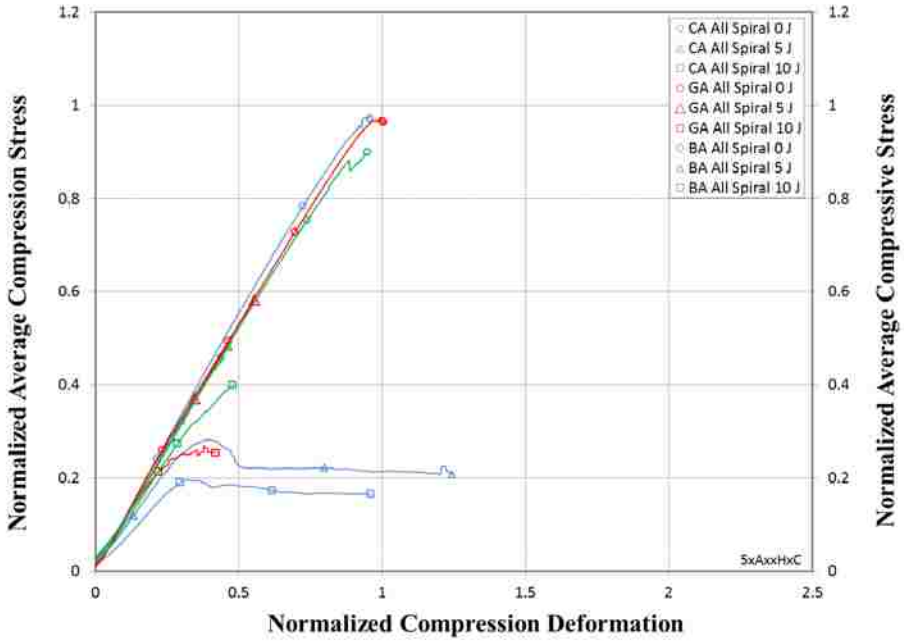

Figure E.6: Normalized Compression Stress-Deformation Curves of All Spiral Sleeve Configurations

E.2 Normalized Average Curves for Full and Half Coverage Configurations

Figure E.7 contains all 18 normalized configurations. Figure E.8 – Figure E.10 compare the normalized compression stresses as a function of impact energy levels.

Figure E.11 and Figure E.12 compare the normalized compression stresses as a function of sleeve coverage (full and half), respectively.

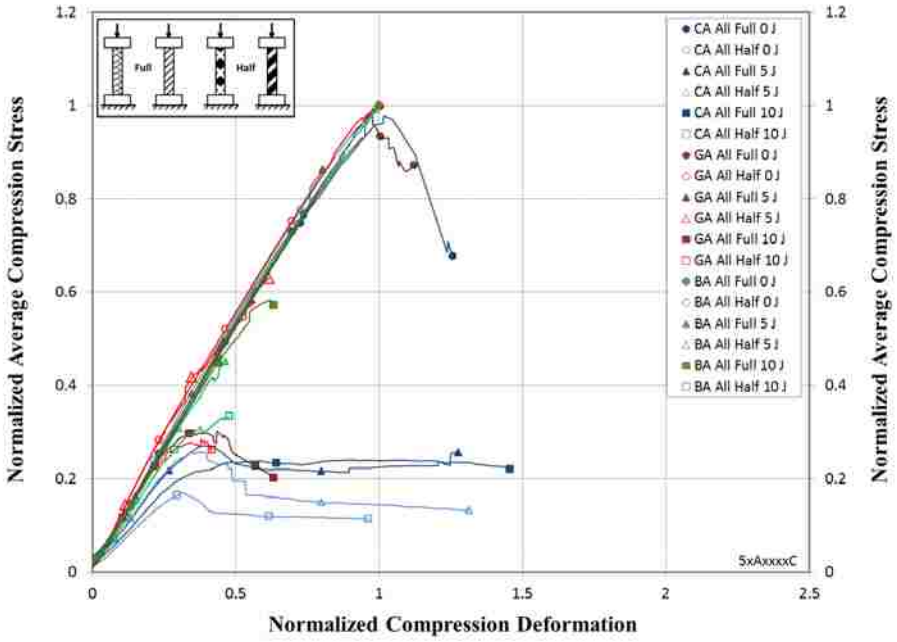

Figure E.7: Normalized Compression Stress-Deformation Plot, Full vs. Half Coverage

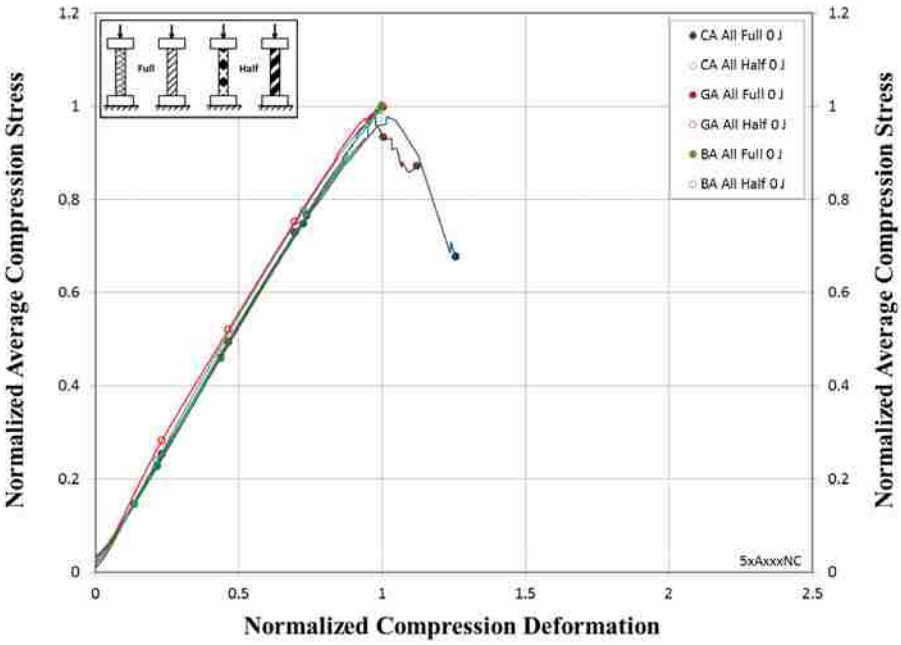

Figure E.8: Normalized Compression Stress-Deformation Curves, Undamaged, Full vs. Half Coverage Configurations

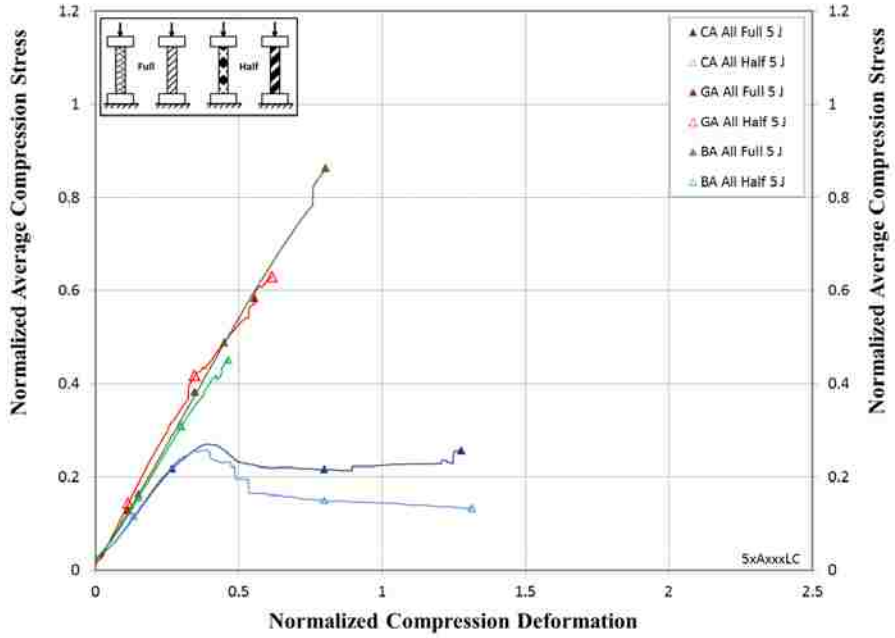

Figure E.9: Normalized Compression Stress-Deformation Curves, 5 J of Impact, Full vs. Half Coverage Configurations

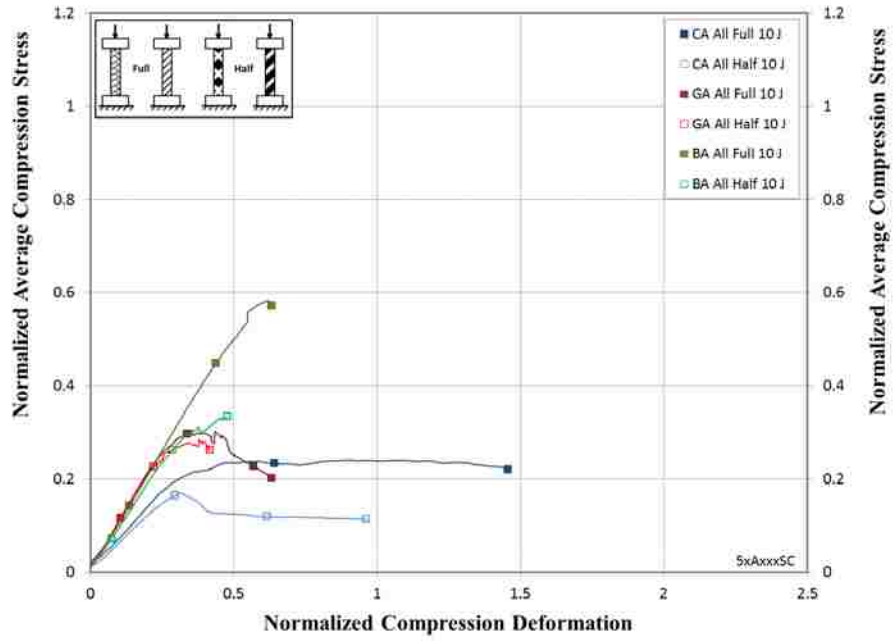

Figure E.10: Normalized Compression Stress-Deformation Curves, 10 J of Impact, Full vs. Half Coverage Configurations

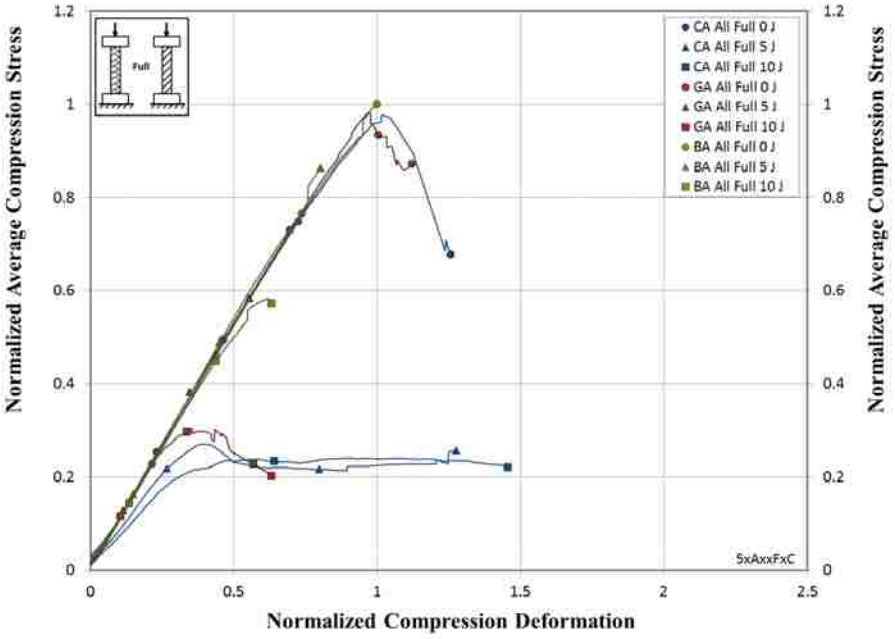

Figure E.11: Normalized Compression Stress-Deformation Curves of All Full Coverage Configurations

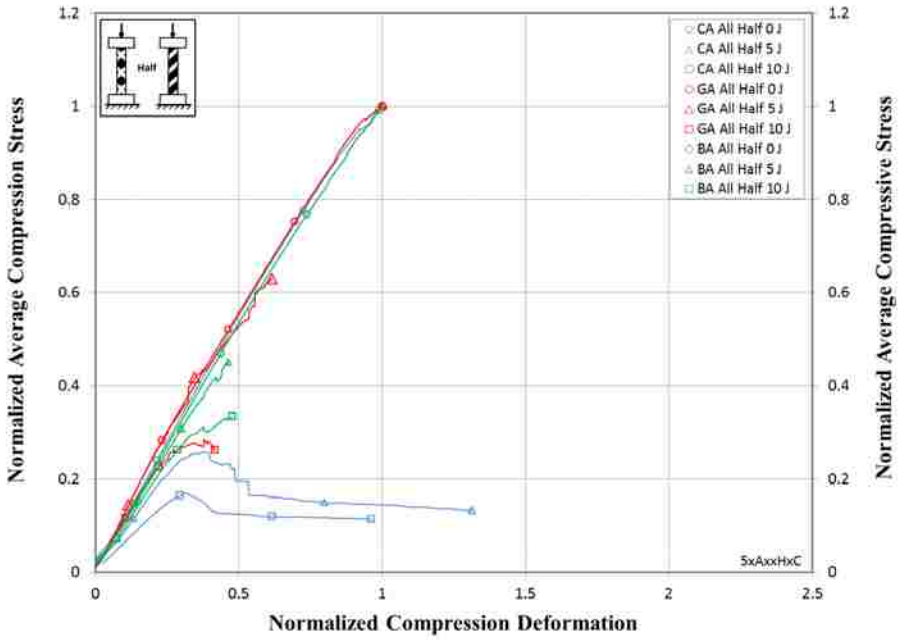

Figure E.12: Normalized Compression Stress-Deformation Curves of All Half Coverage Configurations